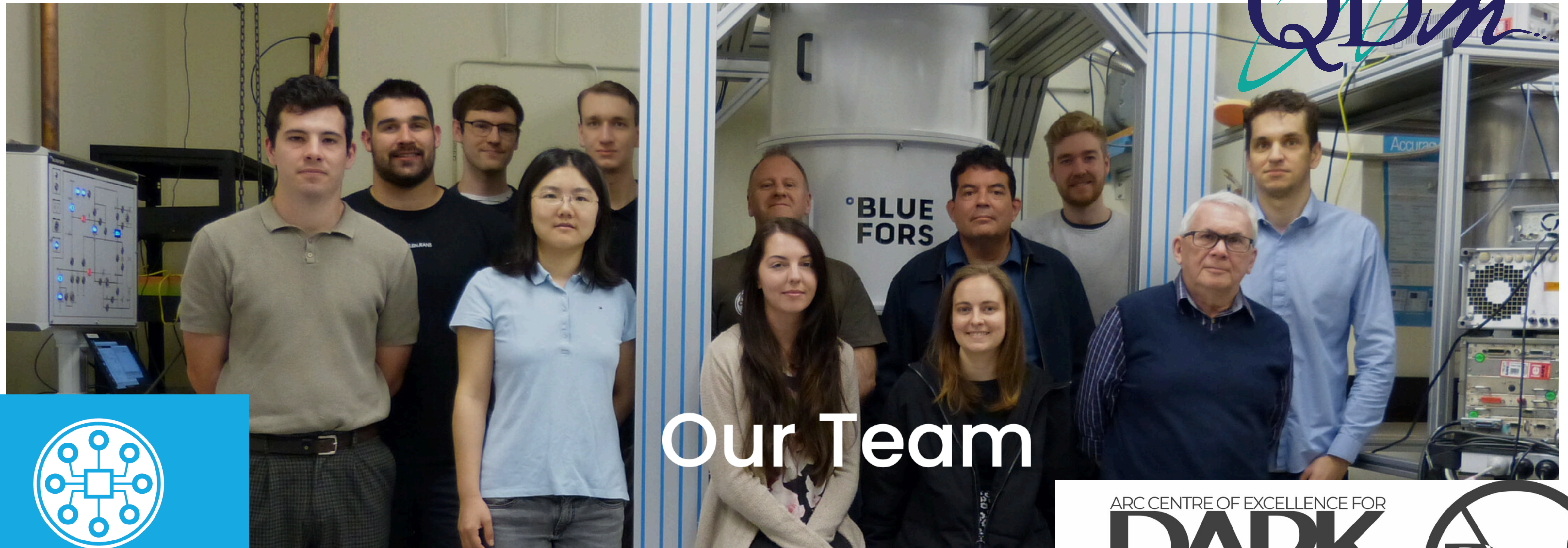
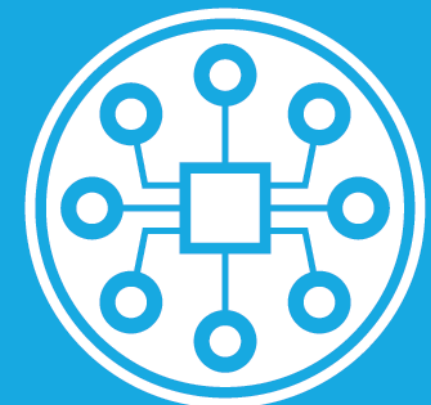


First results from Phase 1a of The ORGAN Experiment

QDM



Our Team



EQUS

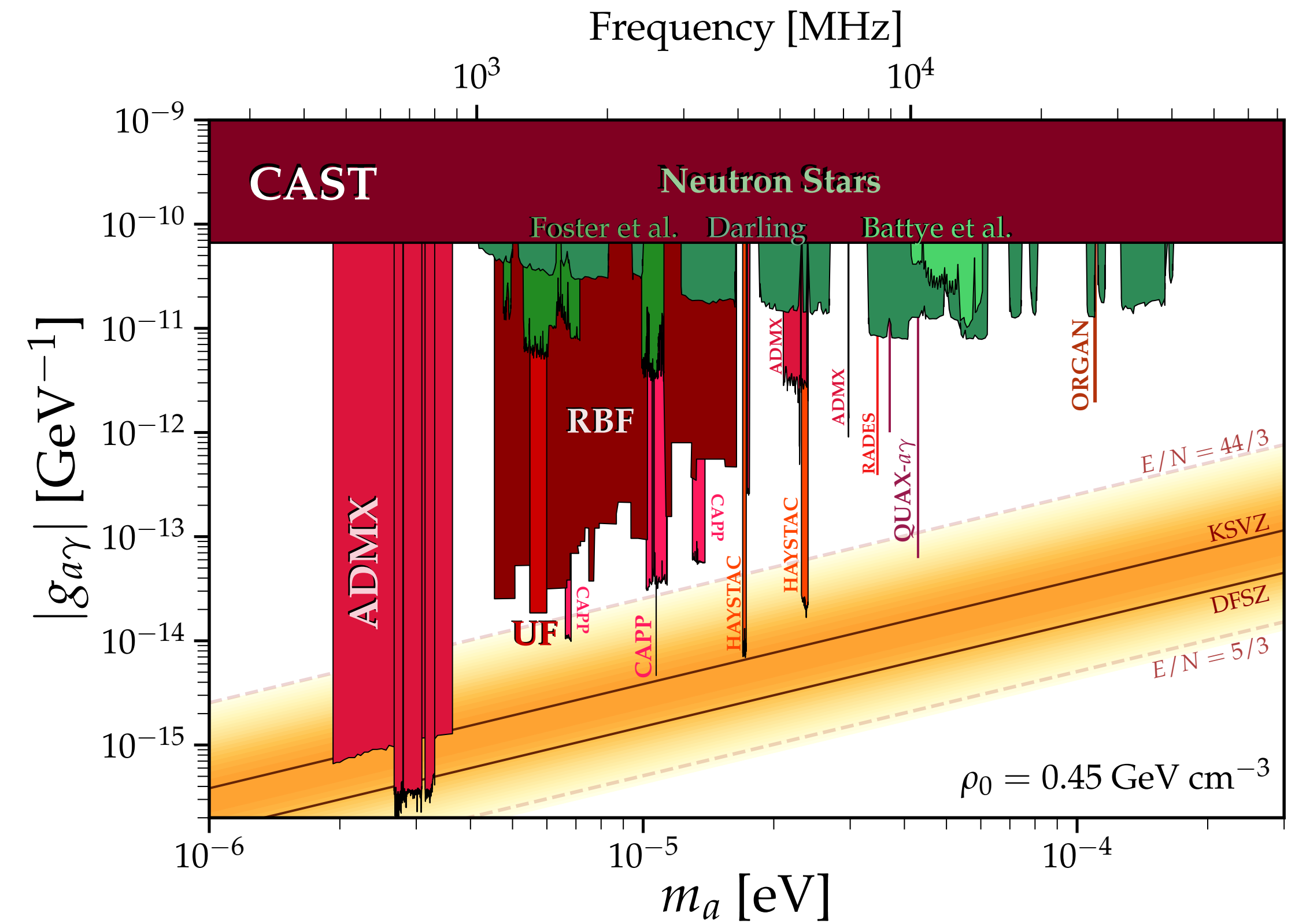
Australian Research Council
Centre of Excellence for
Engineered Quantum Systems

Aaron Quiskamp



ORGAN: Oscillating Resonant Group AxioN Experiment

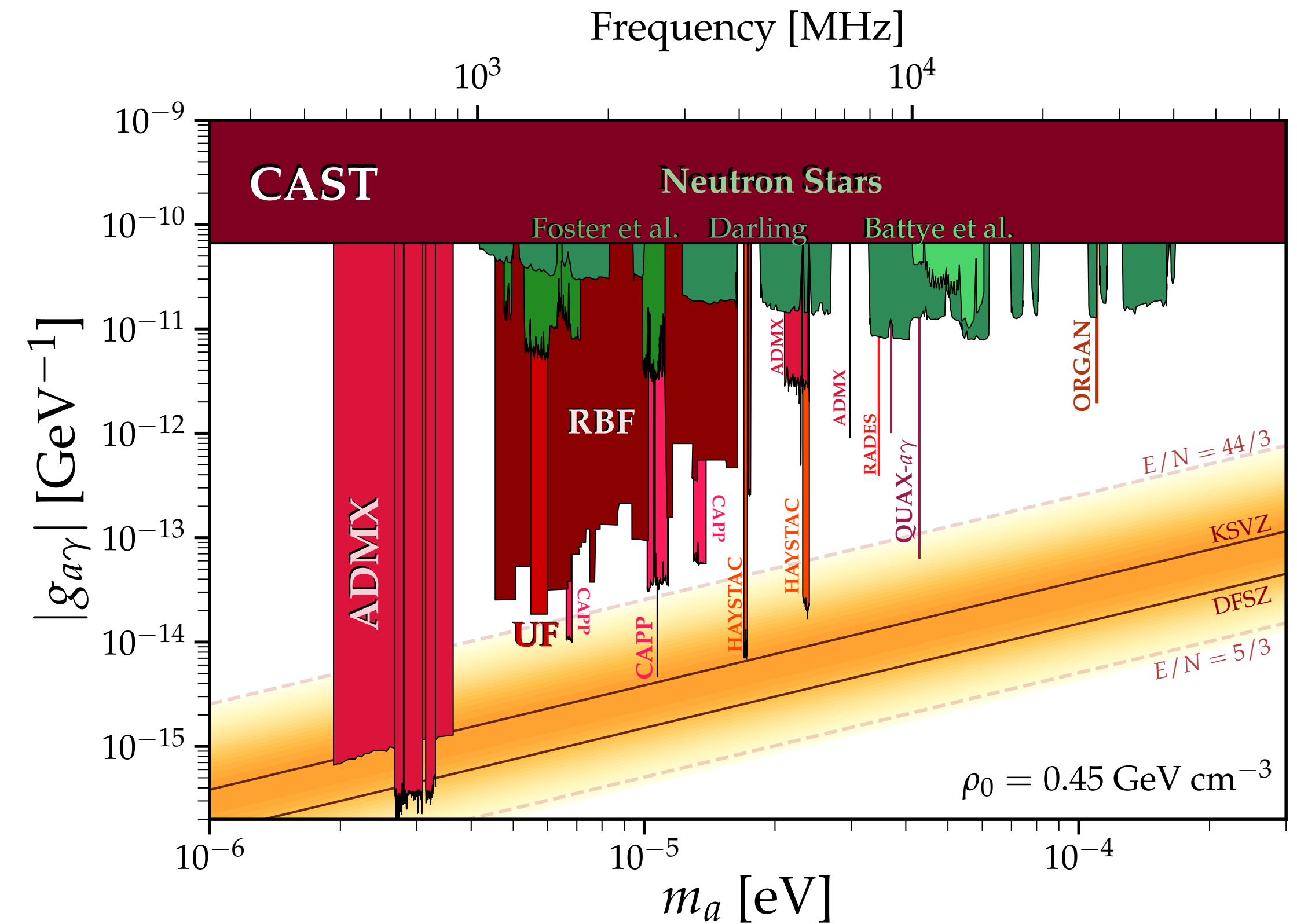
ORGAN: Oscillating Resonant Group AxioN Experiment



cajohare.github.io/AxionLimits

ORGAN: Oscillating Resonant Group AxioN Experiment

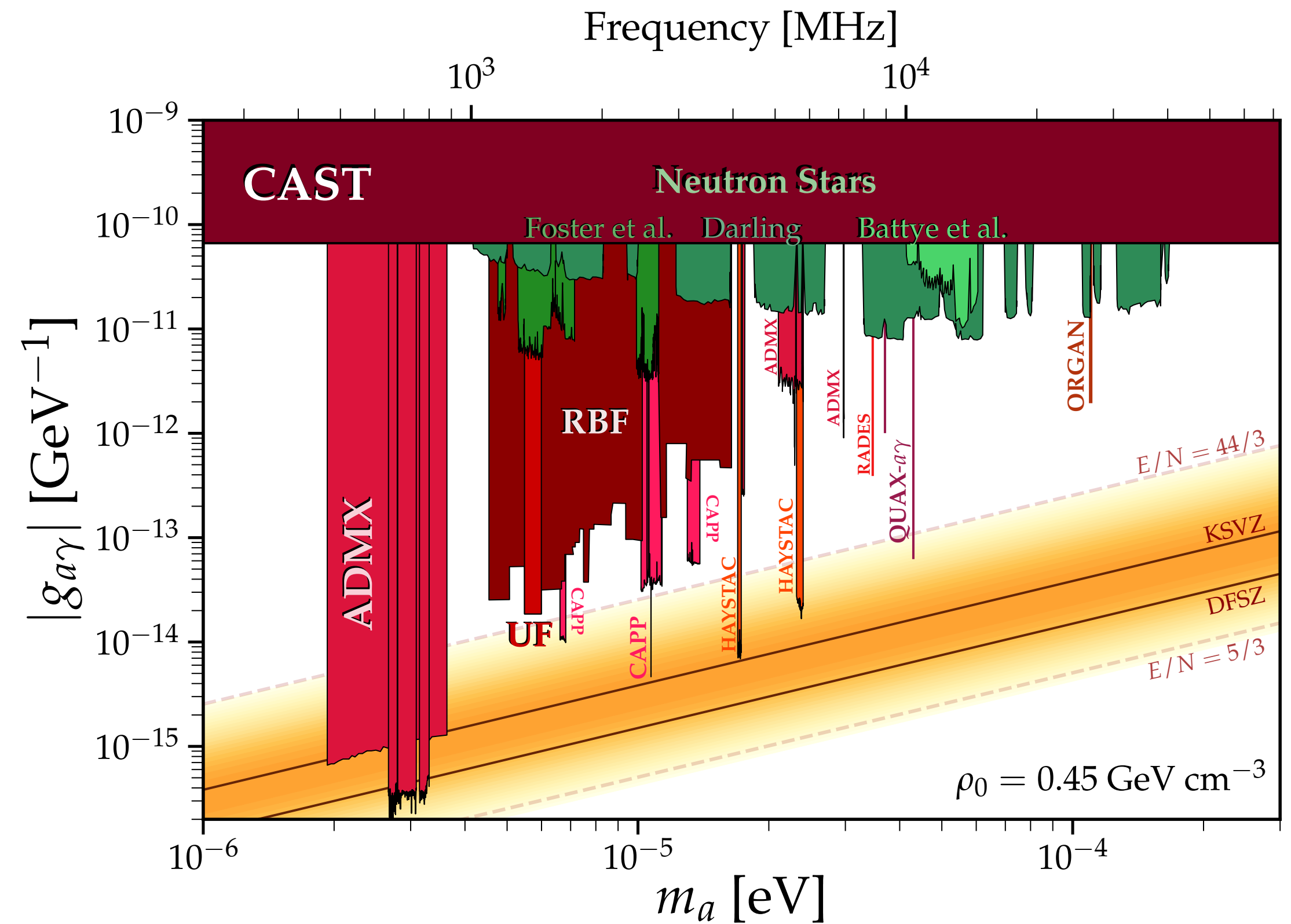
- High frequency (>15 GHz) axion haloscope at UWA



cajohare.github.io/AxionLimits

ORGAN: Oscillating Resonant Group AxioN Experiment

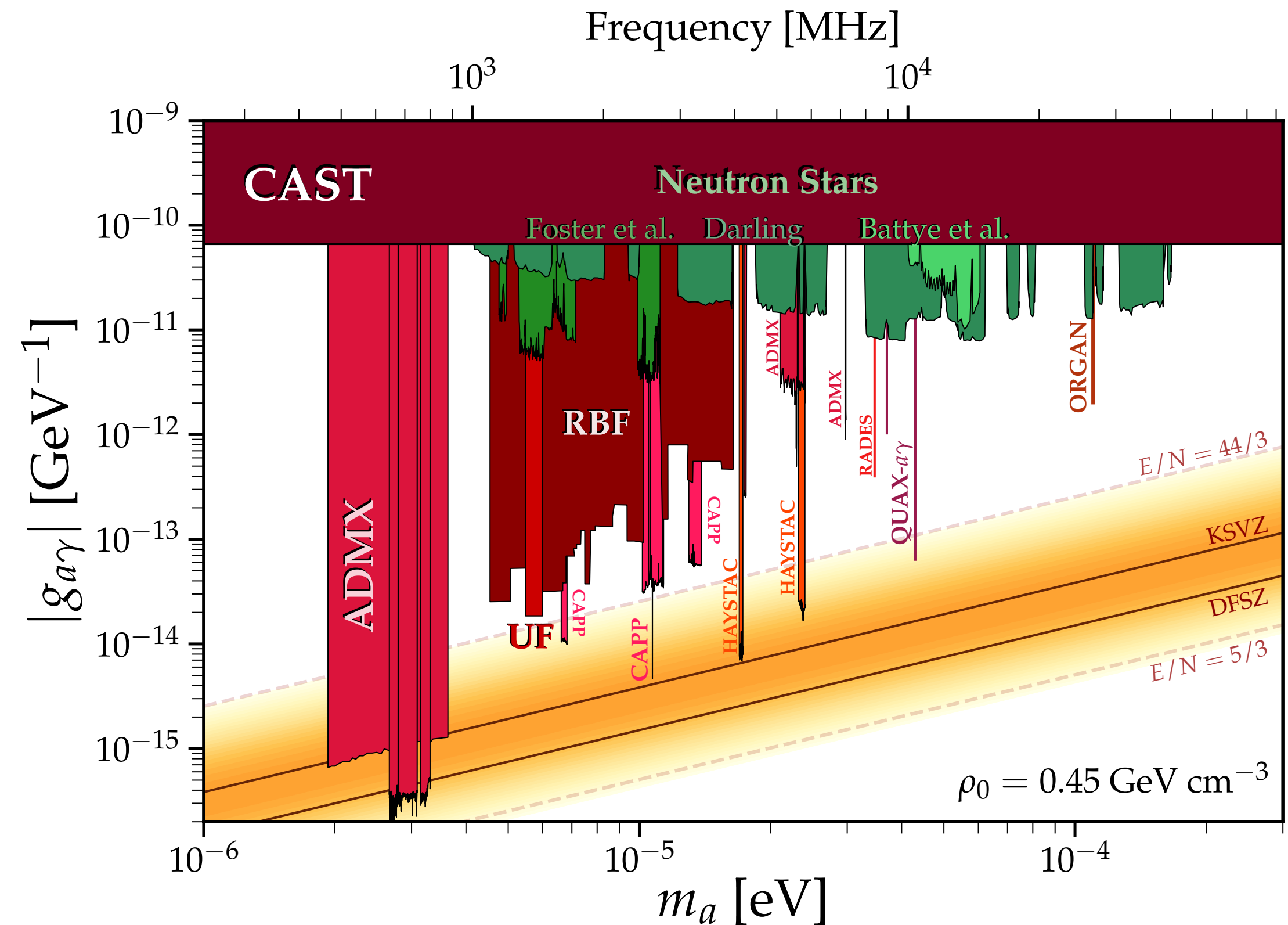
- High frequency (>15 GHz) axion haloscope at UWA
- High frequency parameter space is largely un-probed and ripe for exploration



cajohare.github.io/AxionLimits

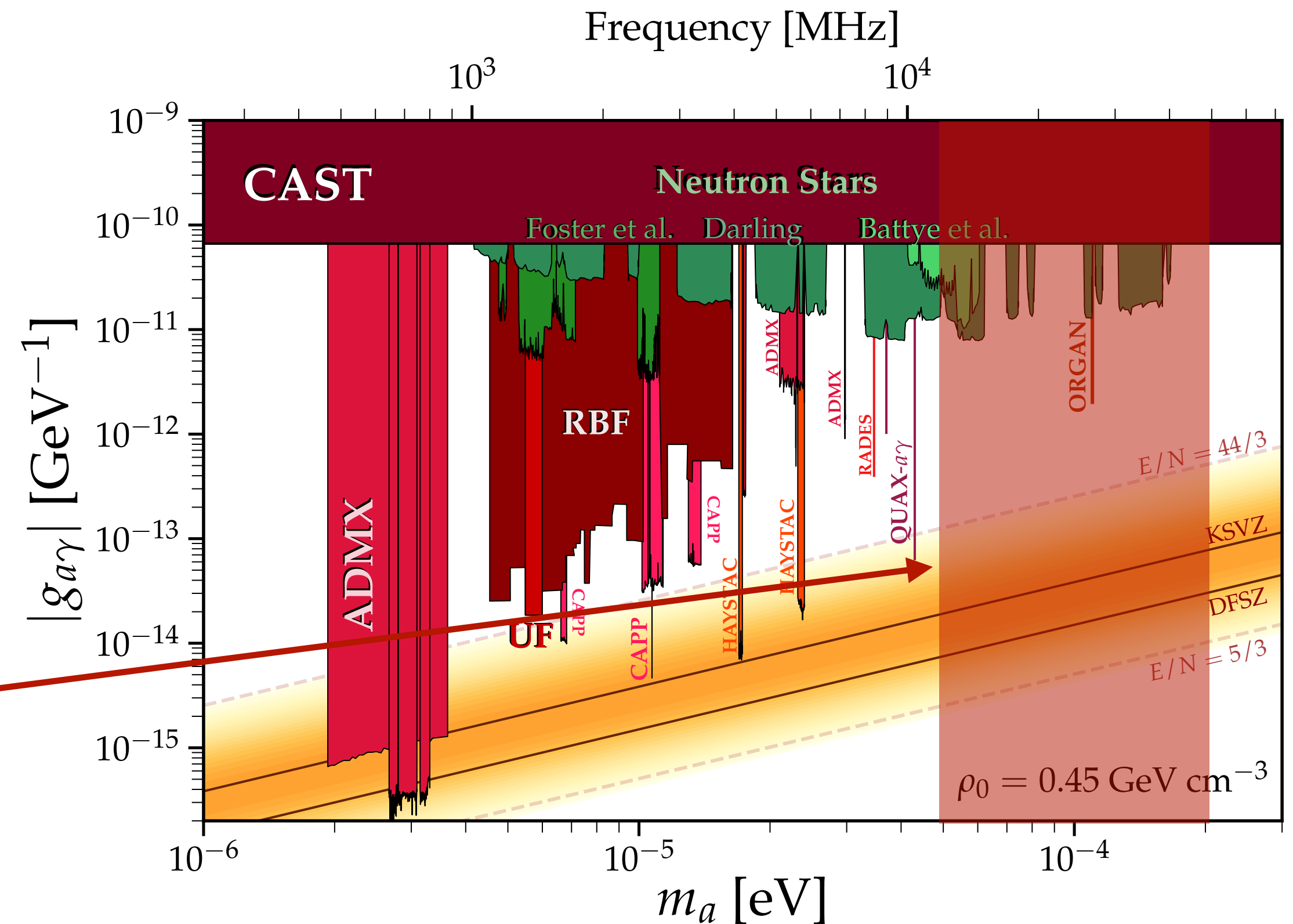
ORGAN: Oscillating Resonant Group AxioN Experiment

- High frequency (>15 GHz) axion haloscope at UWA
- High frequency parameter space is largely un-probed and ripe for exploration
- SMASH model predicts axion mass (m_a) between 50 and 200 μeV

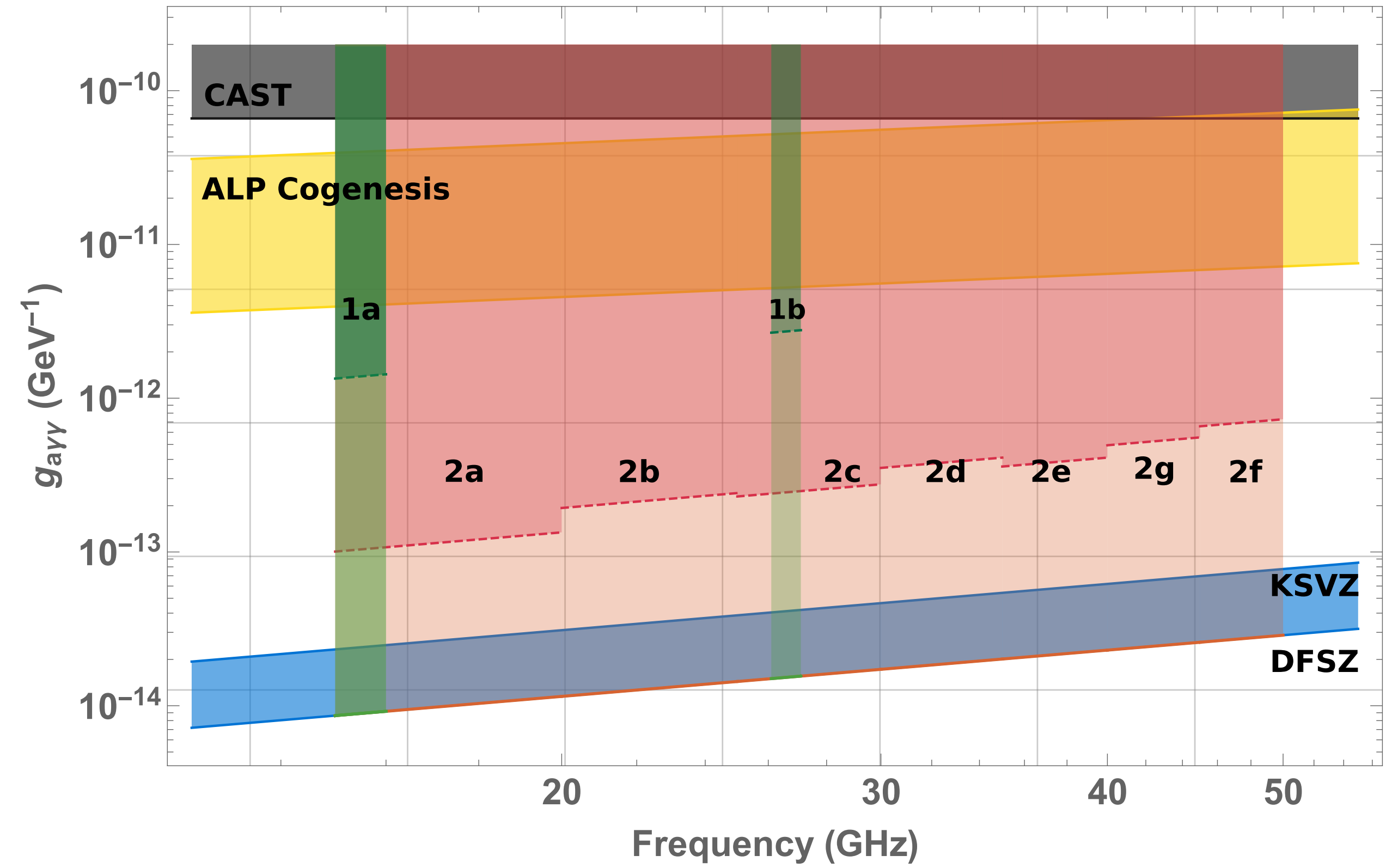


ORGAN: Oscillating Resonant Group AxioN Experiment

- High frequency (>15 GHz) axion haloscope at UWA
- High frequency parameter space is largely un-probed and ripe for exploration
- SMASH model predicts axion mass (m_a) between 50 and 200 μeV

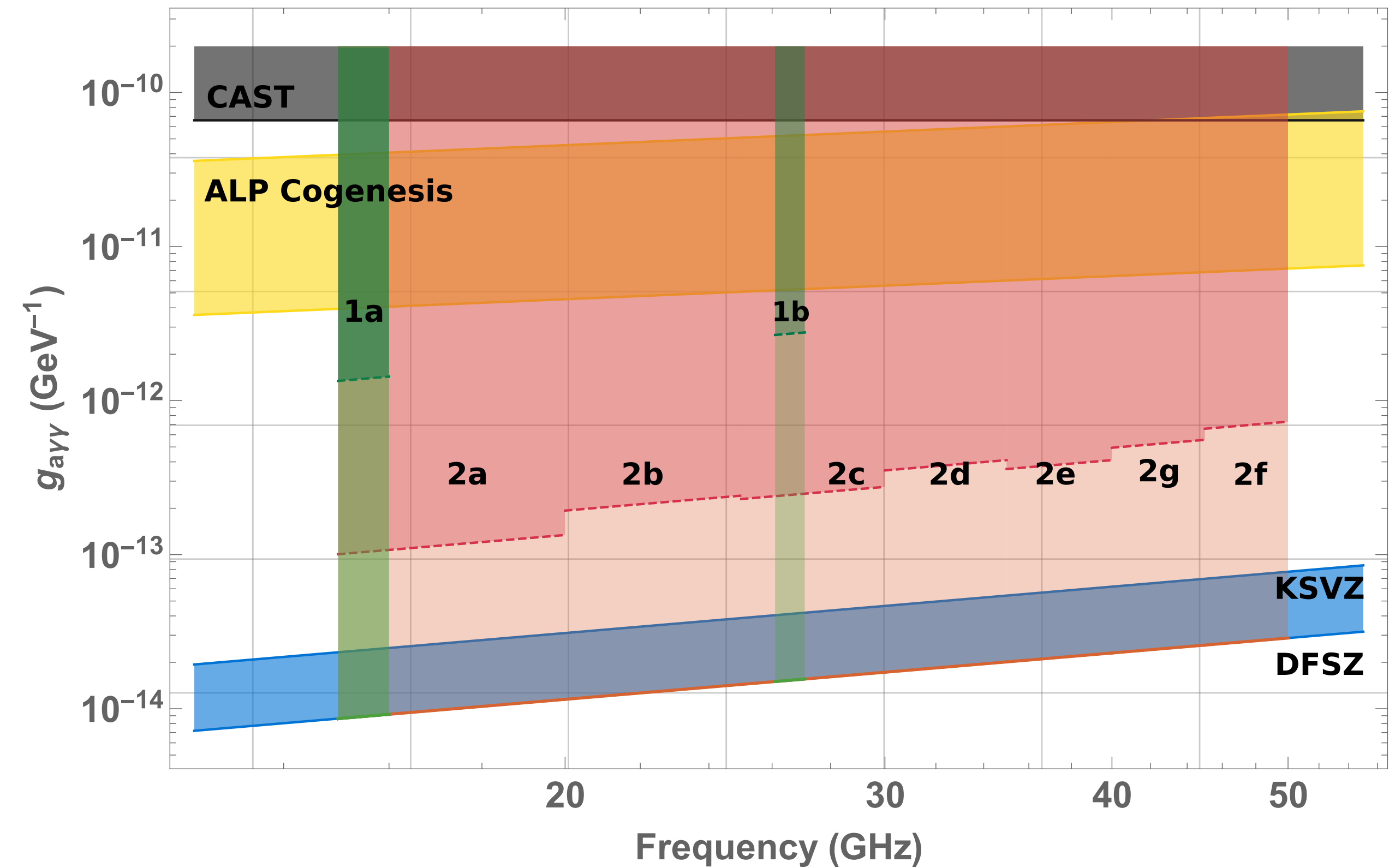


ORGAN Run Plan



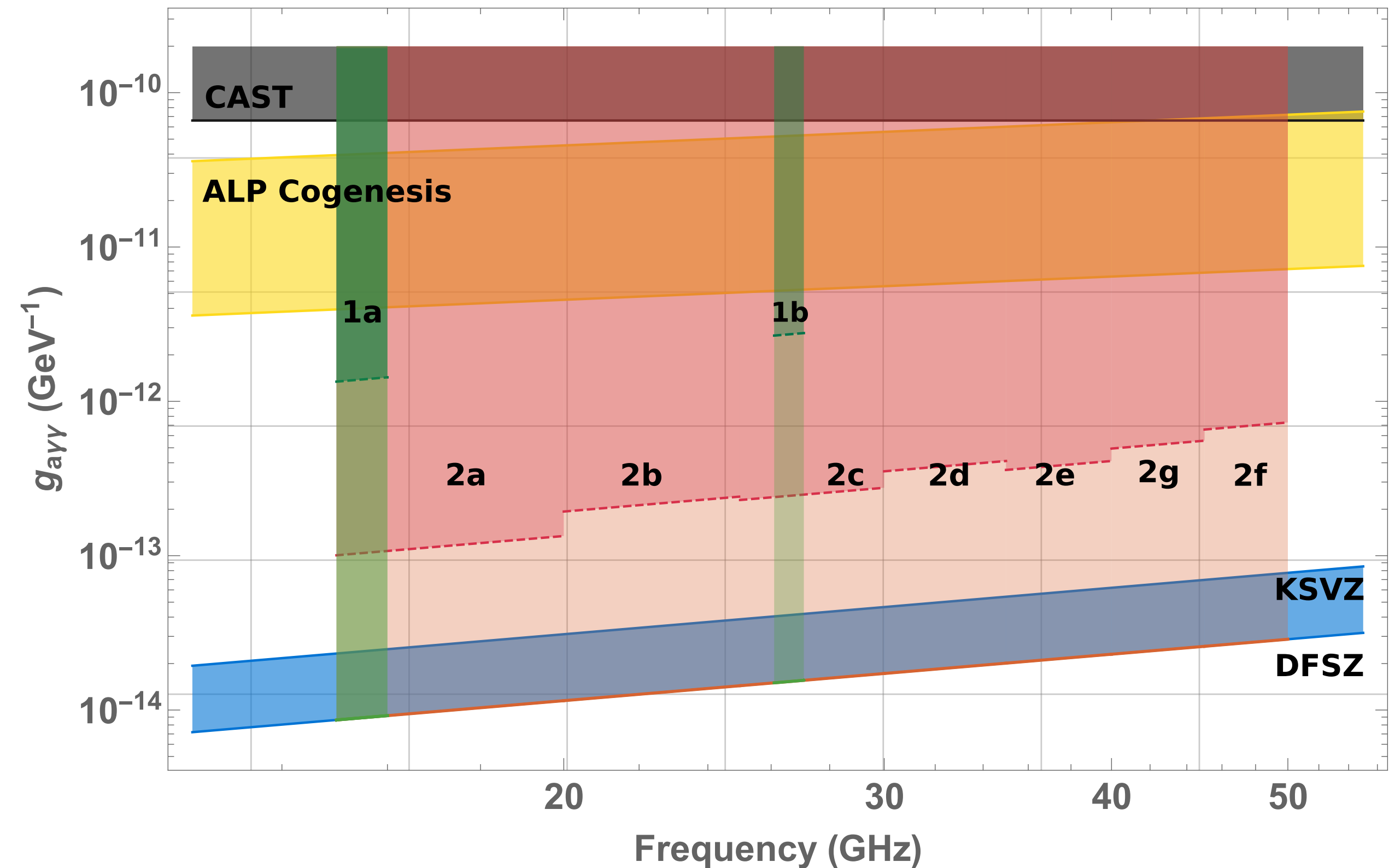
ORGAN Run Plan

- Phase 1: Narrow searches around 15-16 GHz and 26-27 GHz



ORGAN Run Plan

- Phase 1: Narrow searches around 15-16 GHz and 26-27 GHz
- Runs 1a/1b (dark green): HEMT-based amplifiers and TM_{010} tuning rod resonators, form factor of 0.4.



ORGAN Run Plan

- Phase 1: Narrow searches around 15-16 GHz and 26-27 GHz
- Runs 1a/1b (dark green): HEMT-based amplifiers and TM_{010} tuning rod resonators, form factor of 0.4.

Axion Kinetic Misalignment Mechanism

Raymond T. Co¹, Lawrence J. Hall^{2,3} and Keisuke Harigaya⁴

¹Leinweber Center for Theoretical Physics, University of Michigan, Ann Arbor, Michigan 48109, USA

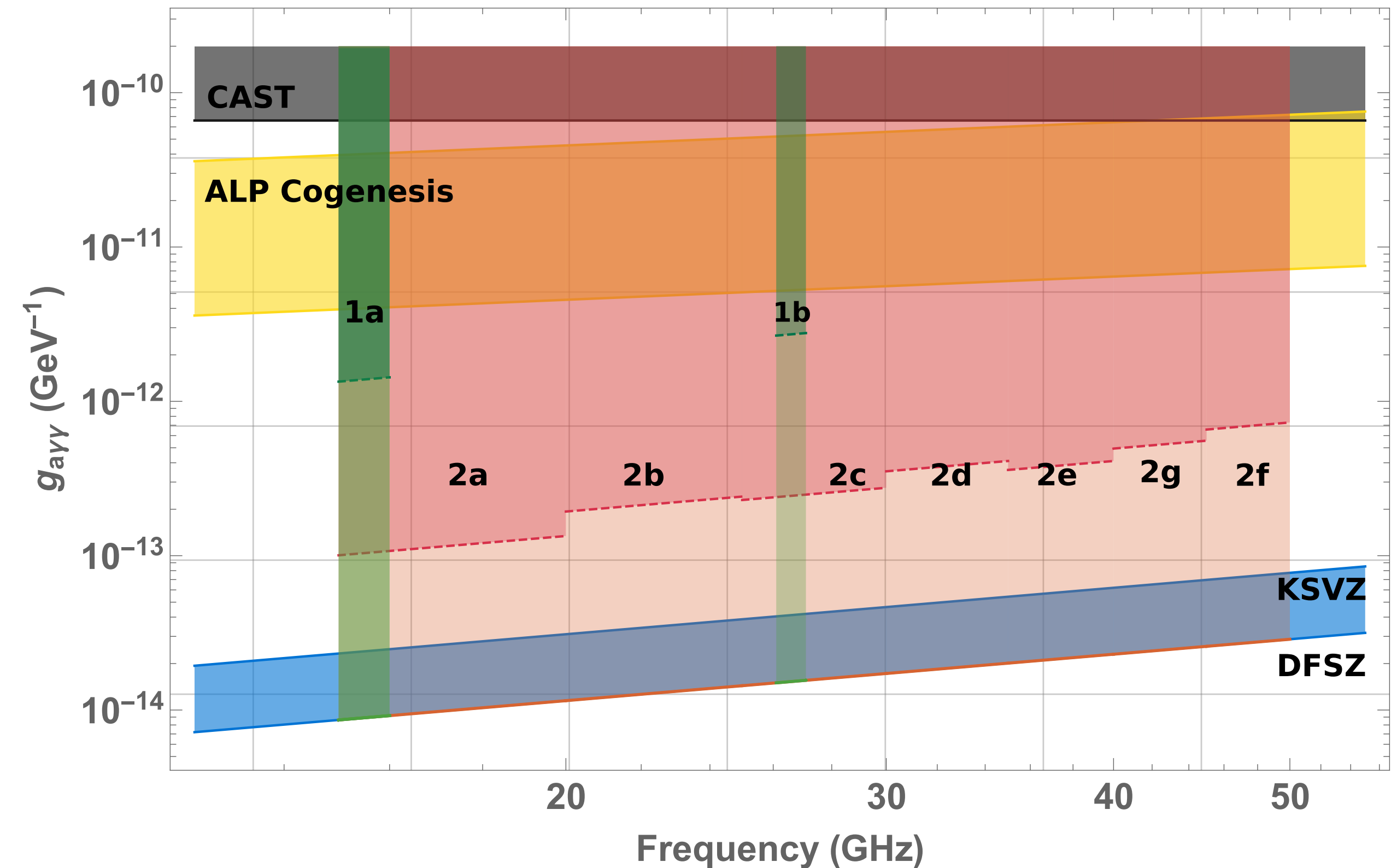
²Department of Physics, University of California, Berkeley, California 94720, USA

³Theoretical Physics Group, Lawrence Berkeley National Laboratory, Berkeley, California 94720, USA

⁴School of Natural Sciences, Institute for Advanced Study, Princeton, New Jersey 08540, USA

(Received 22 November 2019; revised manuscript received 6 April 2020; accepted 8 June 2020; published 26 June 2020)

In the conventional misalignment mechanism, the axion field has a constant initial field value in the early Universe and later begins to oscillate. We present an alternative scenario where the axion field has a nonzero initial velocity, allowing an axion decay constant much below the conventional prediction from axion dark matter. This axion velocity can be generated from explicit breaking of the axion shift symmetry in the early Universe, which may occur as this symmetry is approximate.



ORGAN Run Plan

- Phase 1: Narrow searches around 15-16 GHz and 26-27 GHz
- Runs 1a/1b (dark green): HEMT-based amplifiers and TM_{010} tuning rod resonators, form factor of 0.4.

Axion Kinetic Misalignment Mechanism

Raymond T. Co,¹ Lawrence J. Hall,^{2,3} and Keisuke Harigaya⁴

¹Leinweber Center for Theoretical Physics, University of Michigan, Ann Arbor, Michigan 48109, USA

²Department of Physics, University of California, Berkeley, California 94720, USA

³Theoretical Physics Group, Lawrence Berkeley National Laboratory, Berkeley, California 94720, USA

⁴School of Natural Sciences, Institute for Advanced Study, Princeton, New Jersey 08540, USA

(Received 22 November 2019; revised manuscript received 6 April 2020; accepted 8 June 2020; published 26 June 2020)

In the conventional misalignment mechanism, the axion field has a constant initial field value in the early Universe and later begins to oscillate. We present an alternative scenario where the axion field has a nonzero initial velocity, allowing an axion decay constant much below the conventional prediction from axion dark matter. This axion velocity can be generated from explicit breaking of the axion shift symmetry in the early Universe, which may occur as this symmetry is approximate.

Raymond T. Co,^a Lawrence J. Hall^{b,c} and Keisuke Harigaya^d

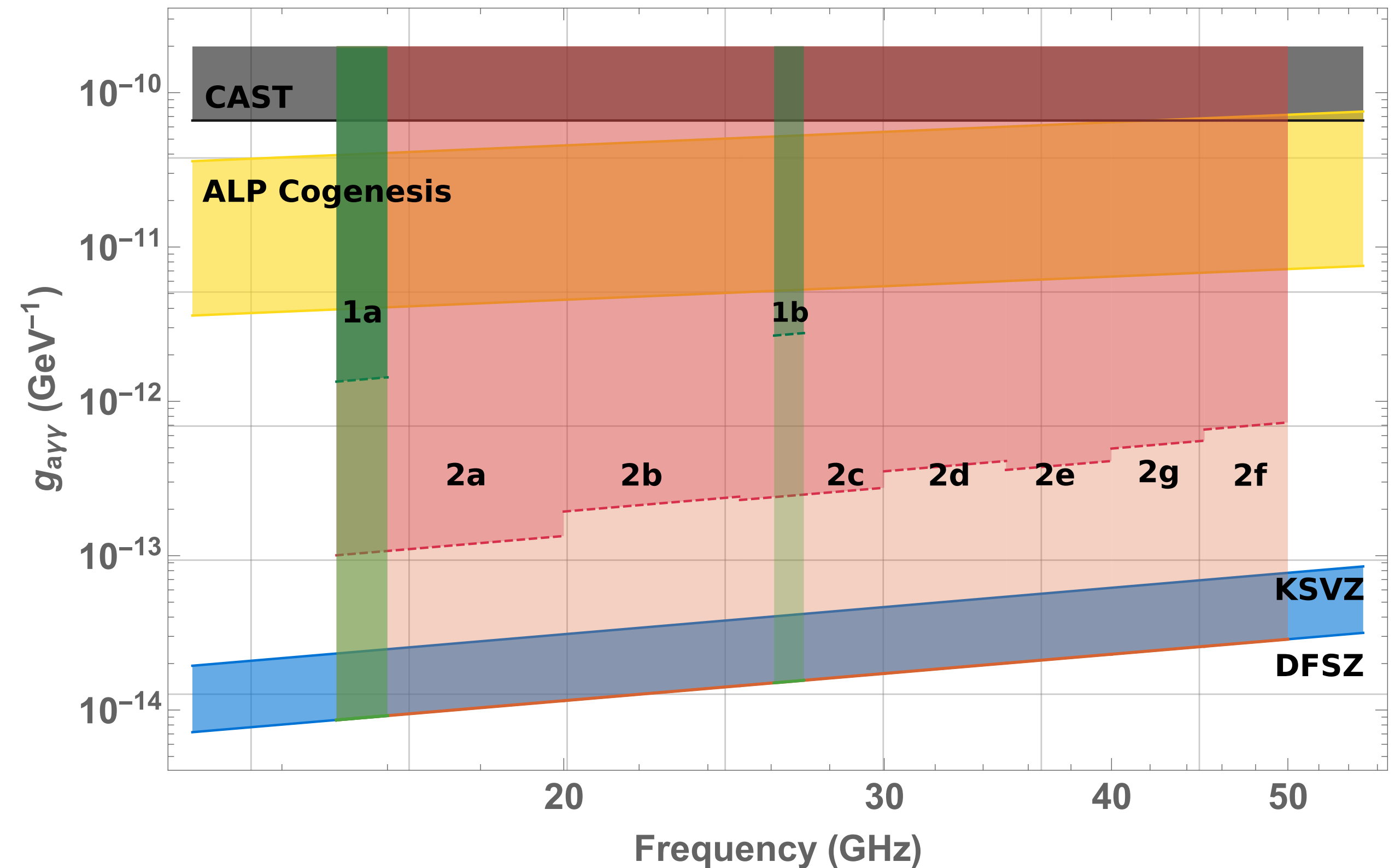
^aLeinweber Center for Theoretical Physics, Department of Physics, University of Michigan, Ann Arbor, MI 48109, U.S.A.

^bDepartment of Physics, University of California, Berkeley, CA 94720, U.S.A.

^cTheoretical Physics Group, Lawrence Berkeley National Laboratory, Berkeley, California 94720, U.S.A.

^dSchool of Natural Sciences, Institute for Advanced Study, Princeton, NJ 08540, U.S.A.

E-mail: rtco@umich.edu, ljhall@lbl.gov, keisukeharigaya@ias.edu



ORGAN Run Plan

- Phase 1: Narrow searches around 15-16 GHz and 26-27 GHz
- Runs 1a/1b (dark green): HEMT-based amplifiers and TM_{010} tuning rod resonators, form factor of 0.4.
- Phase 2: Wider searches (15-50GHz) building on expertise gained in Phase 1

Axion Kinetic Misalignment Mechanism

Raymond T. Co,¹ Lawrence J. Hall,^{2,3} and Keisuke Harigaya⁴

¹Leinweber Center for Theoretical Physics, University of Michigan, Ann Arbor, Michigan 48109, USA

²Department of Physics, University of California, Berkeley, California 94720, USA

³Theoretical Physics Group, Lawrence Berkeley National Laboratory, Berkeley, California 94720, USA

⁴School of Natural Sciences, Institute for Advanced Study, Princeton, New Jersey 08540, USA

(Received 22 November 2019; revised manuscript received 6 April 2020; accepted 8 June 2020; published 26 June 2020)

In the conventional misalignment mechanism, the axion field has a constant initial field value in the early Universe and later begins to oscillate. We present an alternative scenario where the axion field has a nonzero initial velocity, allowing an axion decay constant much below the conventional prediction from axion dark matter. This axion velocity can be generated from explicit breaking of the axion shift symmetry in the early Universe, which may occur as this symmetry is approximate.

Predictions for axion couplings from ALPogenesis

Raymond T. Co,^a Lawrence J. Hall^{b,c} and Keisuke Harigaya^d

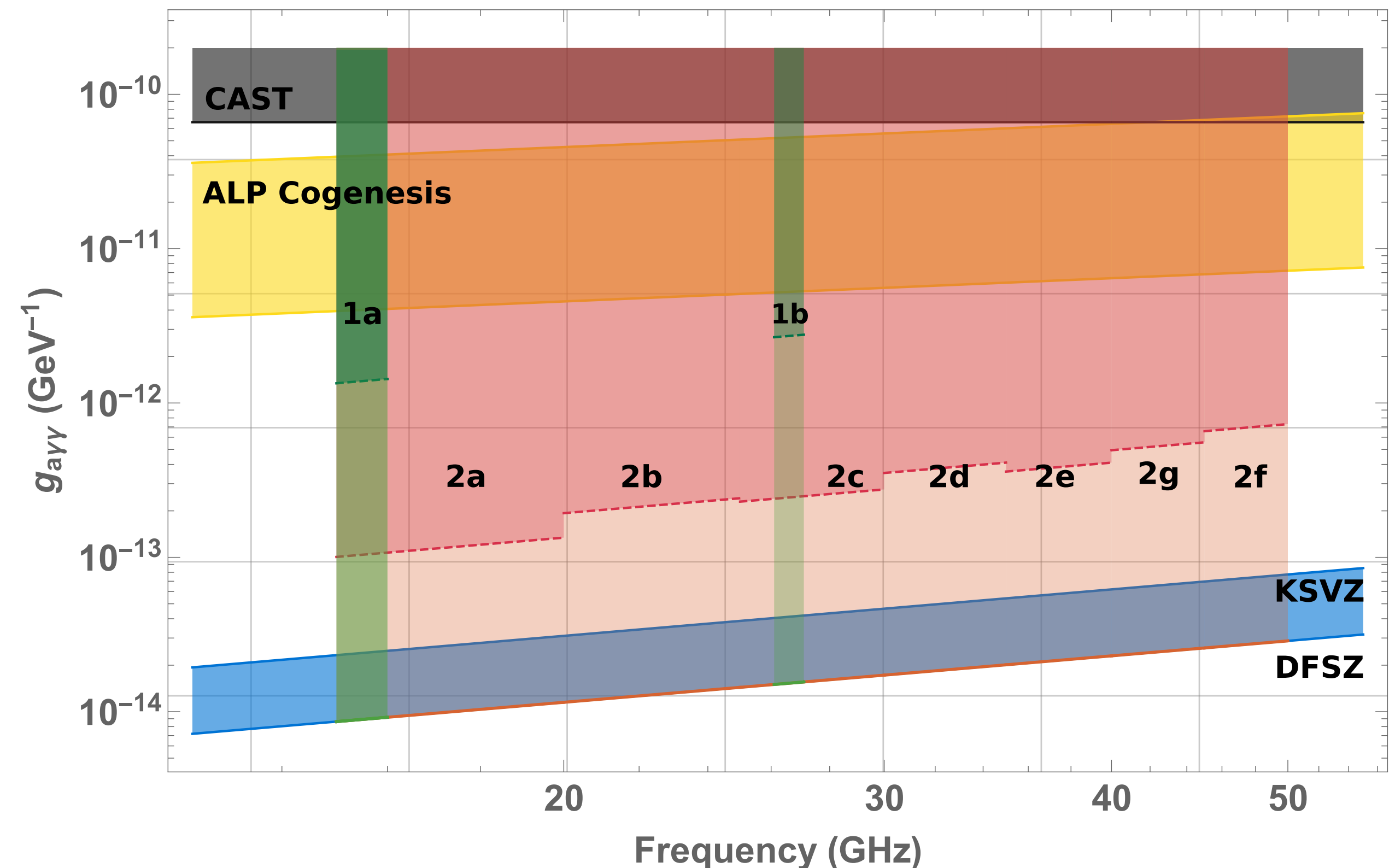
^aLeinweber Center for Theoretical Physics, Department of Physics, University of Michigan, Ann Arbor, MI 48109, U.S.A.

^bDepartment of Physics, University of California, Berkeley, CA 94720, U.S.A.

^cTheoretical Physics Group, Lawrence Berkeley National Laboratory, Berkeley, California 94720, U.S.A.

^dSchool of Natural Sciences, Institute for Advanced Study, Princeton, NJ 08540, U.S.A.

E-mail: rtco@umich.edu, ljhall@lbl.gov, keisukeharigaya@ias.edu



ORGAN Run Plan

- Phase 1: Narrow searches around 15-16 GHz and 26-27 GHz
- Runs 1a/1b (dark green): HEMT-based amplifiers and TM_{010} tuning rod resonators, form factor of 0.4.
- Phase 2: Wider searches (15-50GHz) building on expertise gained in Phase 1
- Phase 2, dark red: Quantum limited linear amplifiers (2-4 cavities)

Axion Kinetic Misalignment Mechanism

Raymond T. Co^{a,1}, Lawrence J. Hall^{b,2,3} and Keisuke Harigaya^{d,4}

¹Leinweber Center for Theoretical Physics, University of Michigan, Ann Arbor, Michigan 48109, USA

²Department of Physics, University of California, Berkeley, California 94720, USA

³Theoretical Physics Group, Lawrence Berkeley National Laboratory, Berkeley, California 94720, USA

⁴School of Natural Sciences, Institute for Advanced Study, Princeton, New Jersey 08540, USA

(Received 22 November 2019; revised manuscript received 6 April 2020; accepted 8 June 2020; published 26 June 2020)

In the conventional misalignment mechanism, the axion field has a constant initial field value in the early Universe and later begins to oscillate. We present an alternative scenario where the axion field has a nonzero initial velocity, allowing an axion decay constant much below the conventional prediction from axion dark matter. This axion velocity can be generated from explicit breaking of the axion shift symmetry in the early Universe, which may occur as this symmetry is approximate.

Predictions for axion couplings from ALPogenesis

Raymond T. Co^a, Lawrence J. Hall^{b,c} and Keisuke Harigaya^d

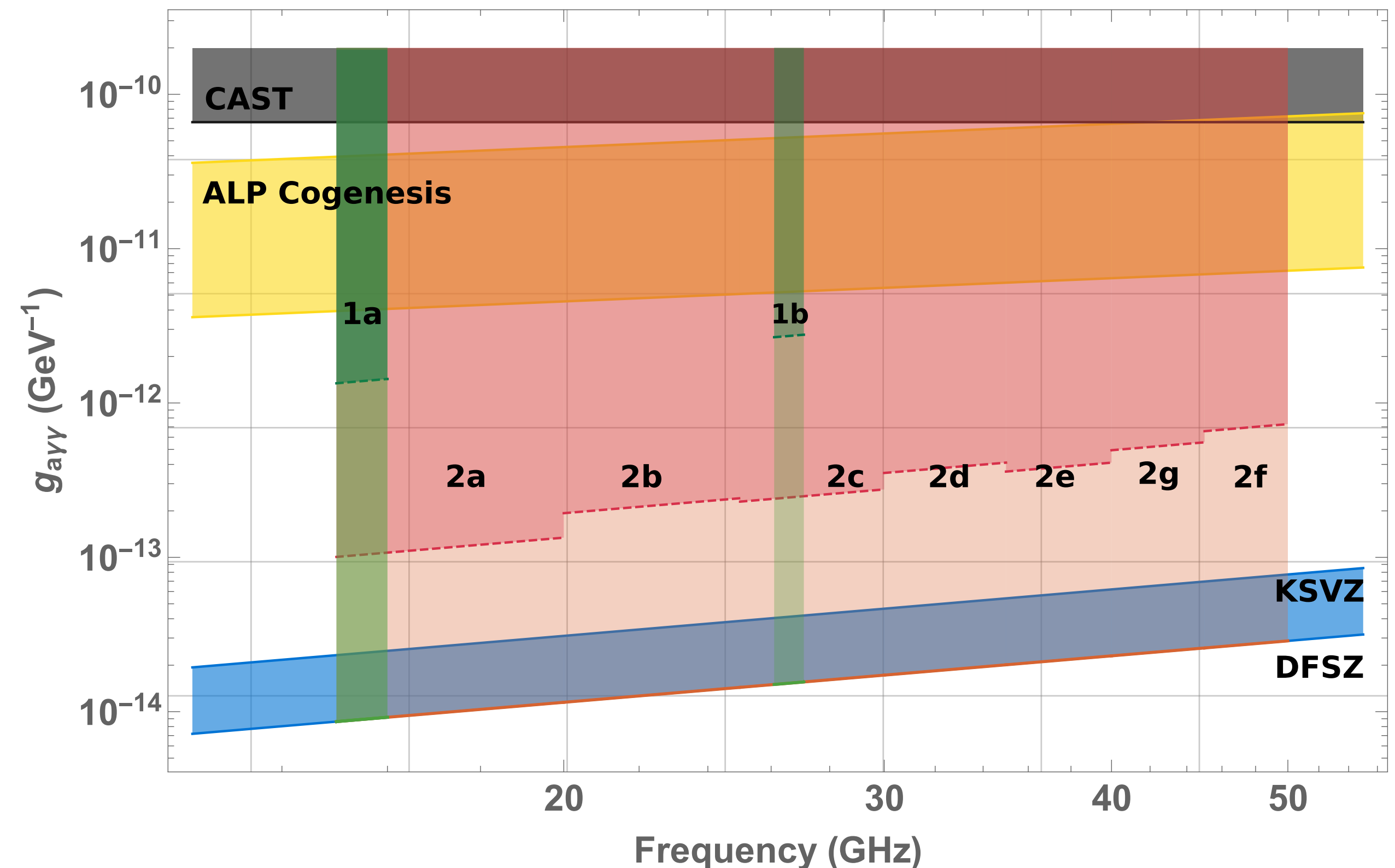
^aLeinweber Center for Theoretical Physics, Department of Physics, University of Michigan, Ann Arbor, MI 48109, U.S.A.

^bDepartment of Physics, University of California, Berkeley, CA 94720, U.S.A.

^cTheoretical Physics Group, Lawrence Berkeley National Laboratory, Berkeley, California 94720, U.S.A.

^dSchool of Natural Sciences, Institute for Advanced Study, Princeton, NJ 08540, U.S.A.

E-mail: rtco@umich.edu, ljhall@lbl.gov, keisukeharigaya@ias.edu



ORGAN Run Plan

- Phase 1: Narrow searches around 15-16 GHz and 26-27 GHz
- Runs 1a/1b (dark green): HEMT-based amplifiers and TM_{010} tuning rod resonators, form factor of 0.4.
- Phase 2: Wider searches (15-50GHz) building on expertise gained in Phase 1
- Phase 2, dark red: Quantum limited linear amplifiers (2-4 cavities)
- Light red/green: Single photon counter

Axion Kinetic Misalignment Mechanism

Raymond T. Co,¹ Lawrence J. Hall,^{2,3} and Keisuke Harigaya⁴

¹Leinweber Center for Theoretical Physics, University of Michigan, Ann Arbor, Michigan 48109, USA

²Department of Physics, University of California, Berkeley, California 94720, USA

³Theoretical Physics Group, Lawrence Berkeley National Laboratory, Berkeley, California 94720, USA

⁴School of Natural Sciences, Institute for Advanced Study, Princeton, New Jersey 08540, USA

(Received 22 November 2019; revised manuscript received 6 April 2020; accepted 8 June 2020; published 26 June 2020)

In the conventional misalignment mechanism, the axion field has a constant initial field value in the early Universe and later begins to oscillate. We present an alternative scenario where the axion field has a nonzero initial velocity, allowing an axion decay constant much below the conventional prediction from axion dark matter. This axion velocity can be generated from explicit breaking of the axion shift symmetry in the early Universe, which may occur as this symmetry is approximate.

Predictions for axion couplings from ALPogenesis

Raymond T. Co,^a Lawrence J. Hall^{b,c} and Keisuke Harigaya^d

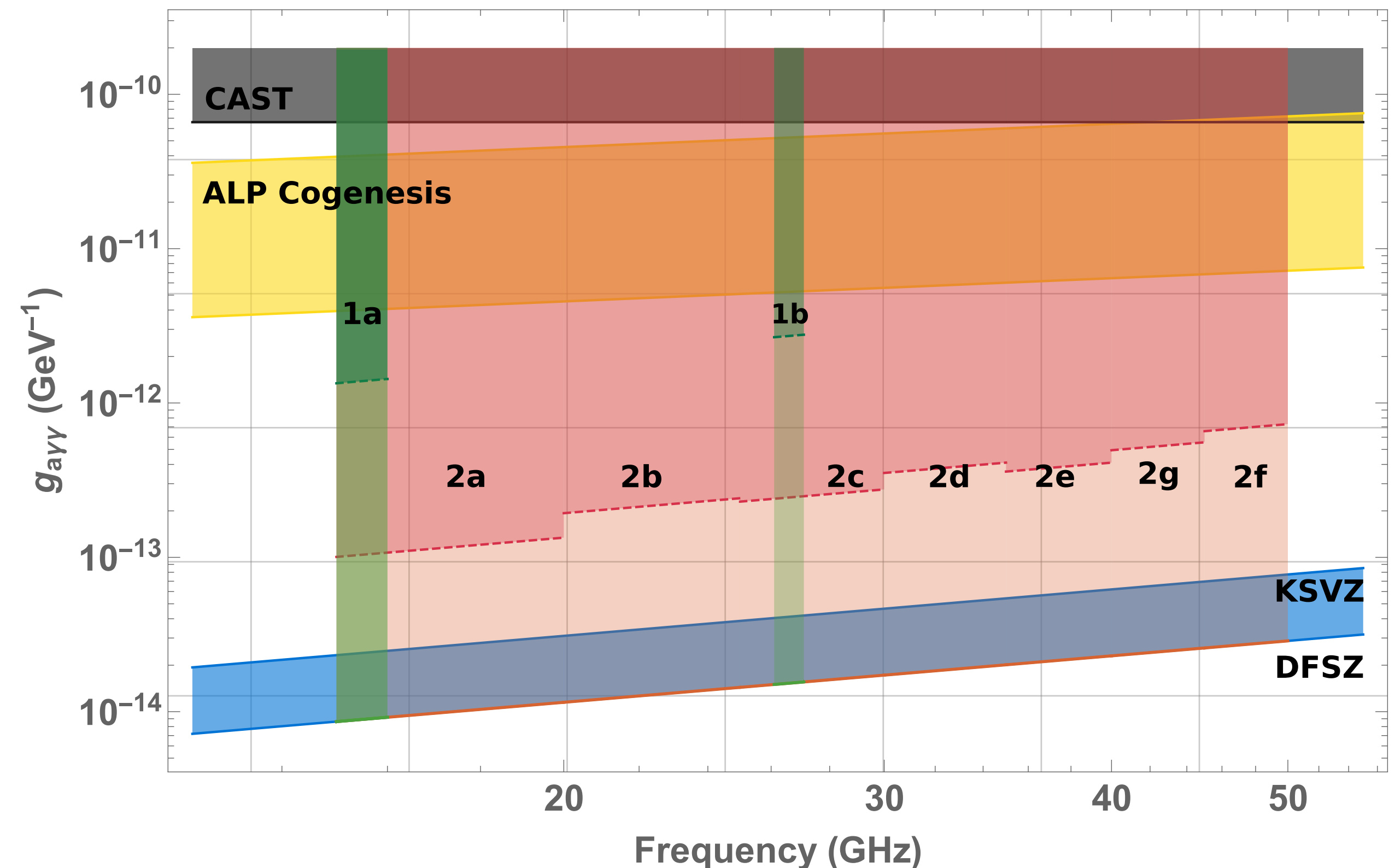
^aLeinweber Center for Theoretical Physics, Department of Physics, University of Michigan, Ann Arbor, MI 48109, U.S.A.

^bDepartment of Physics, University of California, Berkeley, CA 94720, U.S.A.

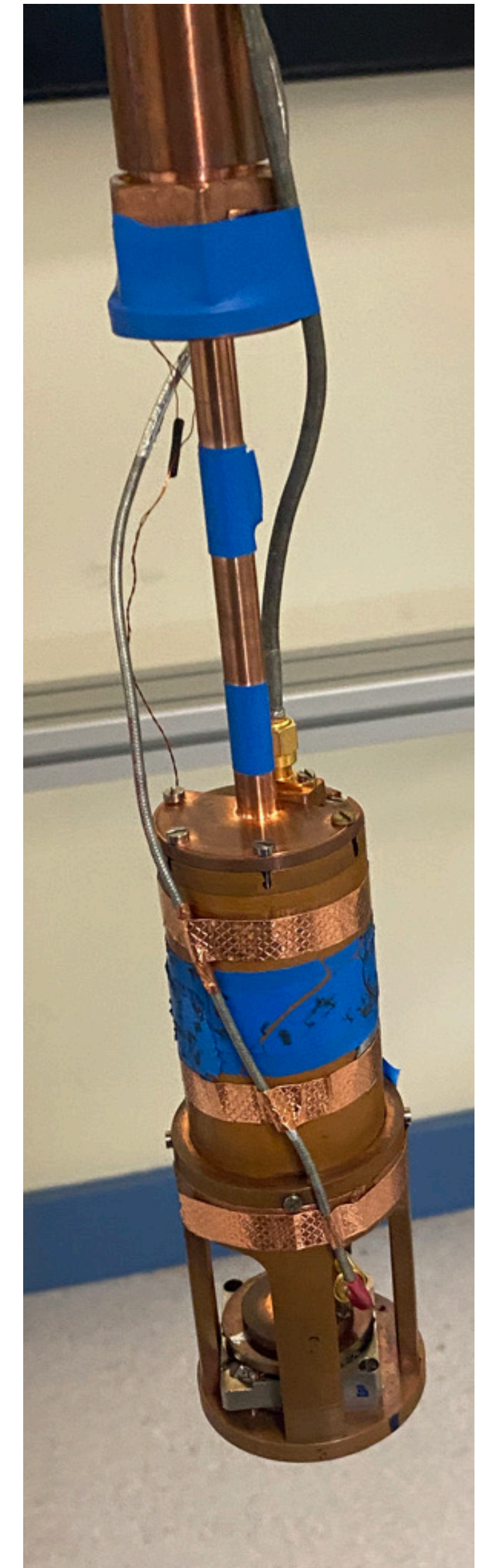
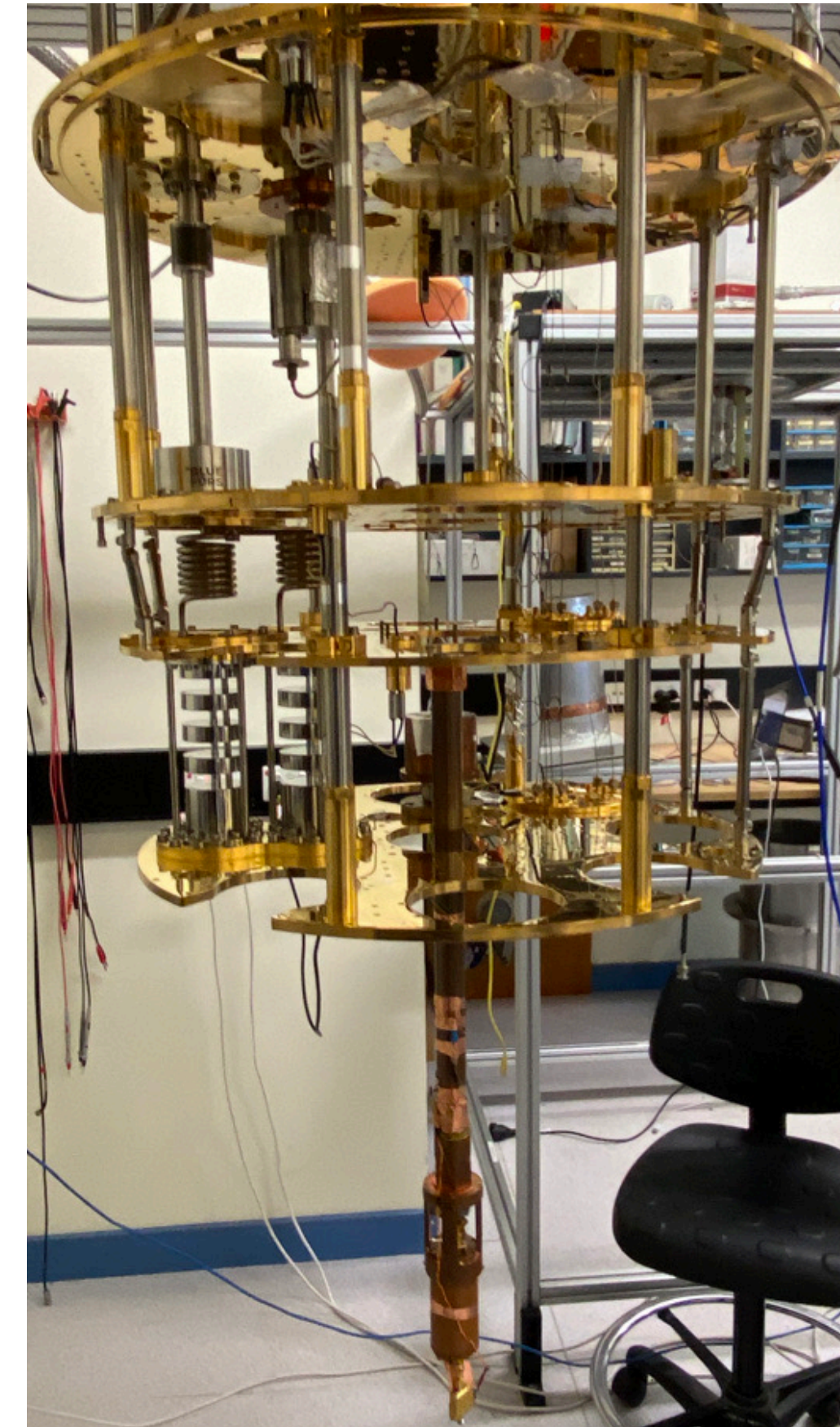
^cTheoretical Physics Group, Lawrence Berkeley National Laboratory, Berkeley, California 94720, U.S.A.

^dSchool of Natural Sciences, Institute for Advanced Study, Princeton, NJ 08540, U.S.A.

E-mail: rtco@umich.edu, ljhall@lbl.gov, keisukeharigaya@ias.edu

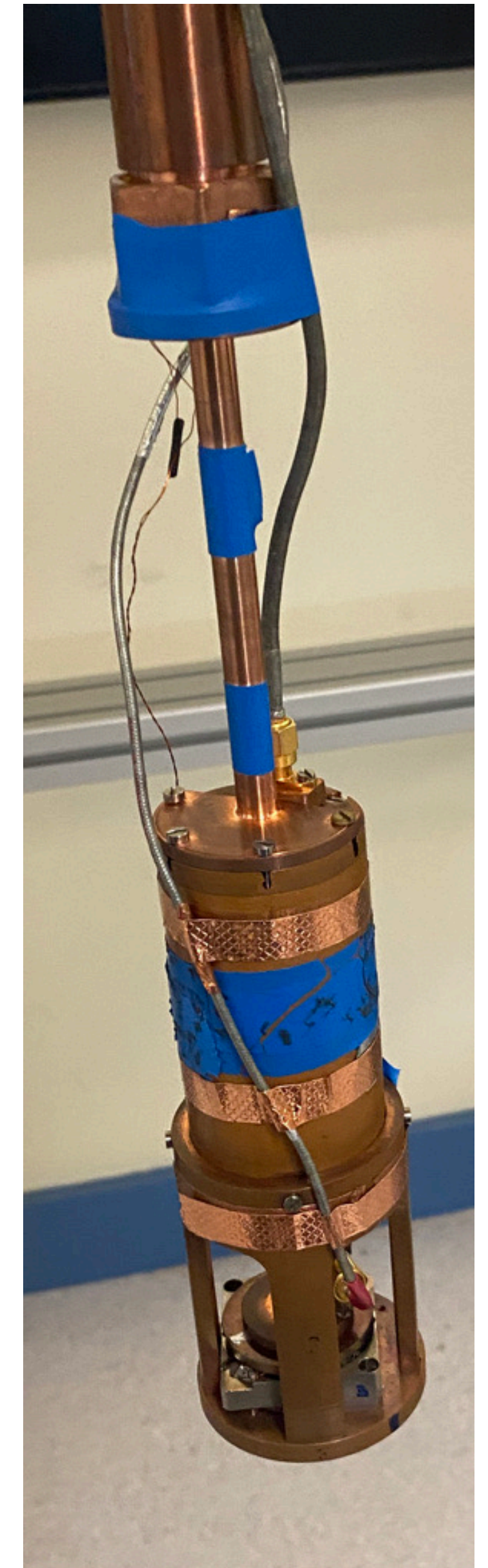
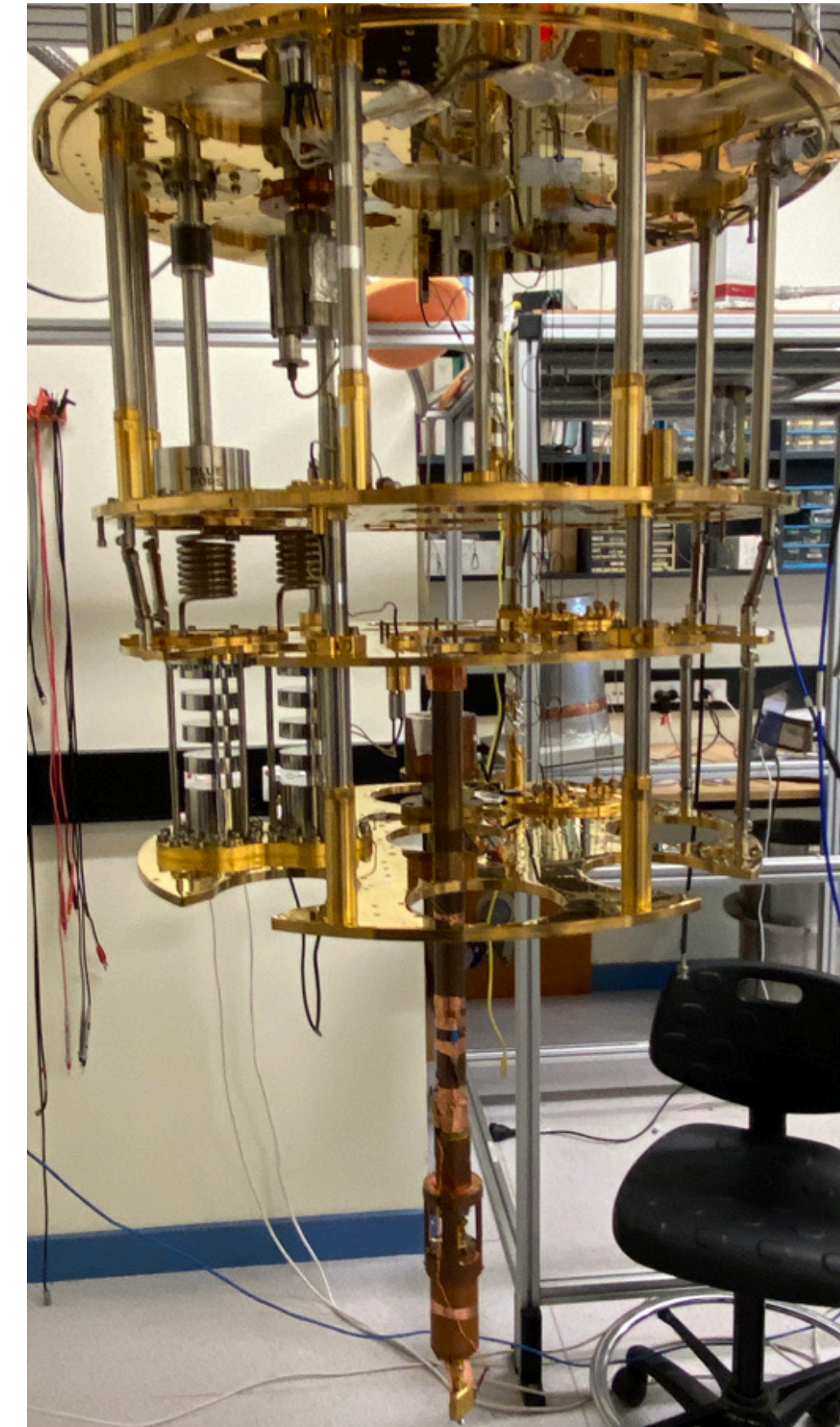


Phase 1a



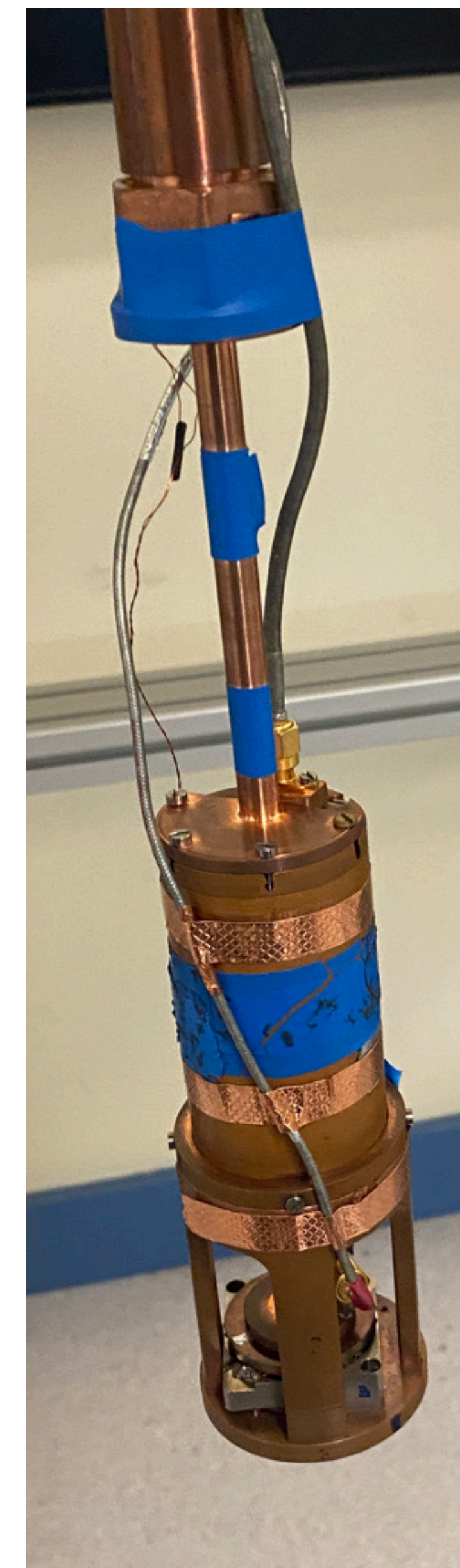
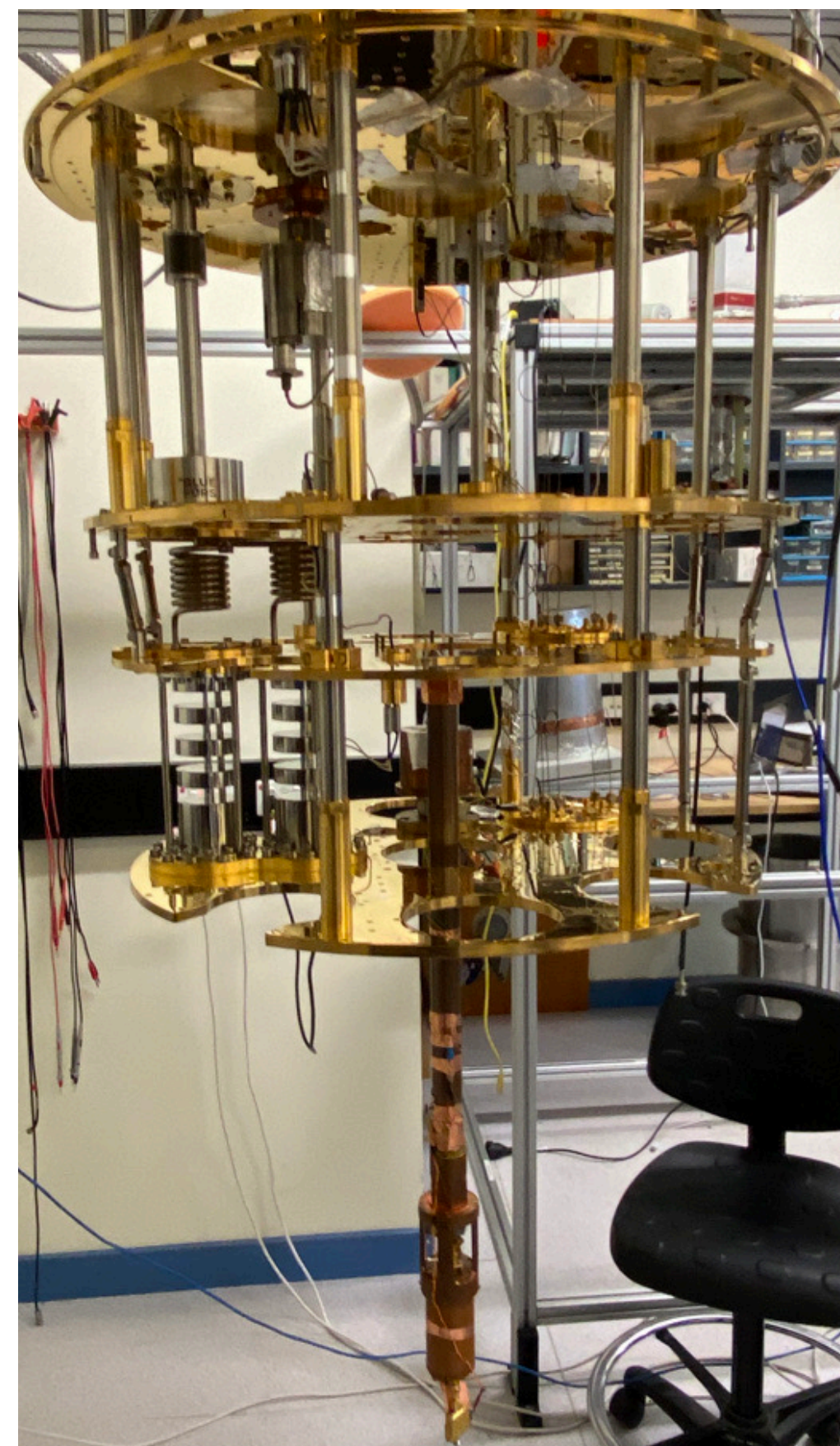
Phase 1a

- Targeting 15.3-16.5 GHz at $\sim 3 \times 10^{-12} g_{\gamma\gamma}$
(ALP co-genesis)



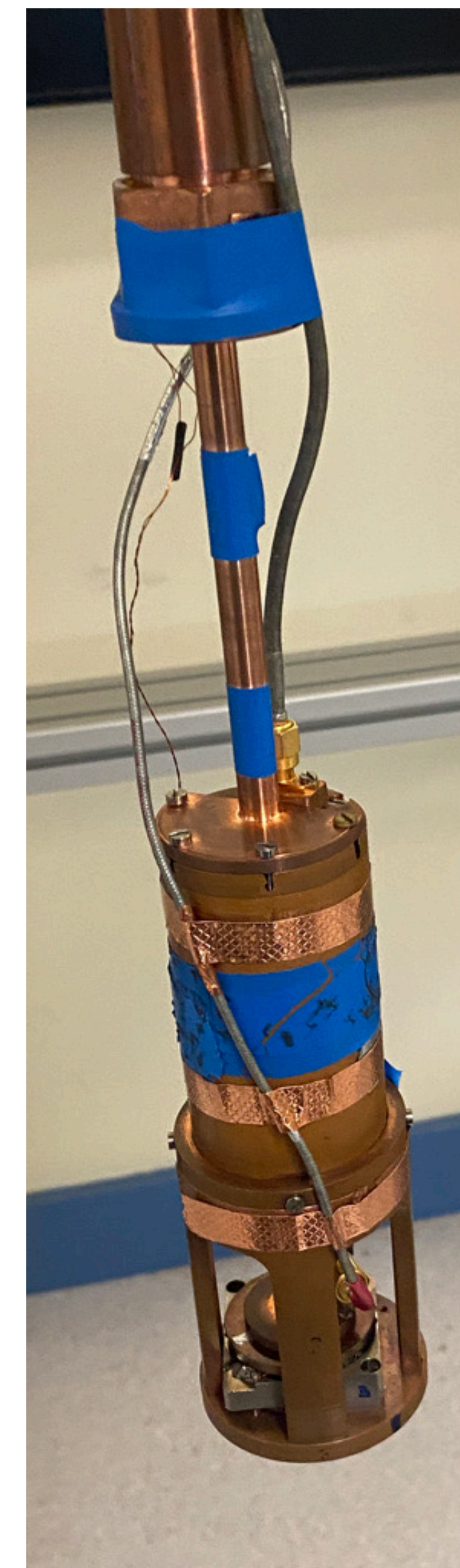
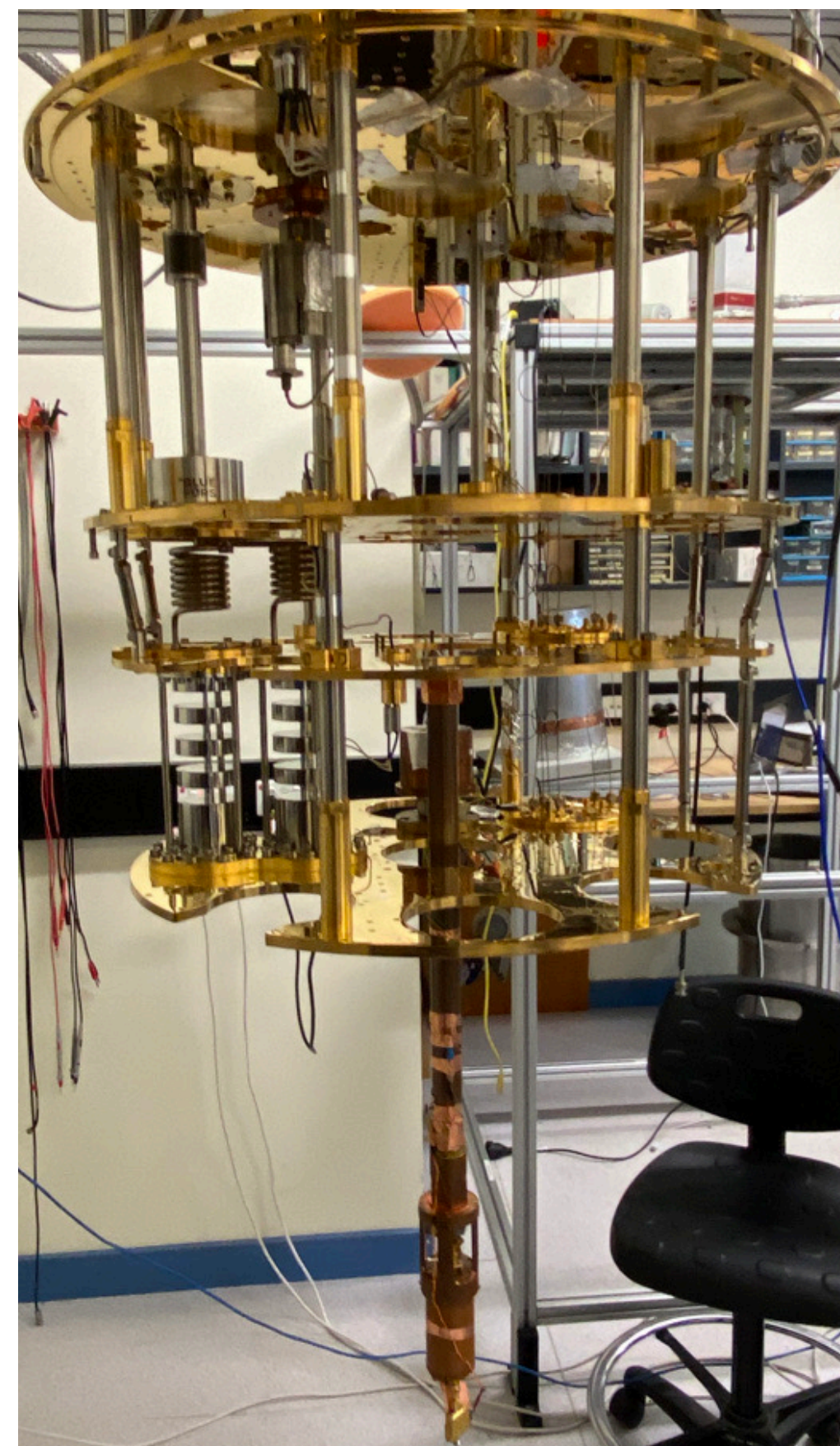
Phase 1a

- Targeting 15.3-16.5 GHz at $\sim 3 \times 10^{-12} g_{a\gamma\gamma}$
(ALP co-genesis)
- Scan rate - How fast we can exclude axions
at a given **mass** and **coupling**



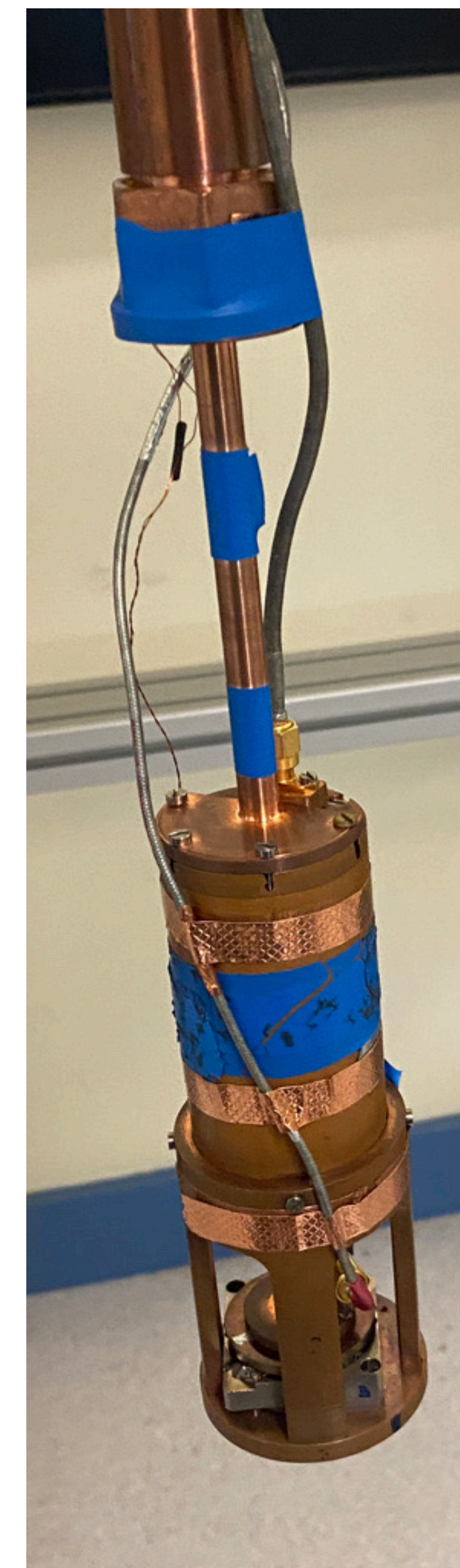
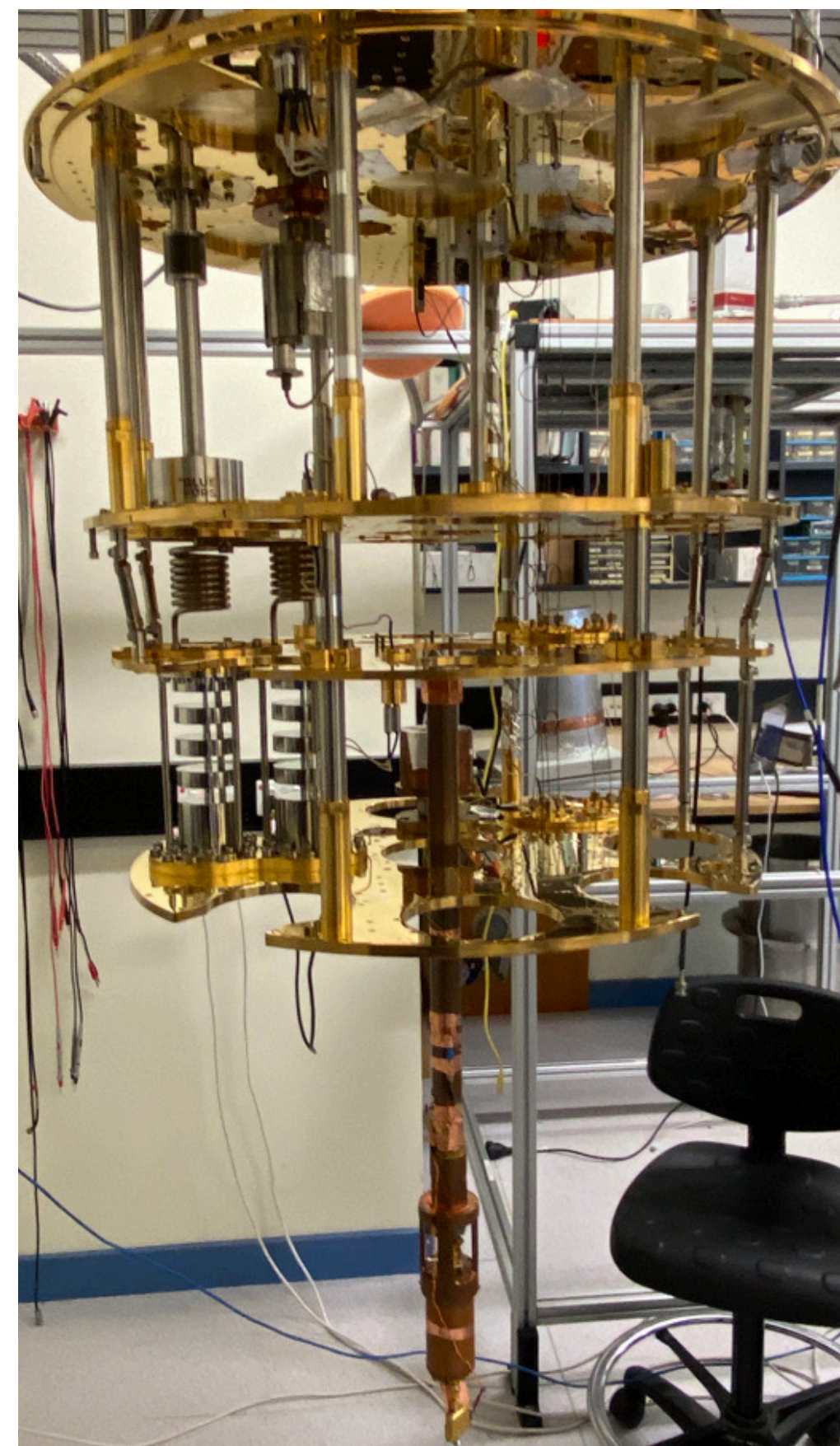
Phase 1a

- Targeting 15.3-16.5 GHz at $\sim 3 \times 10^{-12} g_{a\gamma\gamma}$
(ALP co-genesis)
- Scan rate - How fast we can exclude axions
at a given **mass** and **coupling**
- Scan rate $\propto \omega^{-14/3}$



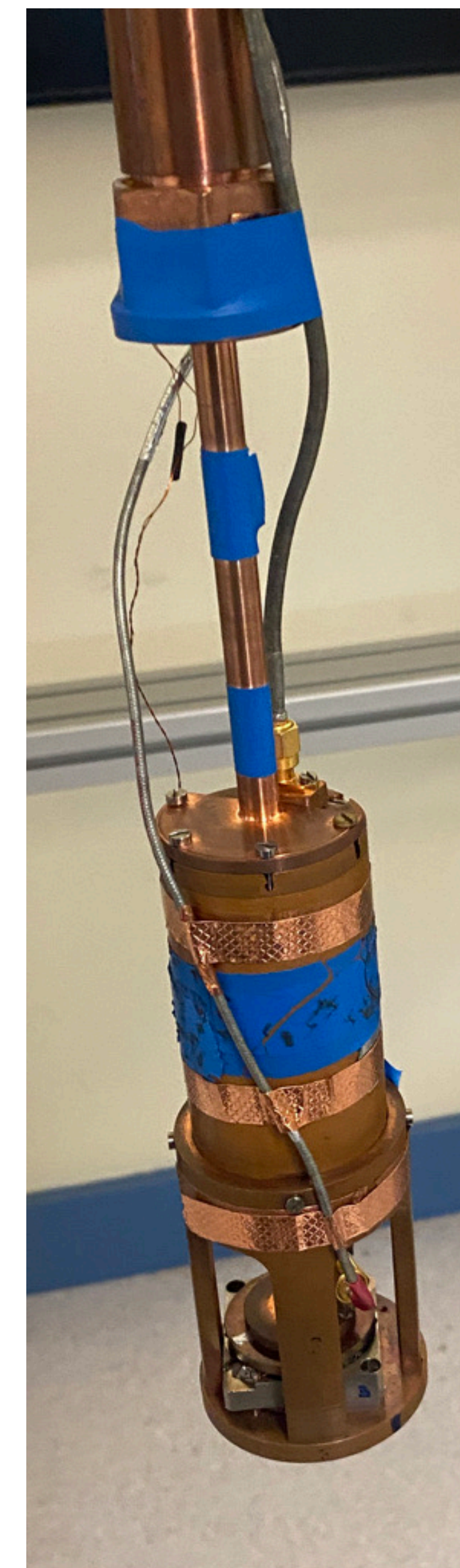
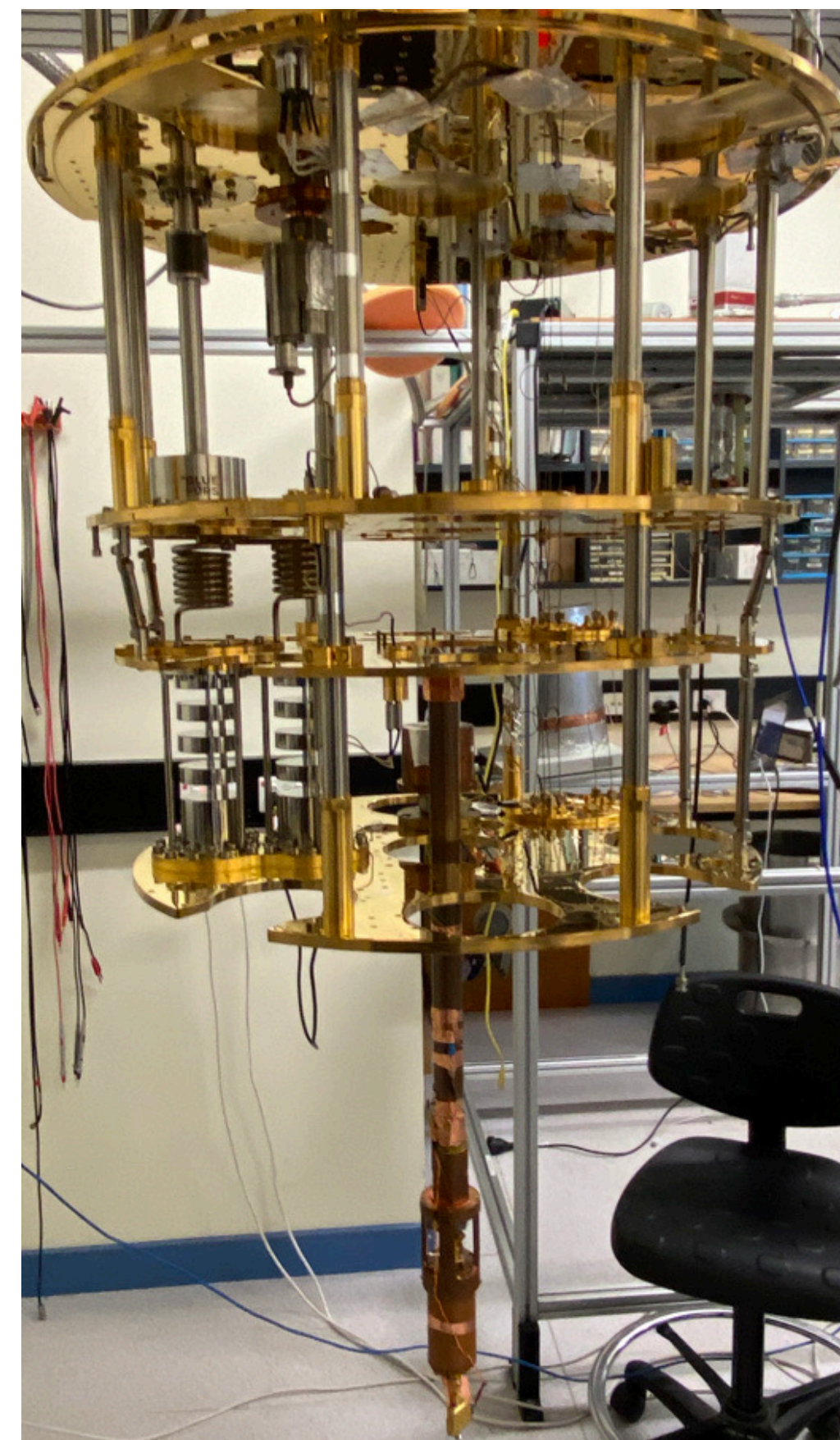
Phase 1a

- Targeting 15.3-16.5 GHz at $\sim 3 \times 10^{-12} g_{a\gamma\gamma}$ (ALP co-genesis)
- Scan rate - How fast we can exclude axions at a given **mass** and **coupling**
- Scan rate $\propto \omega^{-14/3}$
- $\omega \propto R^{-1}$ and $V \propto R^3$ (small cavities)



Phase 1a

- Targeting 15.3-16.5 GHz at $\sim 3 \times 10^{-12} g_{a\gamma\gamma}$ (ALP co-genesis)
- Scan rate - How fast we can exclude axions at a given **mass** and **coupling**
- Scan rate $\propto \omega^{-14/3}$
- $\omega \propto R^{-1}$ and $V \propto R^3$ (small cavities)
- Small cavities = Small machining tolerances



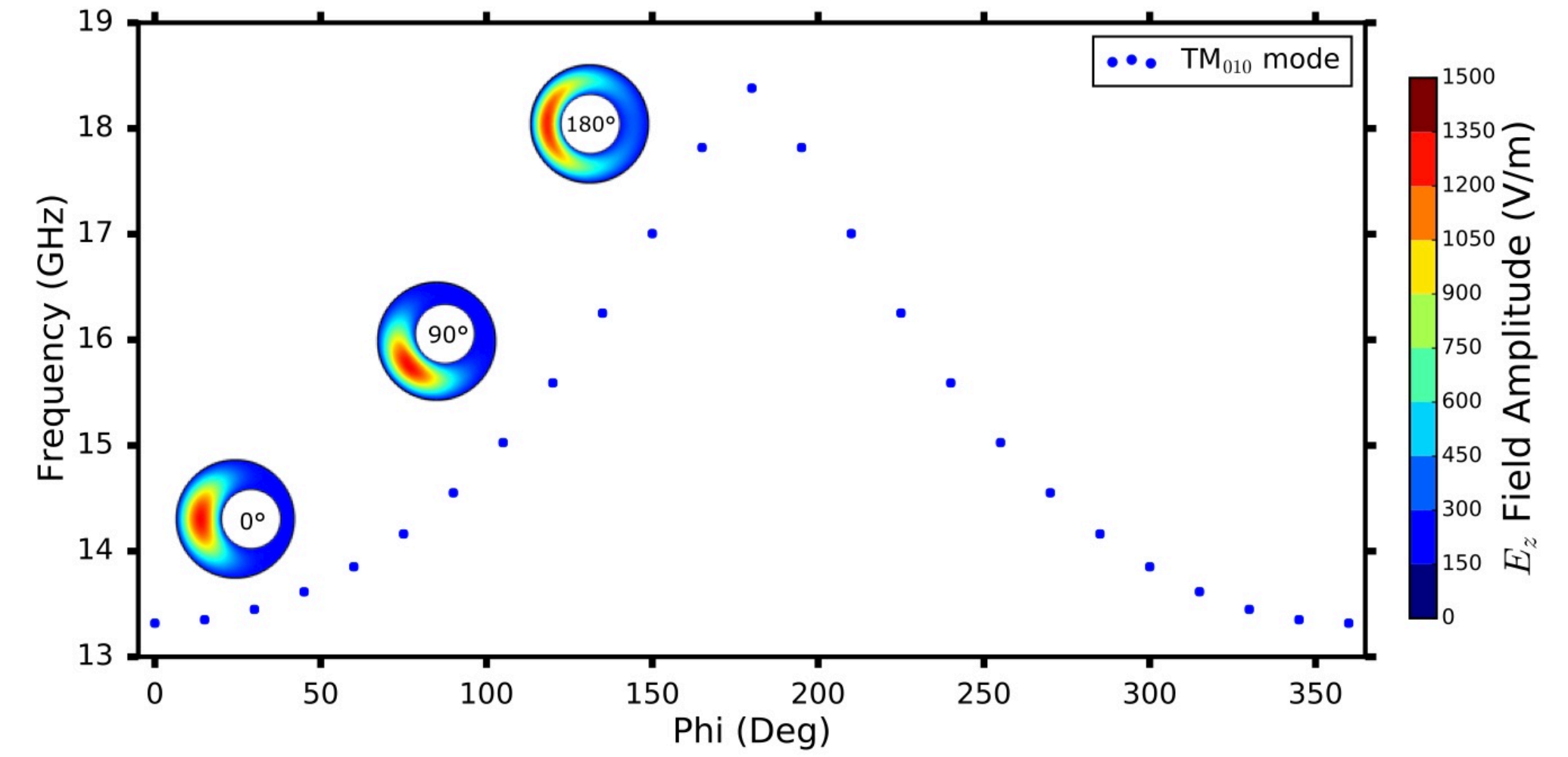
Cavity Characterisation

Cavity Characterisation

- By moving the rod radially the mode is perturbed, shifting the frequency

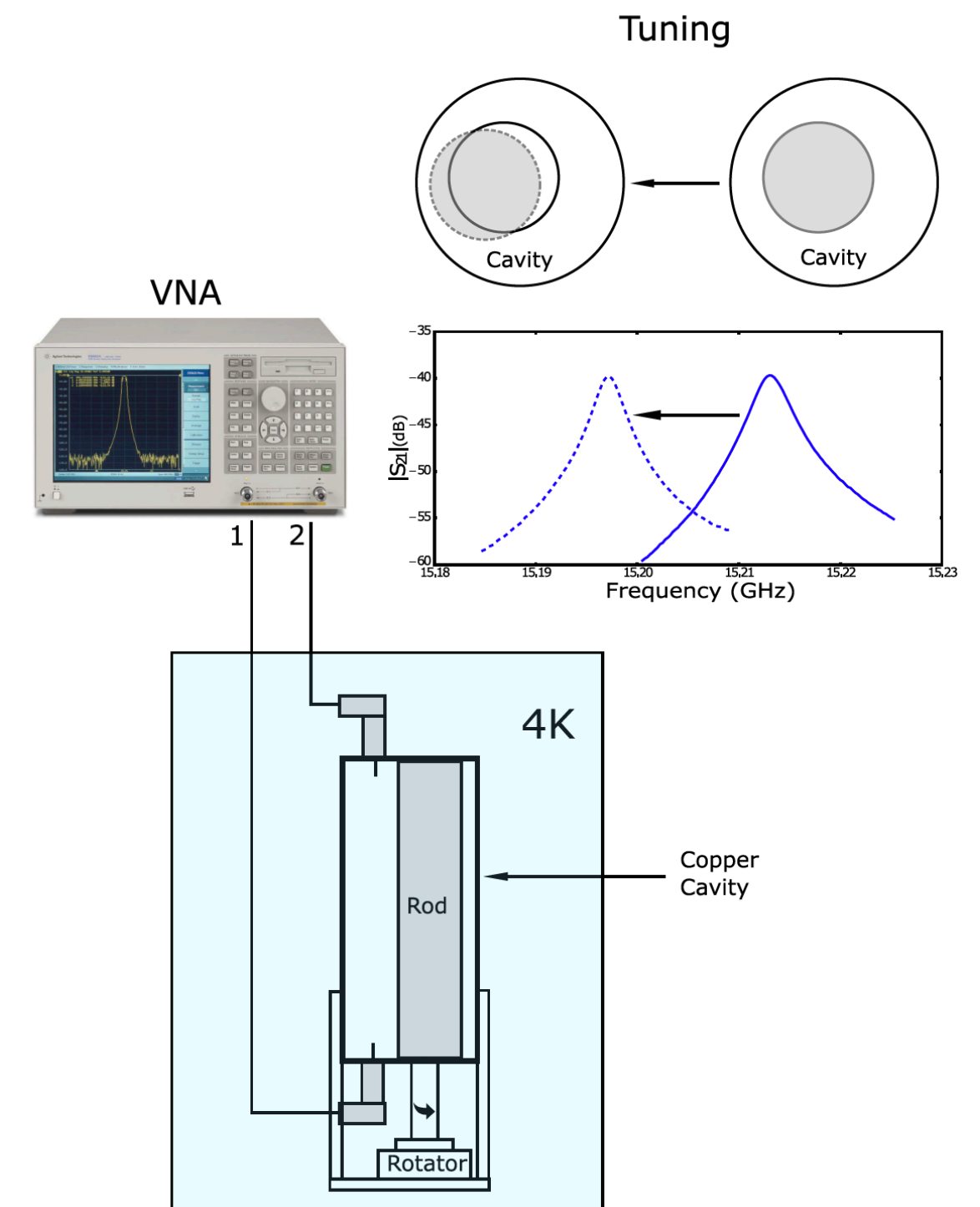
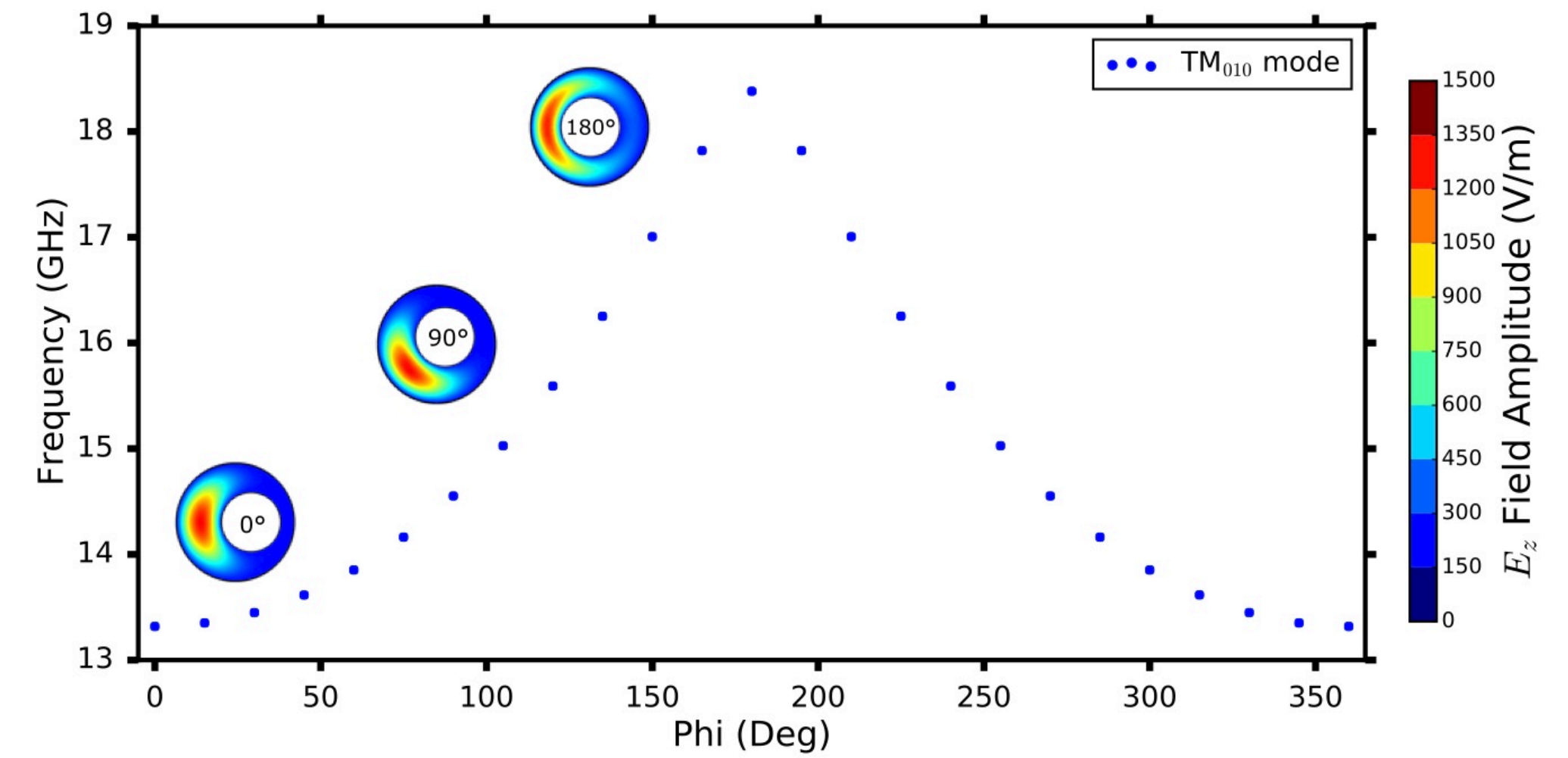
Cavity Characterisation

- By moving the rod radially the mode is perturbed, shifting the frequency



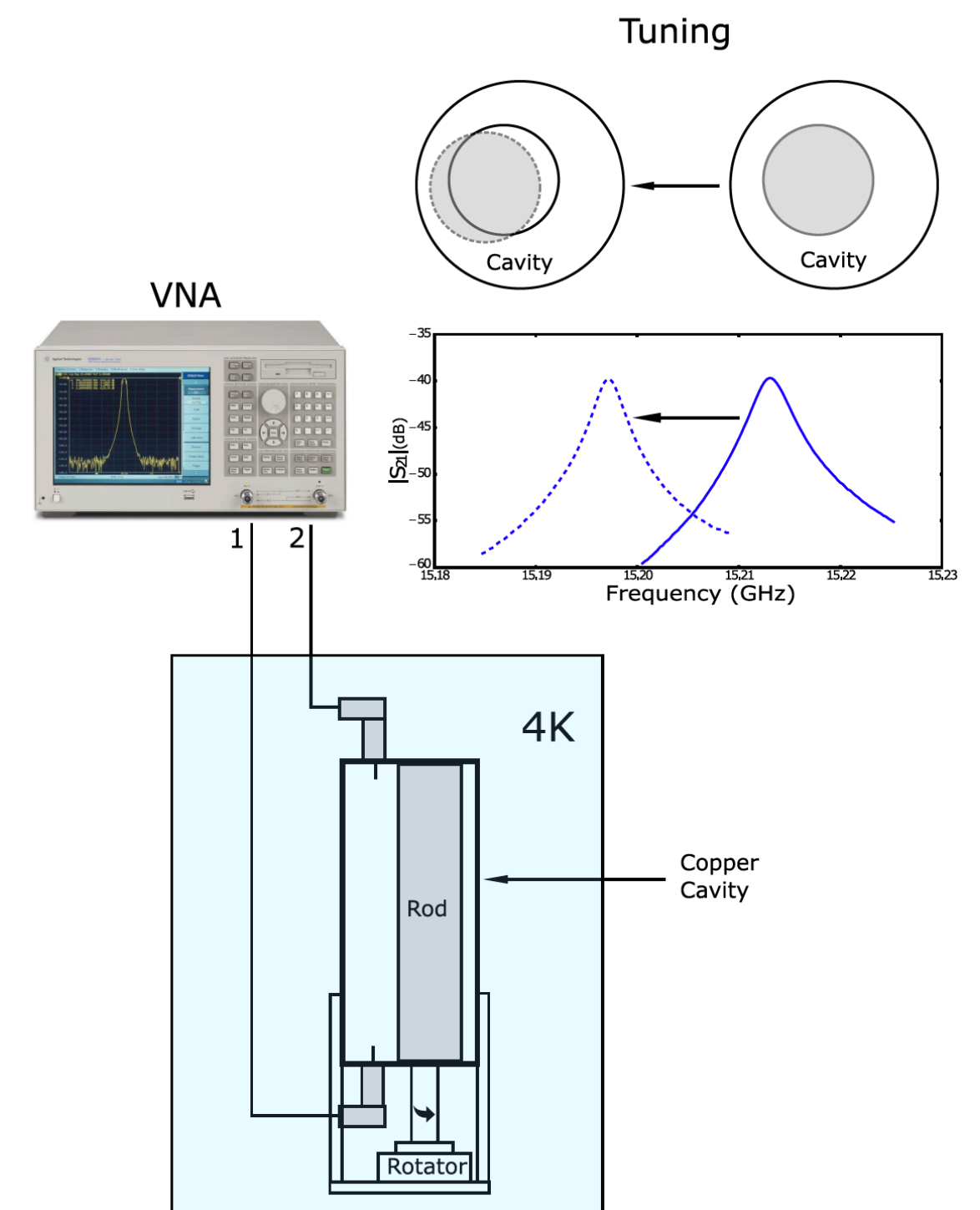
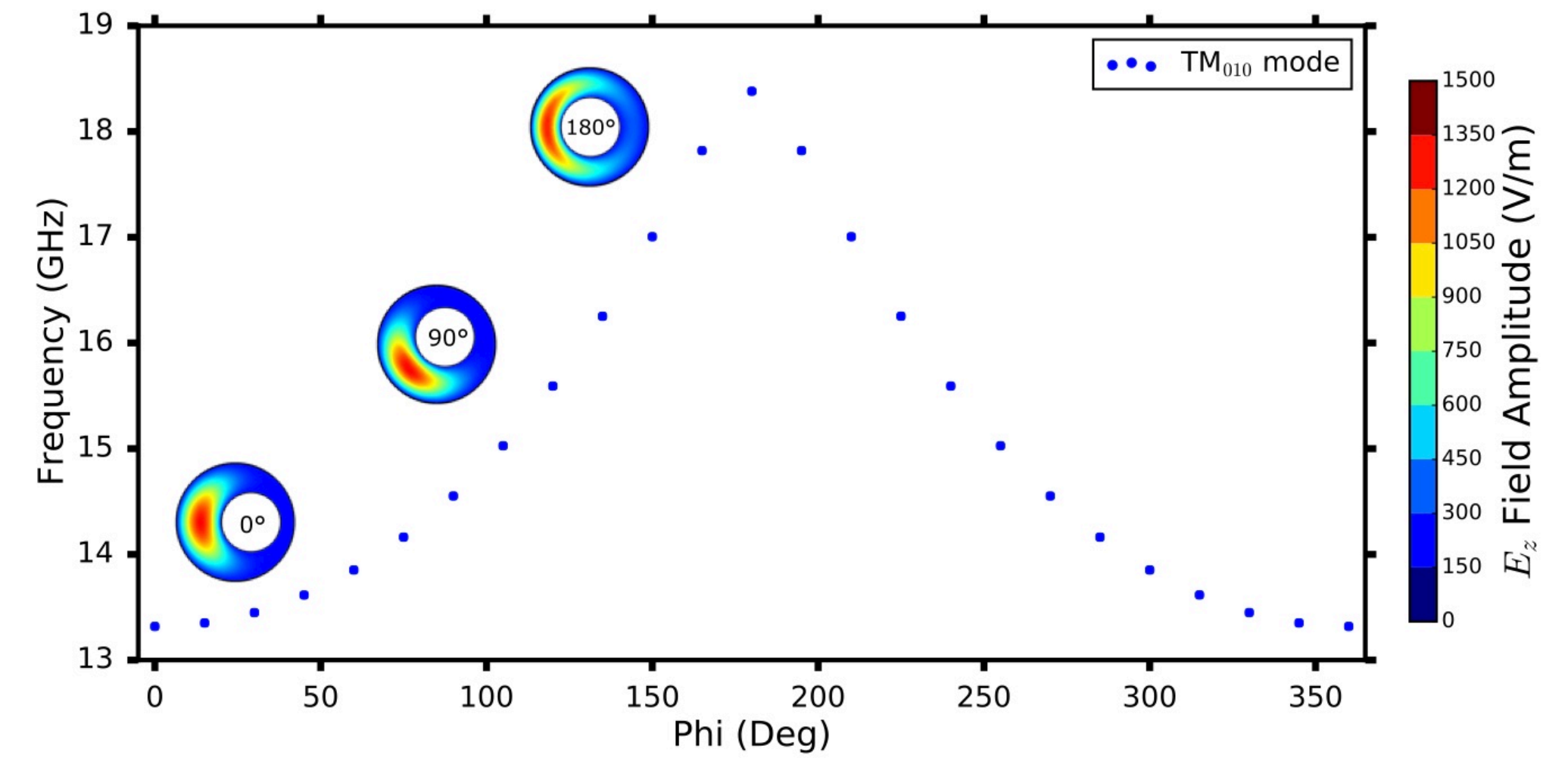
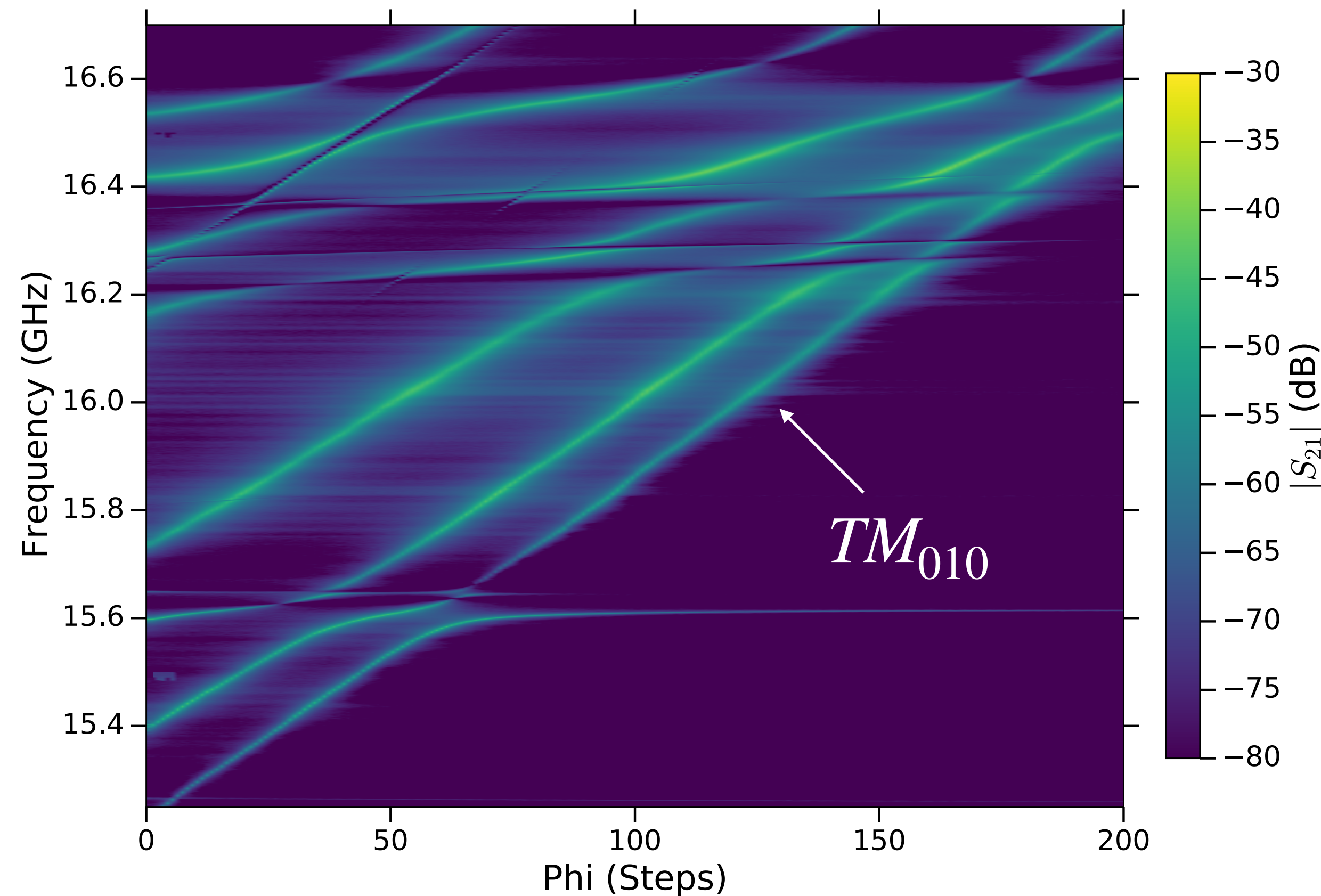
Cavity Characterisation

- By moving the rod radially the mode is perturbed, shifting the frequency



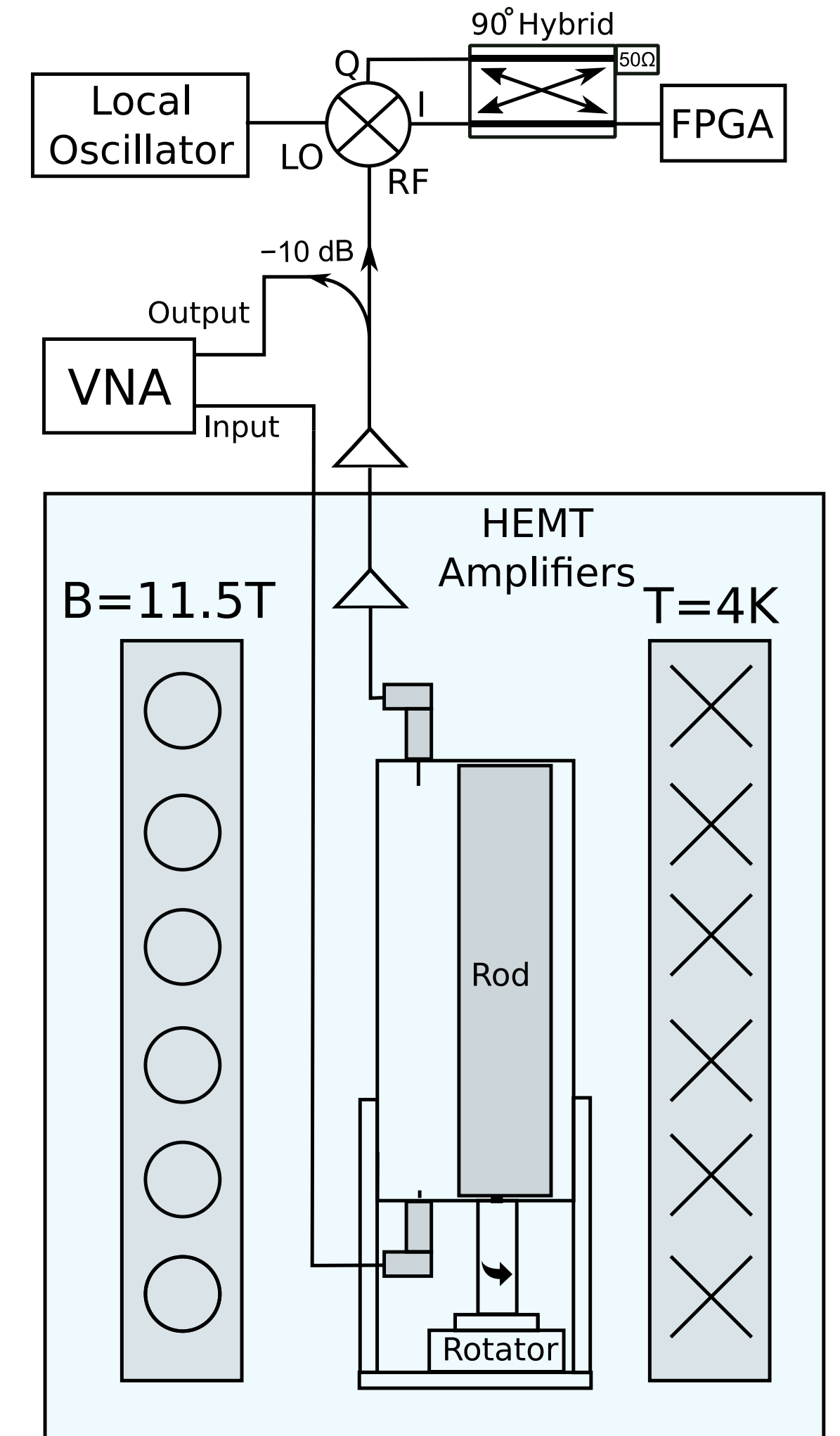
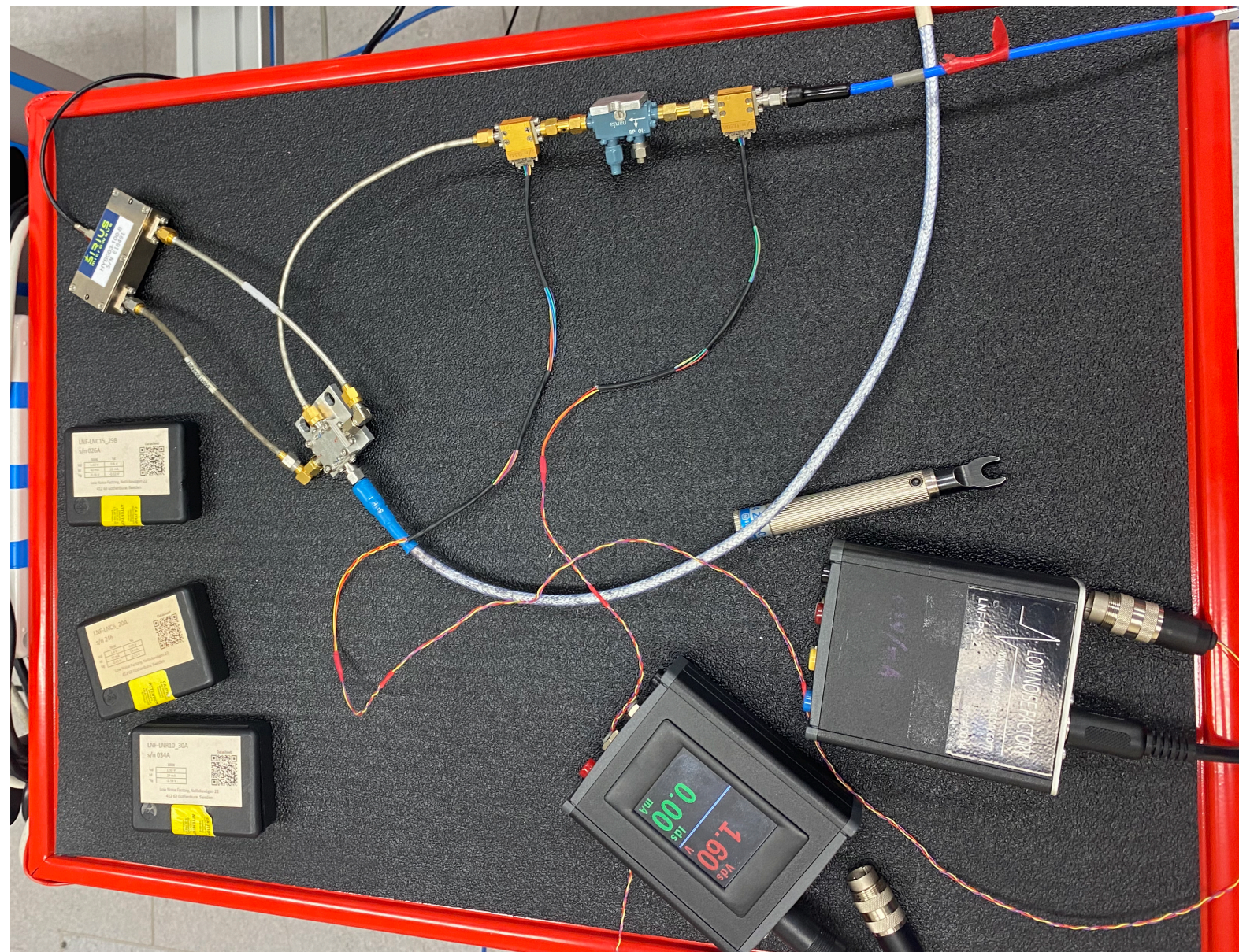
Cavity Characterisation

- By moving the rod radially the mode is perturbed, shifting the frequency



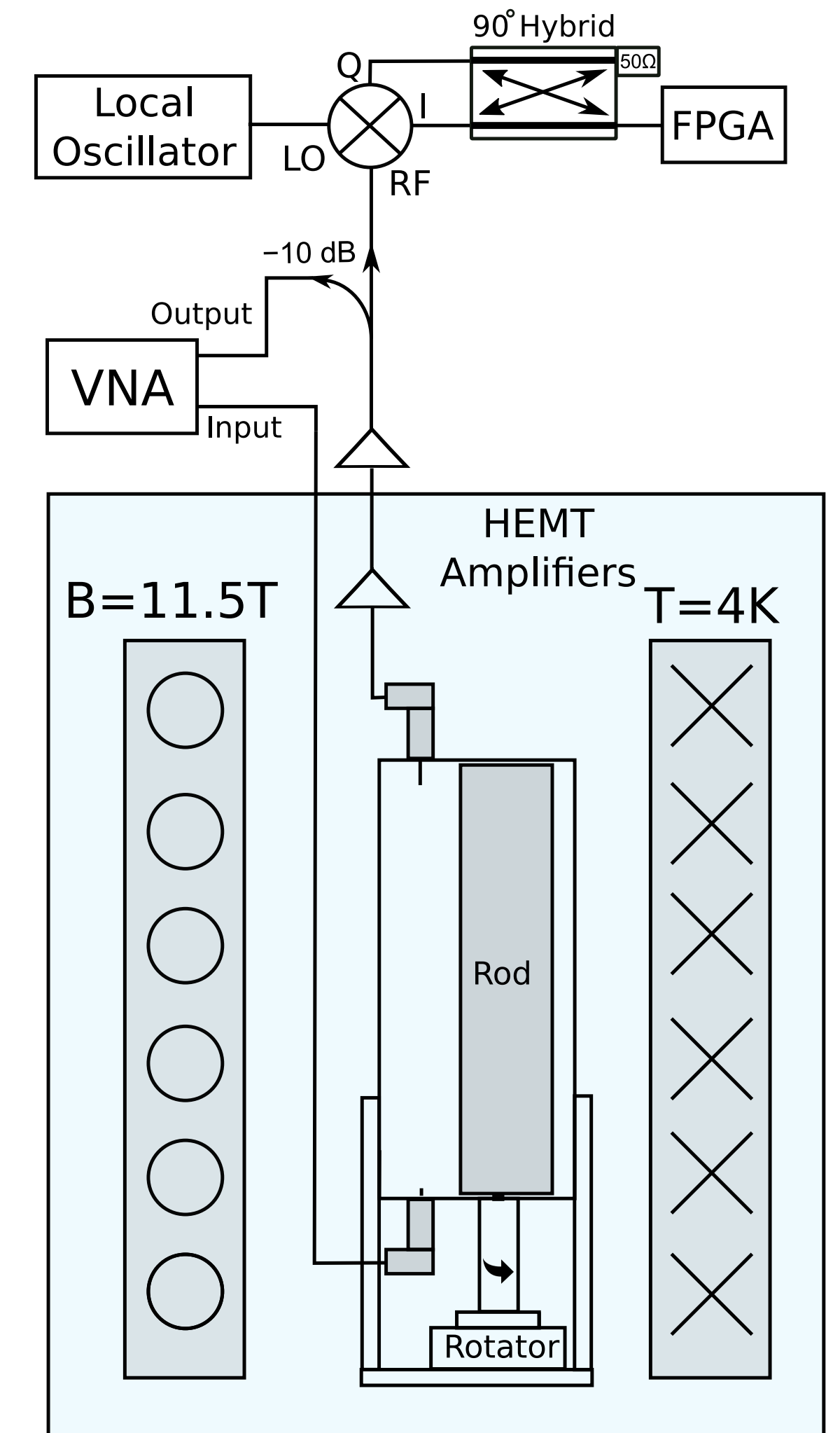
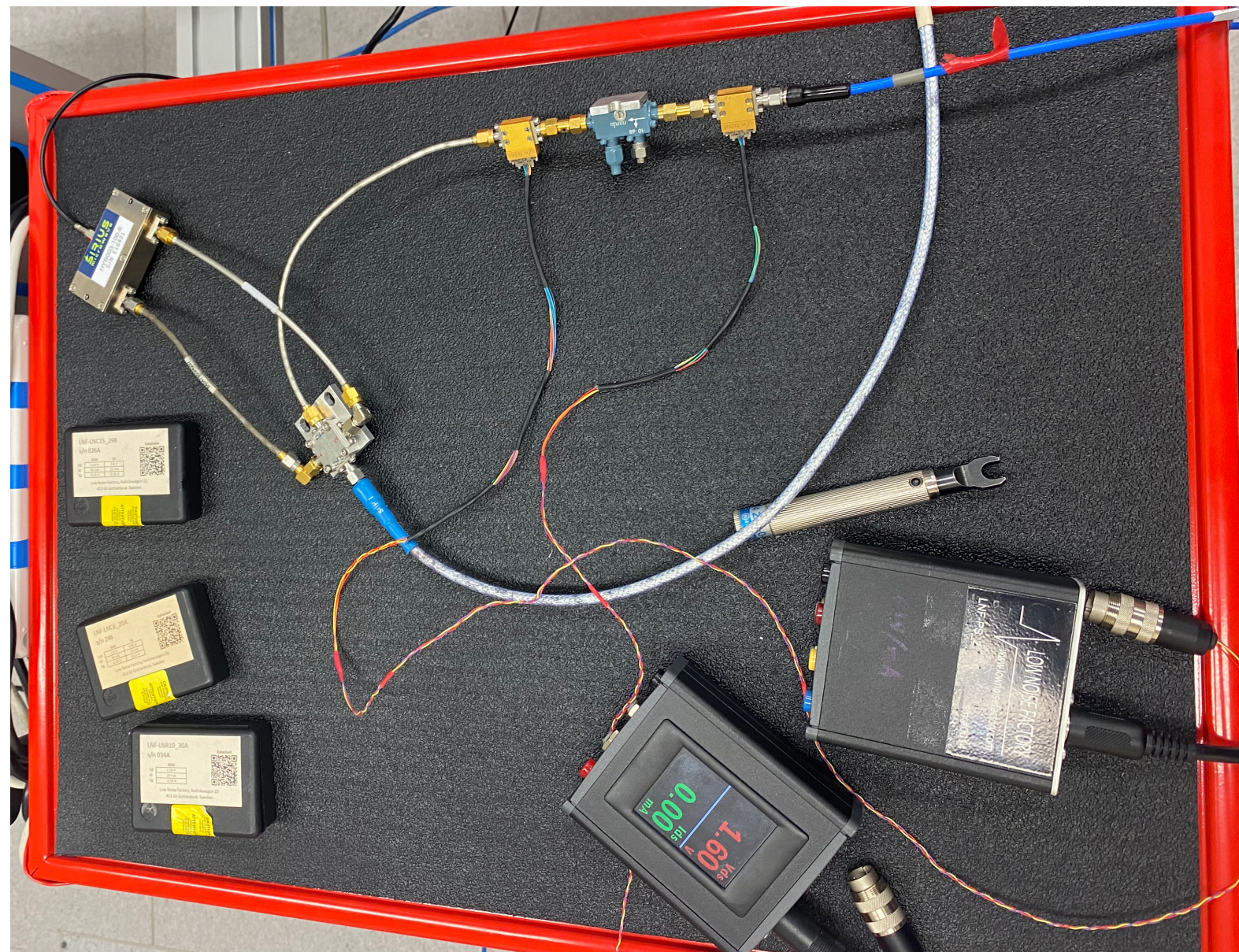
Experimental Setup

- So far we've scanned for ~ 2.5 weeks (~600MHz)



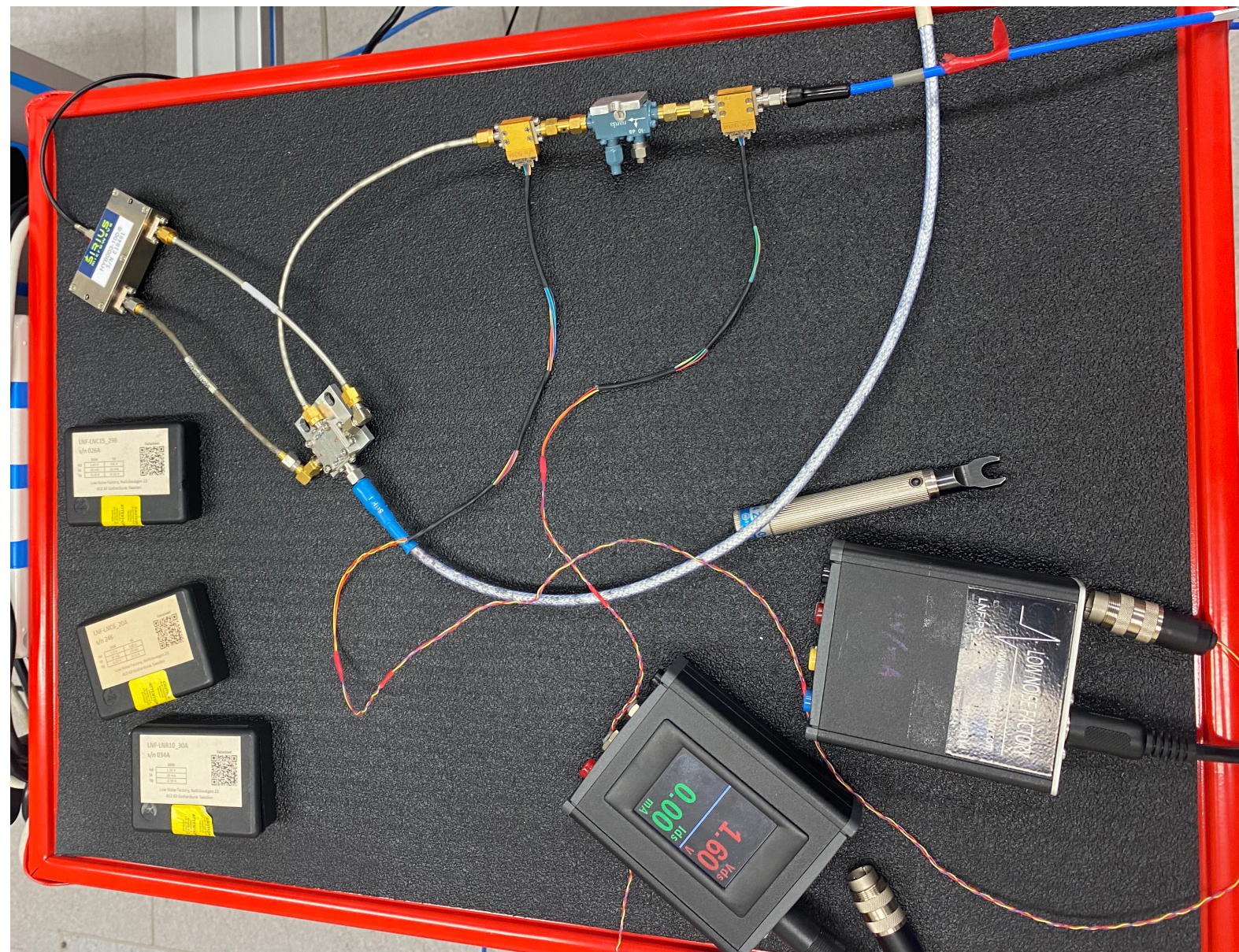
Experimental Setup

- So far we've scanned for ~ 2.5 weeks (~600MHz)
- We use an IQ mixer and hybrid coupler for image rejection of the noisy sideband

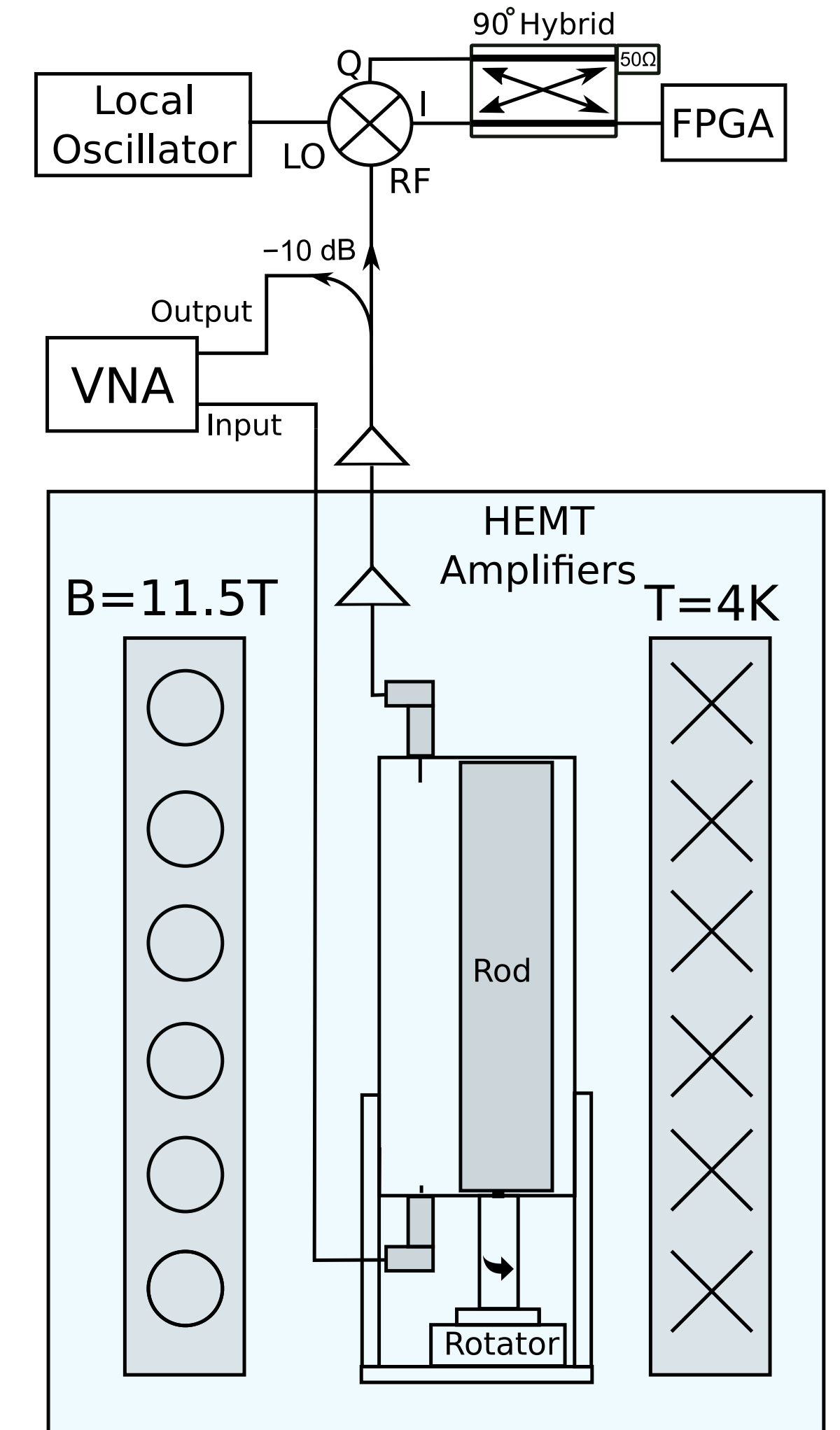


Experimental Setup

- So far we've scanned for ~ 2.5 weeks (~600MHz)
- We use an IQ mixer and hybrid coupler for image rejection of the noisy sideband

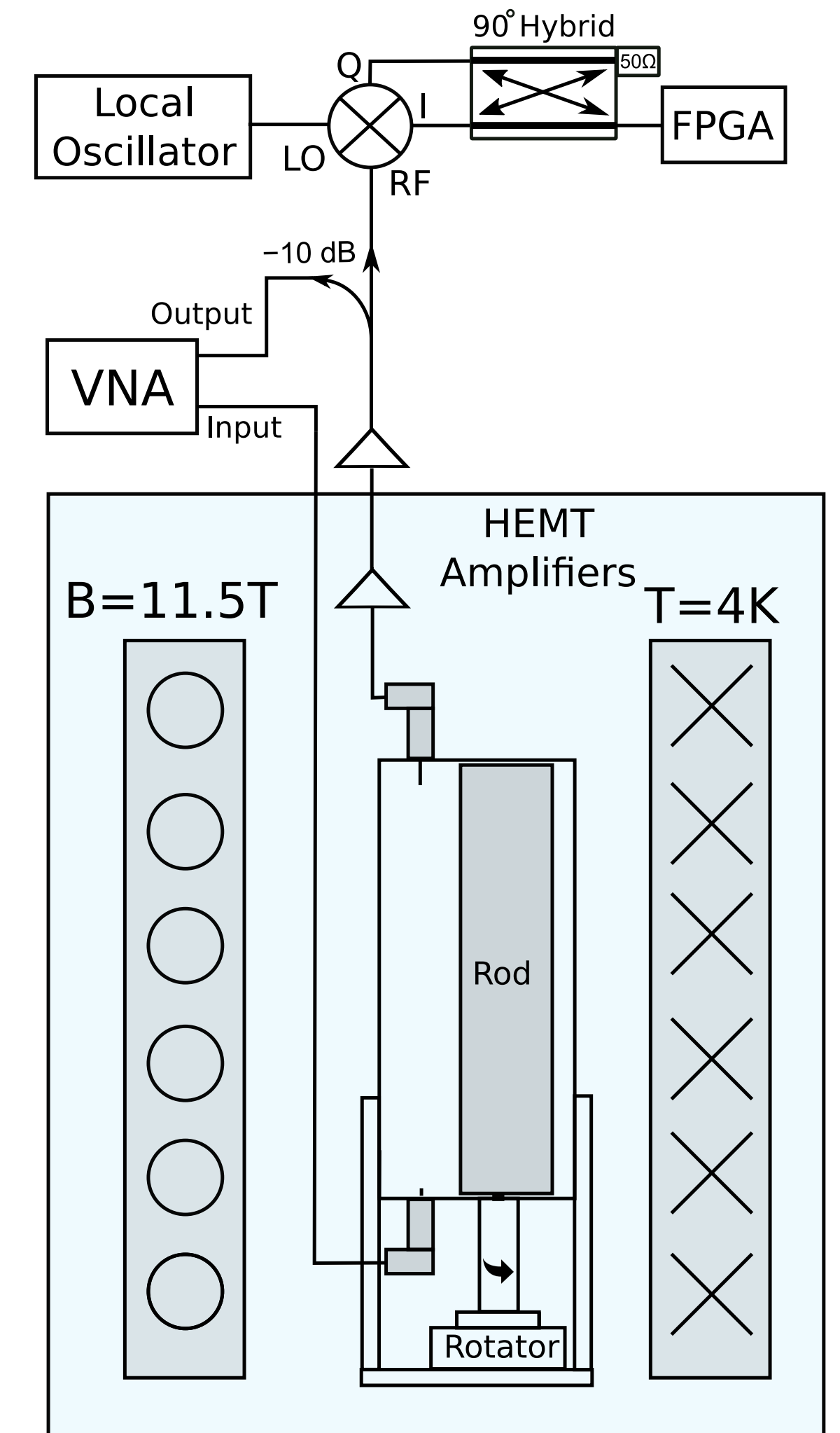
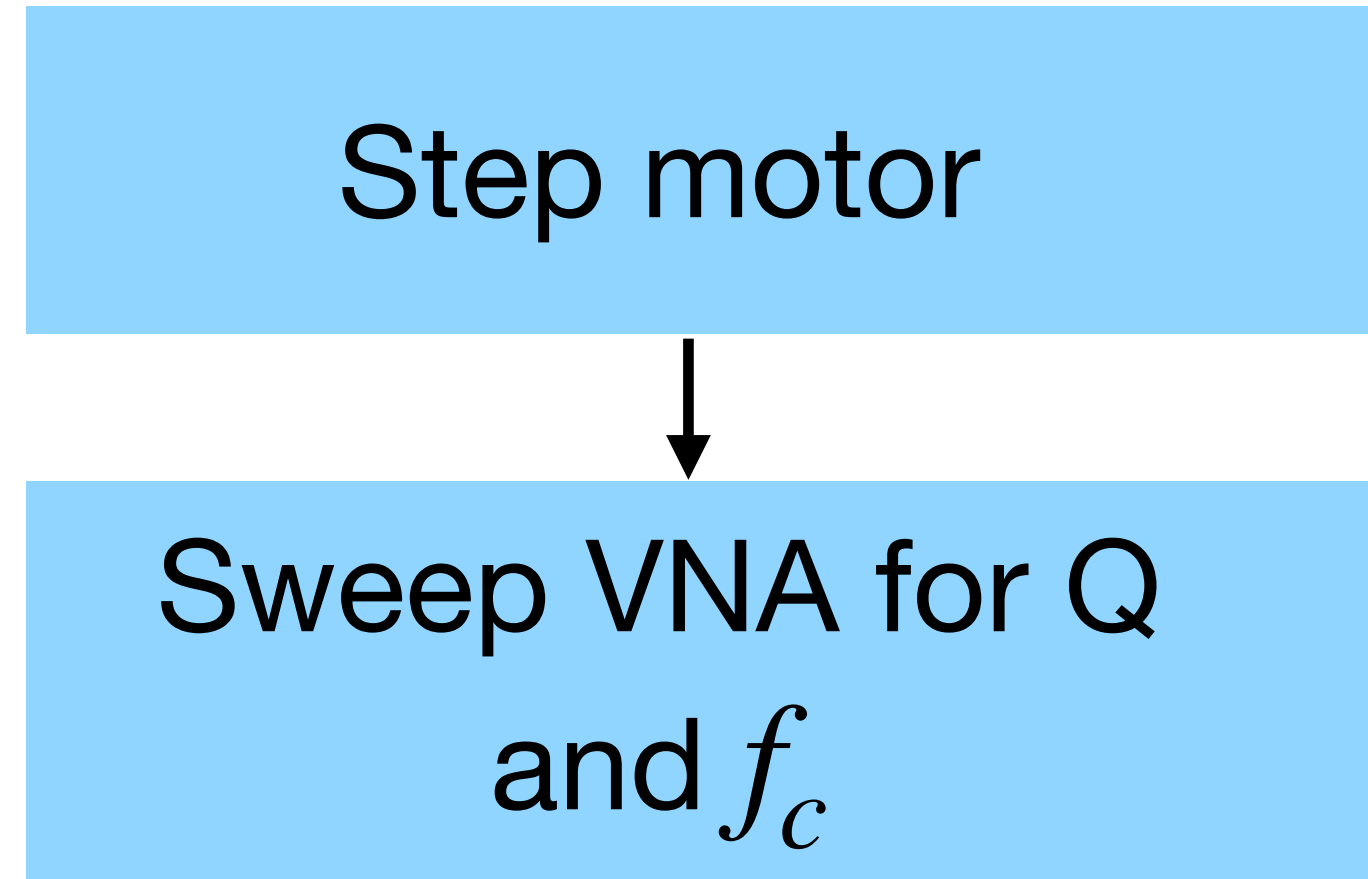
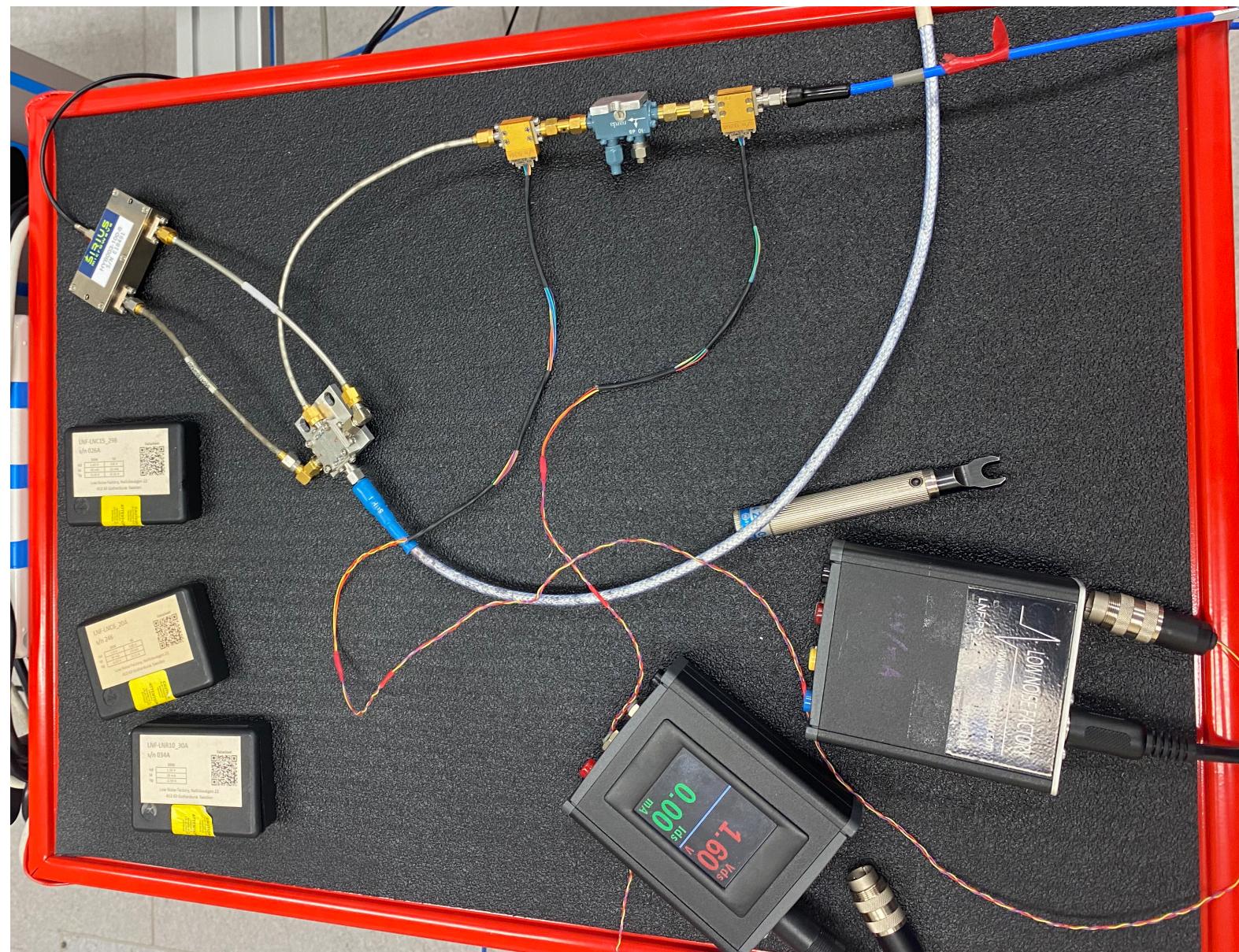


Step motor



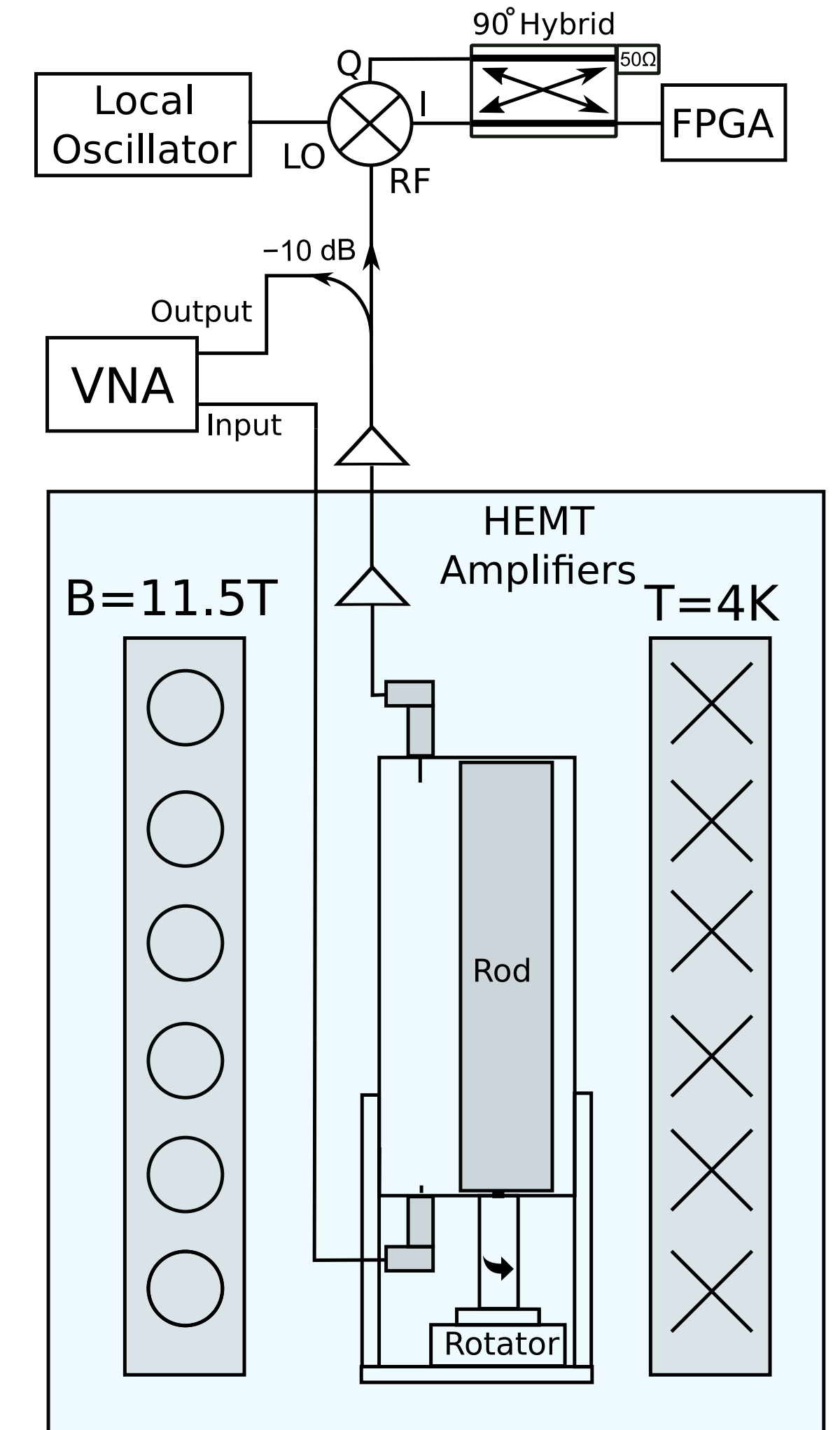
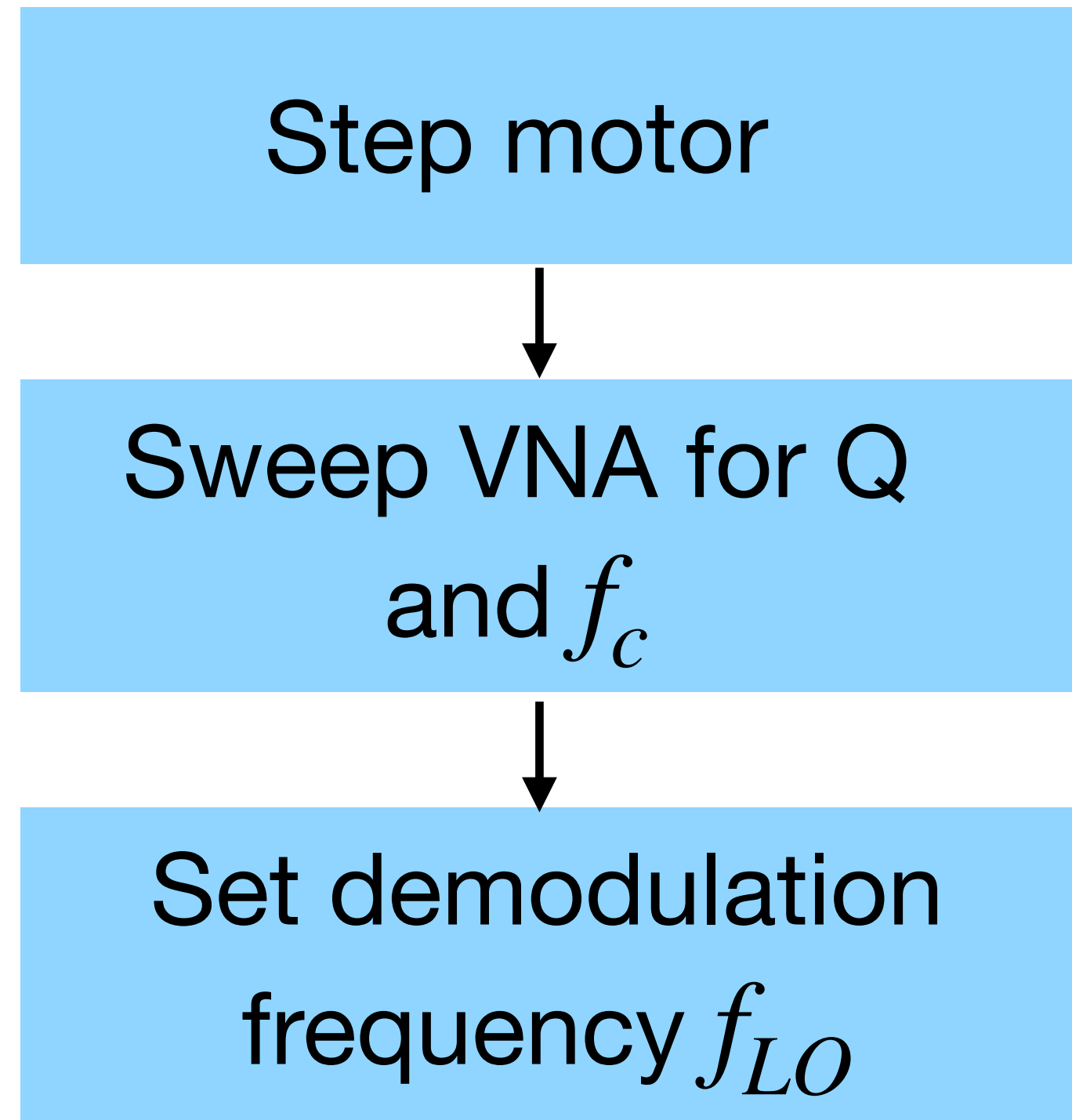
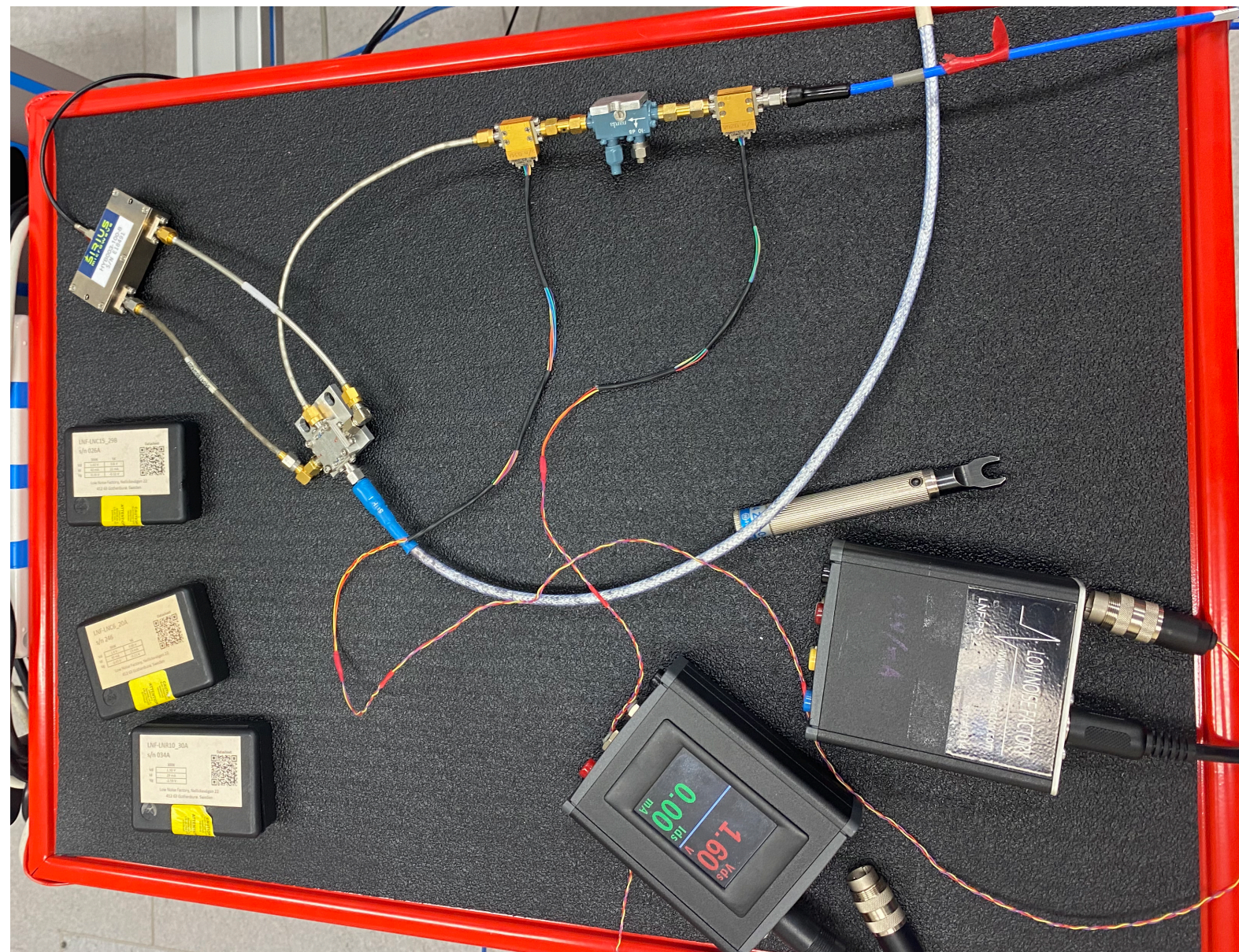
Experimental Setup

- So far we've scanned for ~ 2.5 weeks (~600MHz)
- We use an IQ mixer and hybrid coupler for image rejection of the noisy sideband



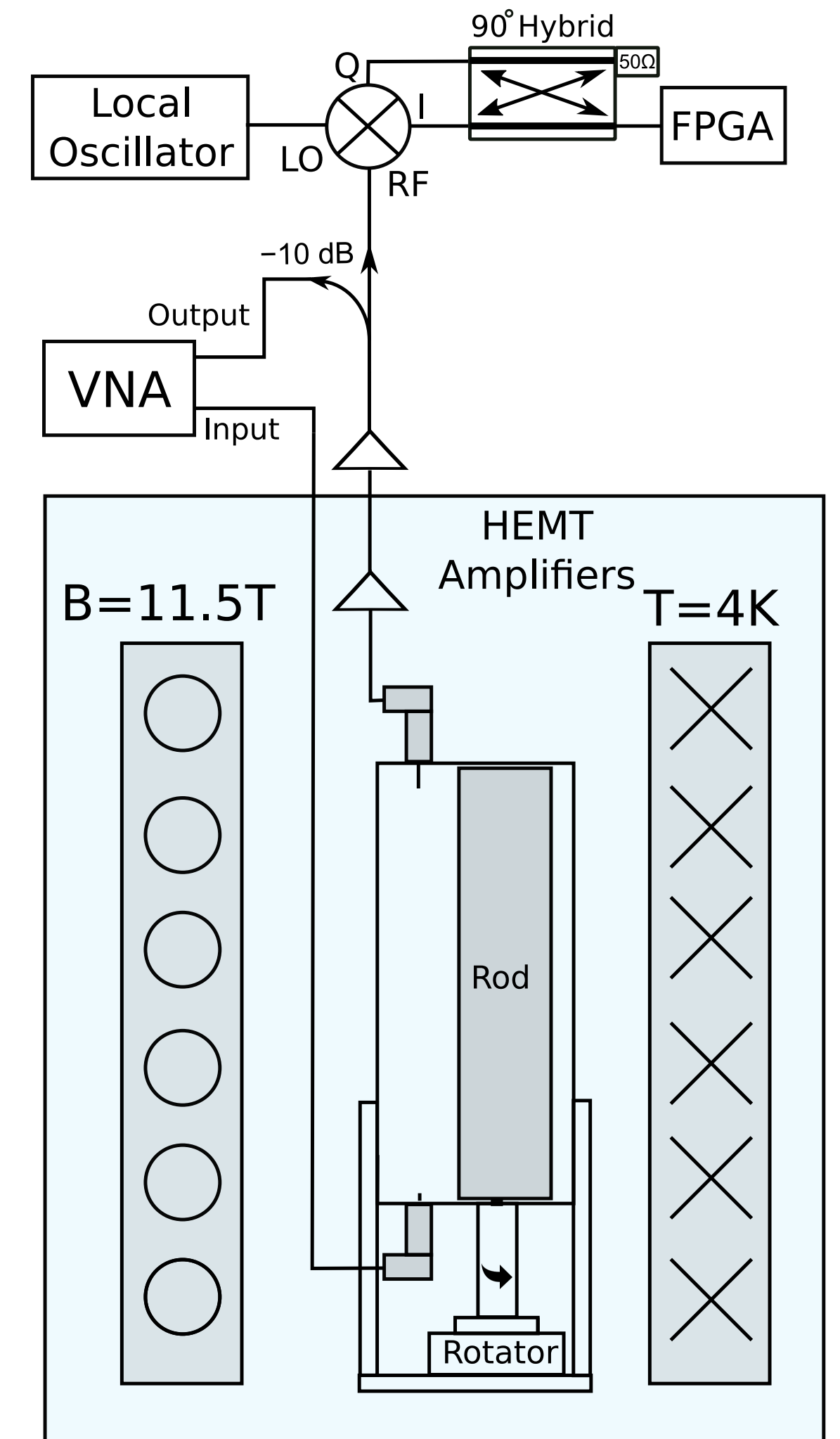
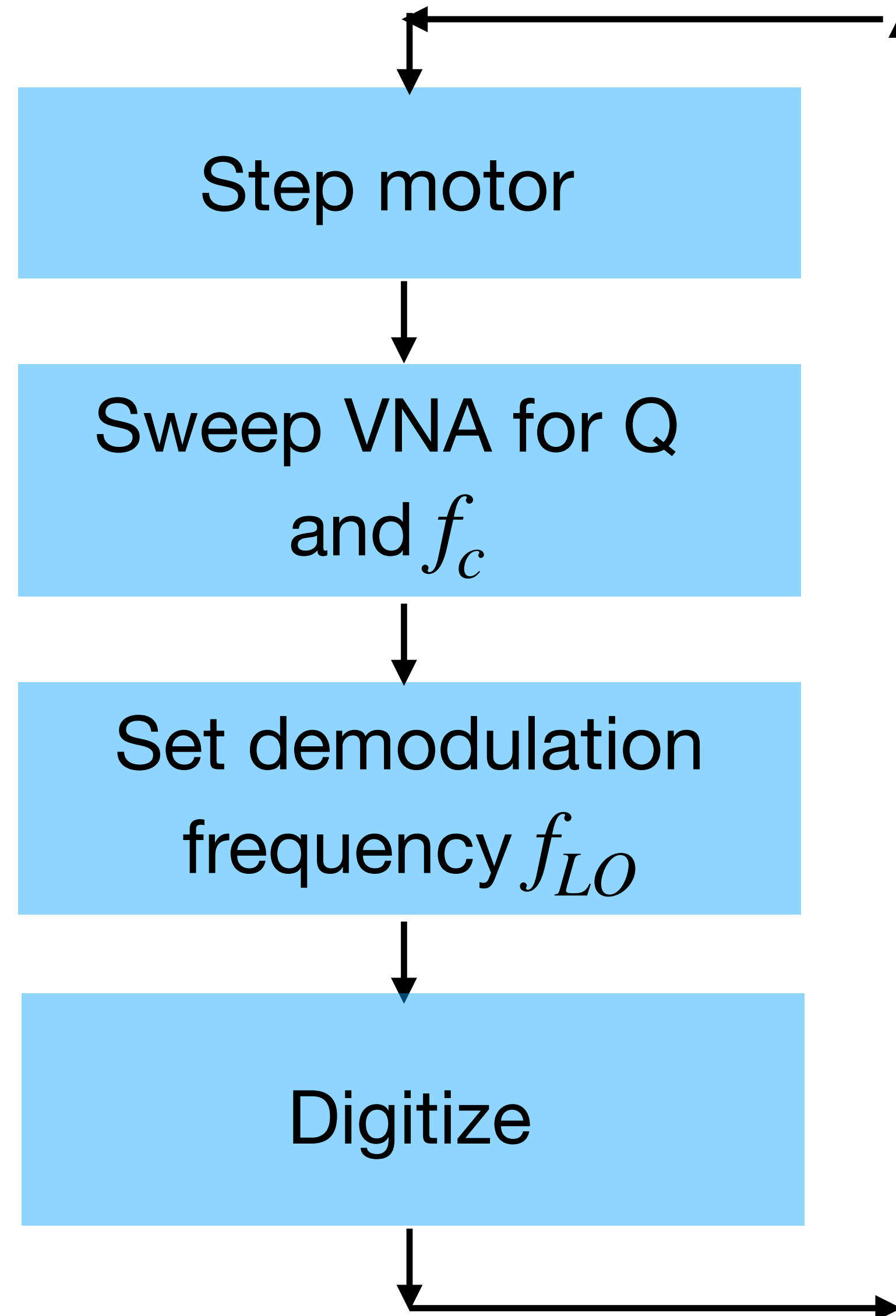
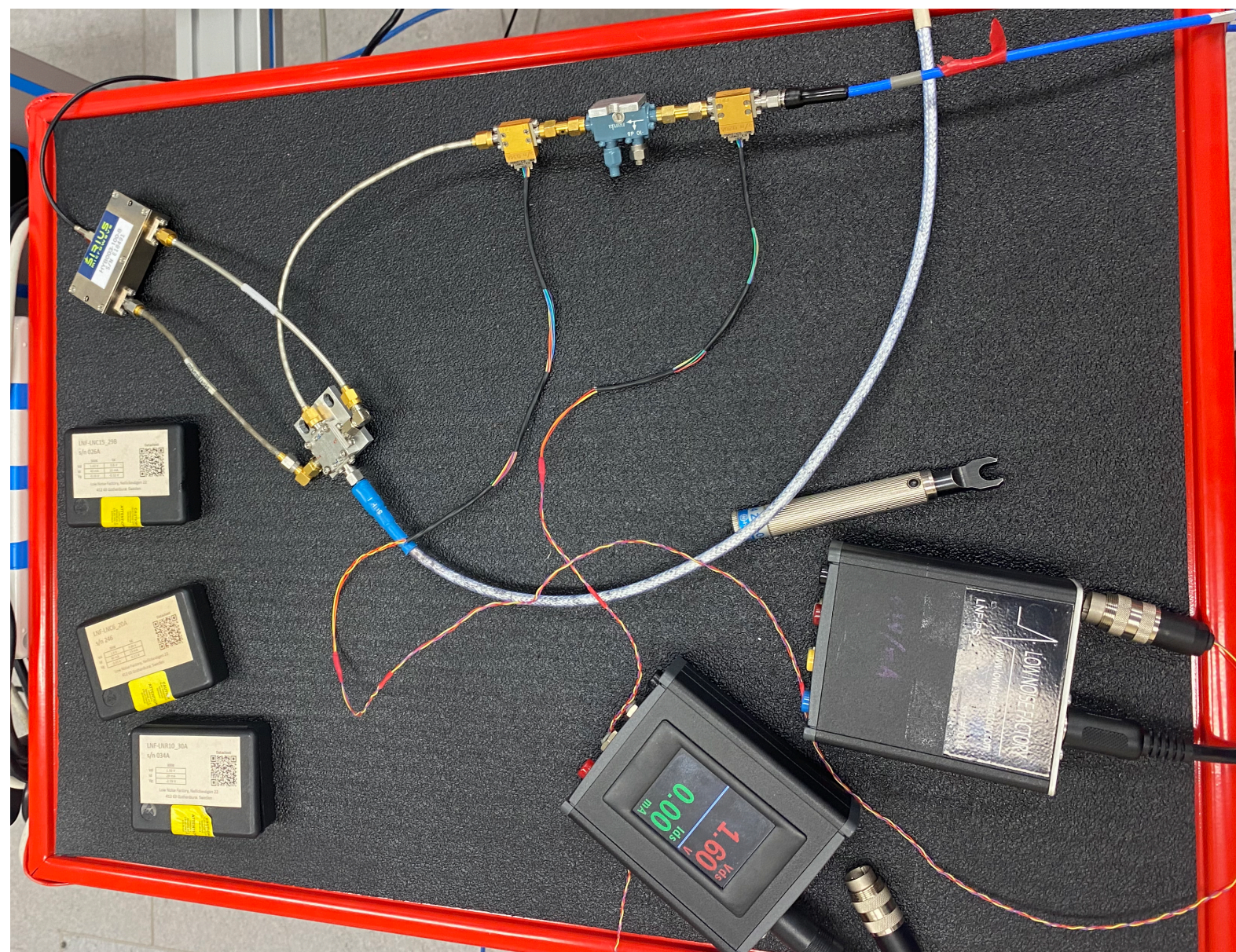
Experimental Setup

- So far we've scanned for ~ 2.5 weeks (~600MHz)
- We use an IQ mixer and hybrid coupler for image rejection of the noisy sideband

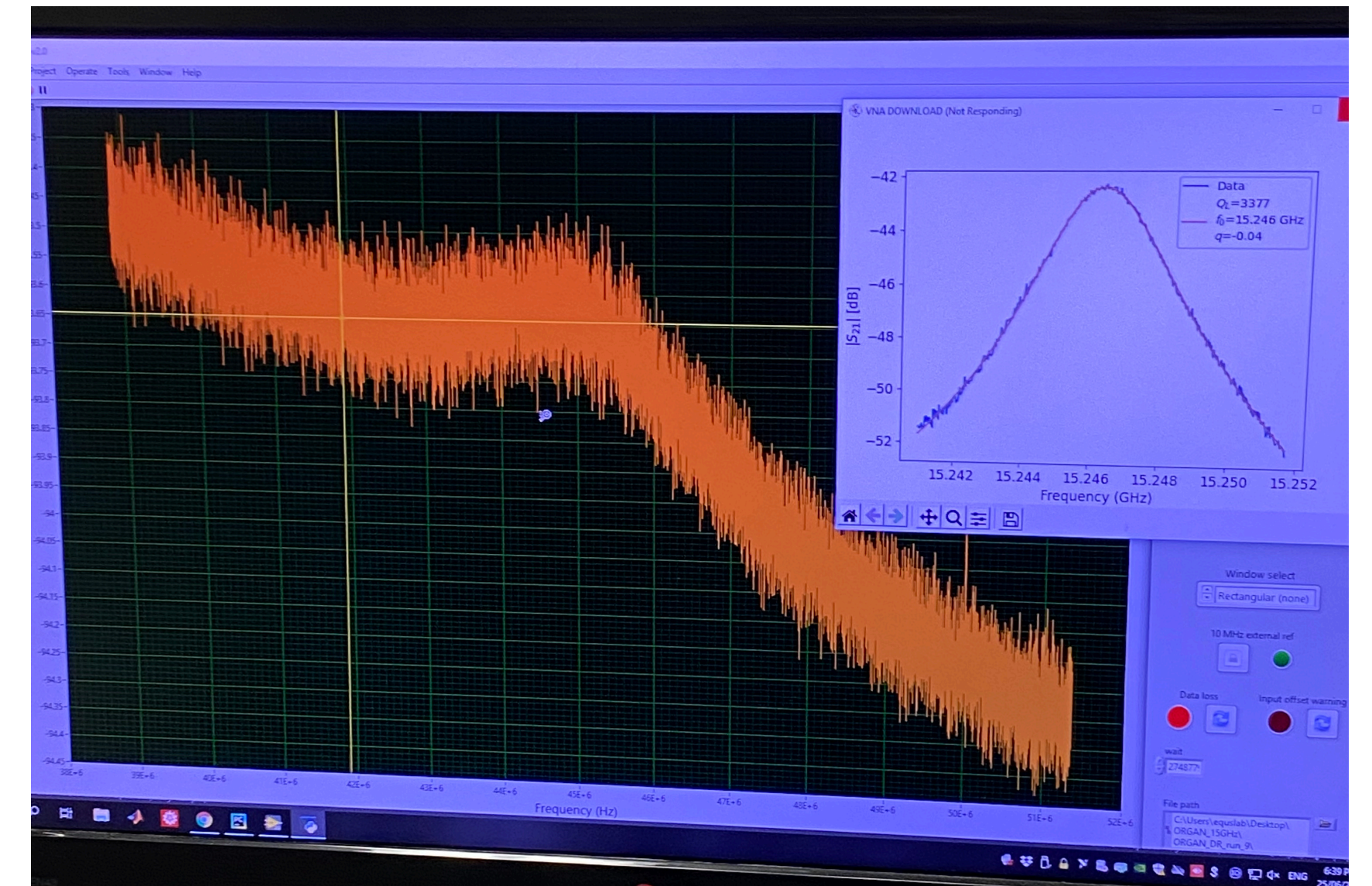


Experimental Setup

- So far we've scanned for ~ 2.5 weeks (~600MHz)
- We use an IQ mixer and hybrid coupler for image rejection of the noisy sideband

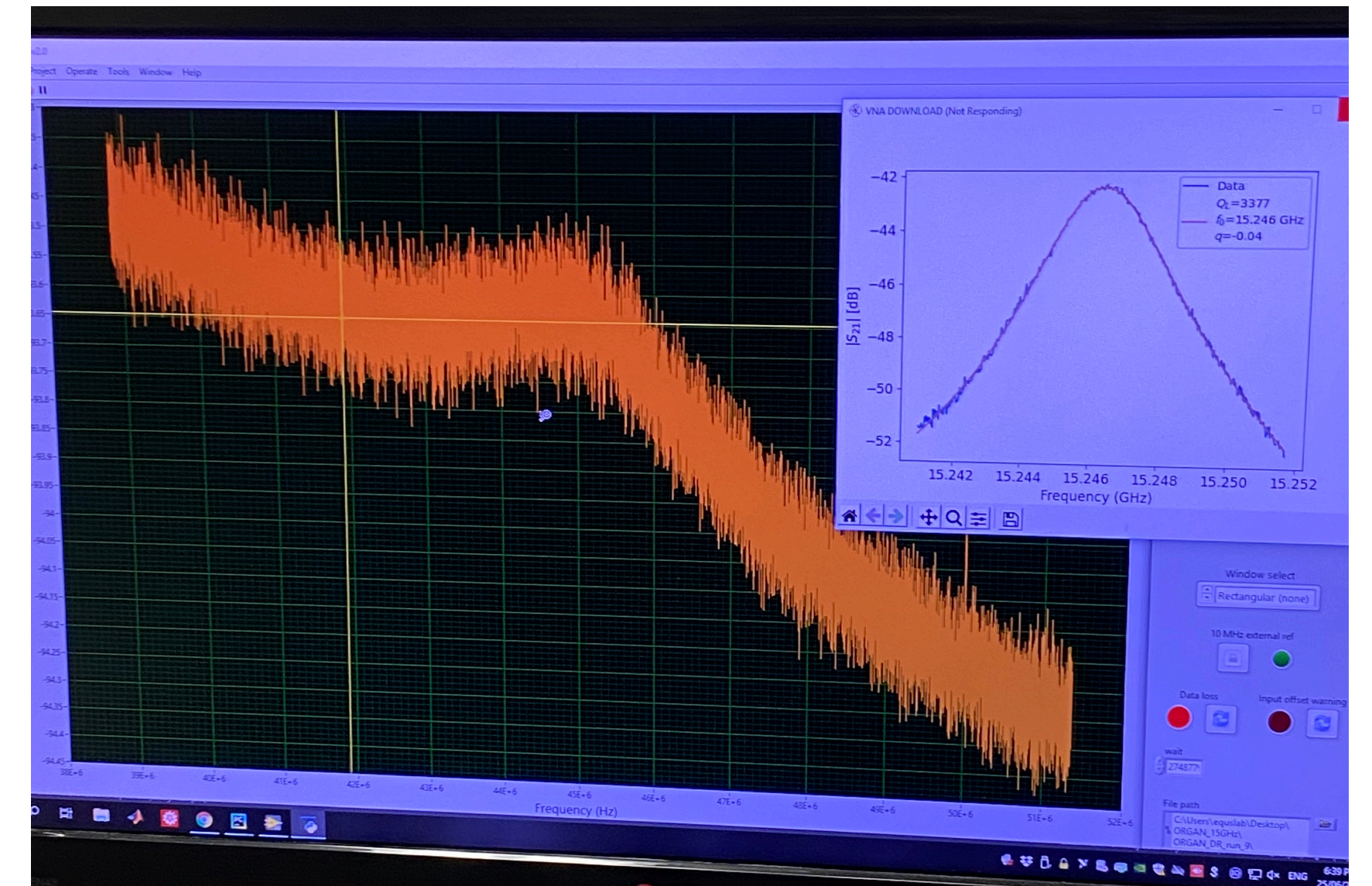


Data Taking



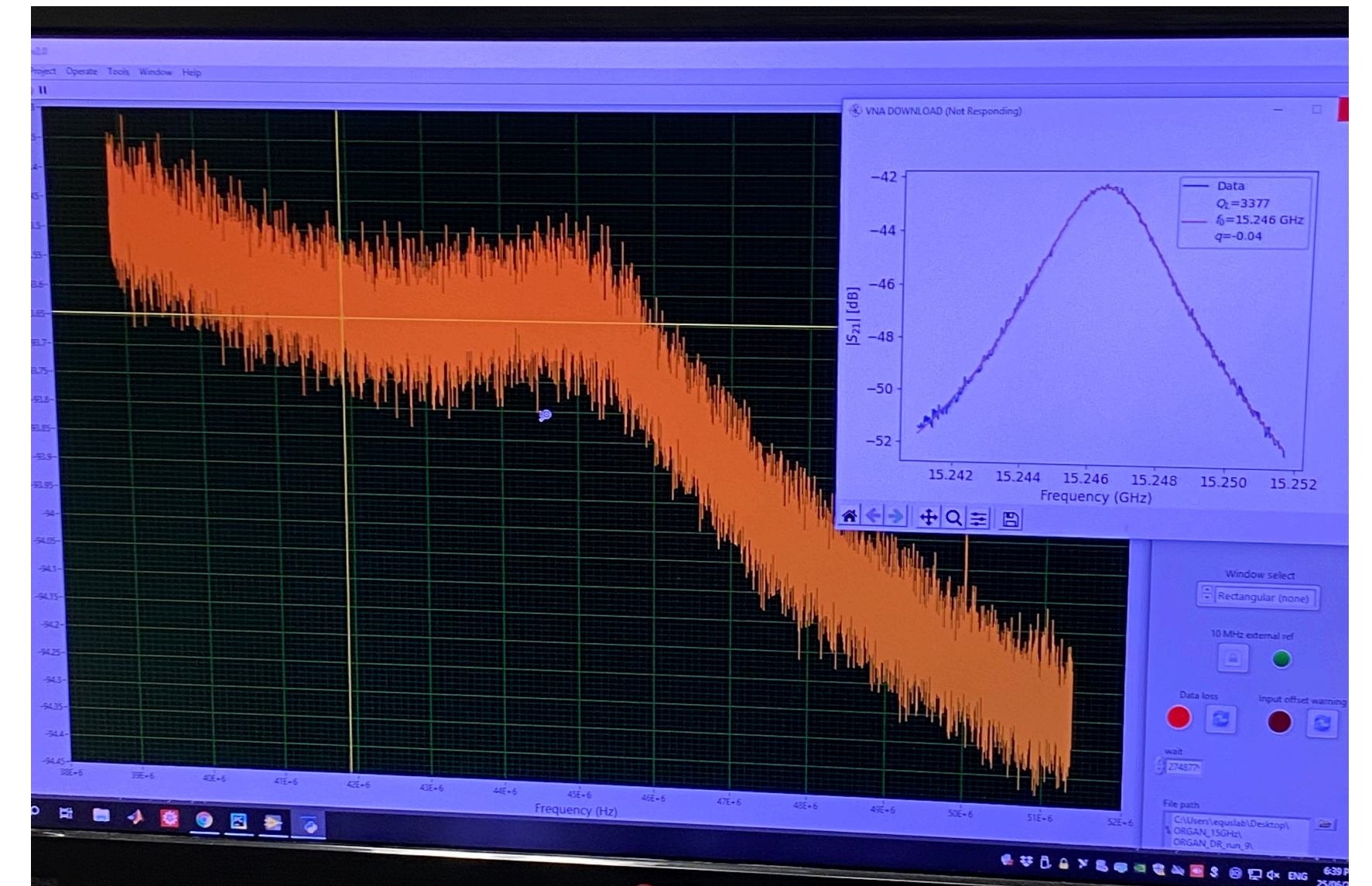
Data Taking

- ~12.5 MHz span, 26,214 point FFT,
 $\Delta\nu_{bin} \approx 477$ Hz



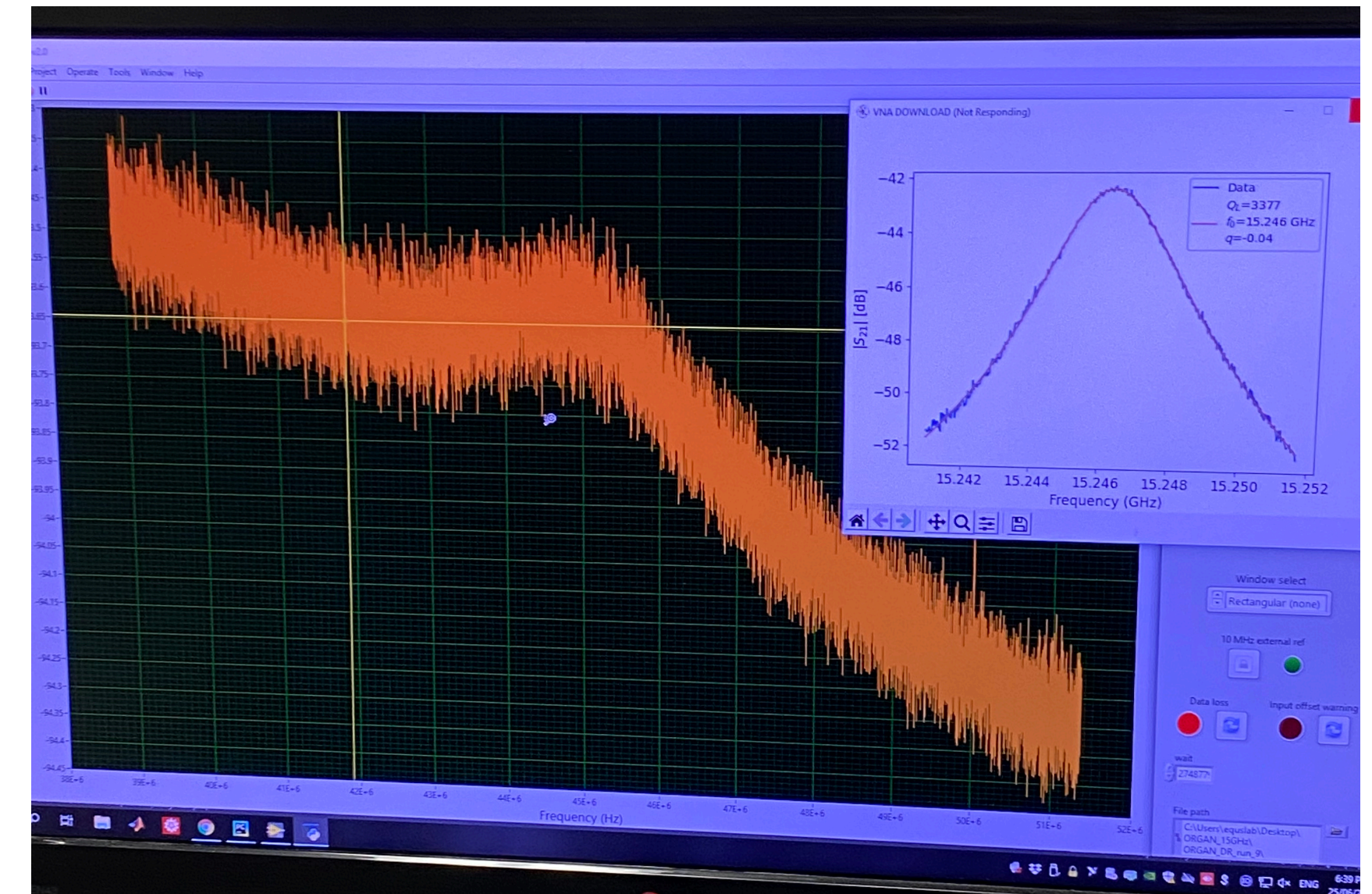
Data Taking

- ~12.5 MHz span, 26,214 point FFT,
 $\Delta\nu_{bin} \approx 477$ Hz
- IF bandwidth gets cropped to
~6MHz



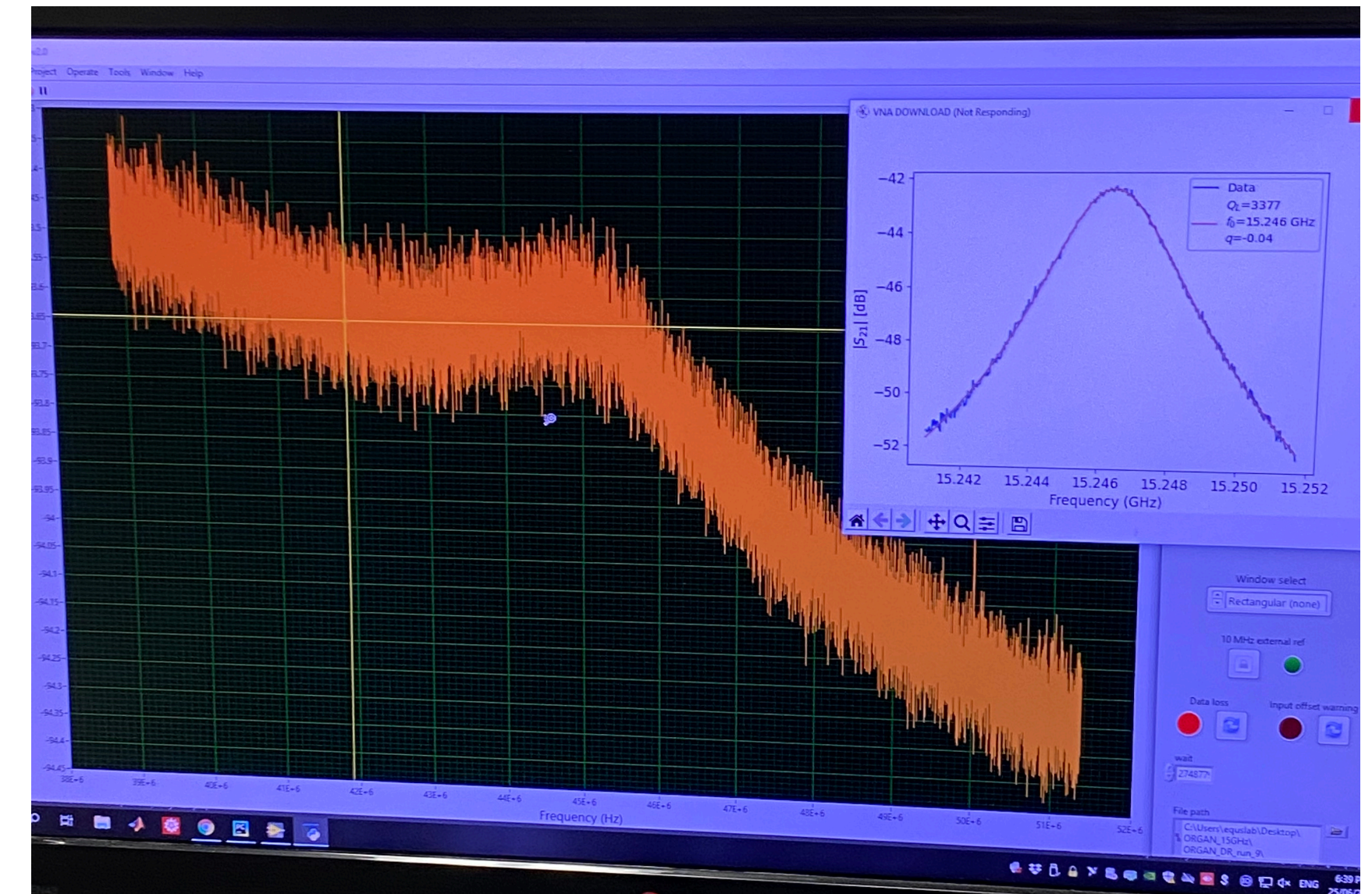
Data Taking

- ~12.5 MHz span, 26,214 point FFT,
 $\Delta\nu_{bin} \approx 477$ Hz
- IF bandwidth gets cropped to
~6MHz
- IF spectrum is free from
contamination



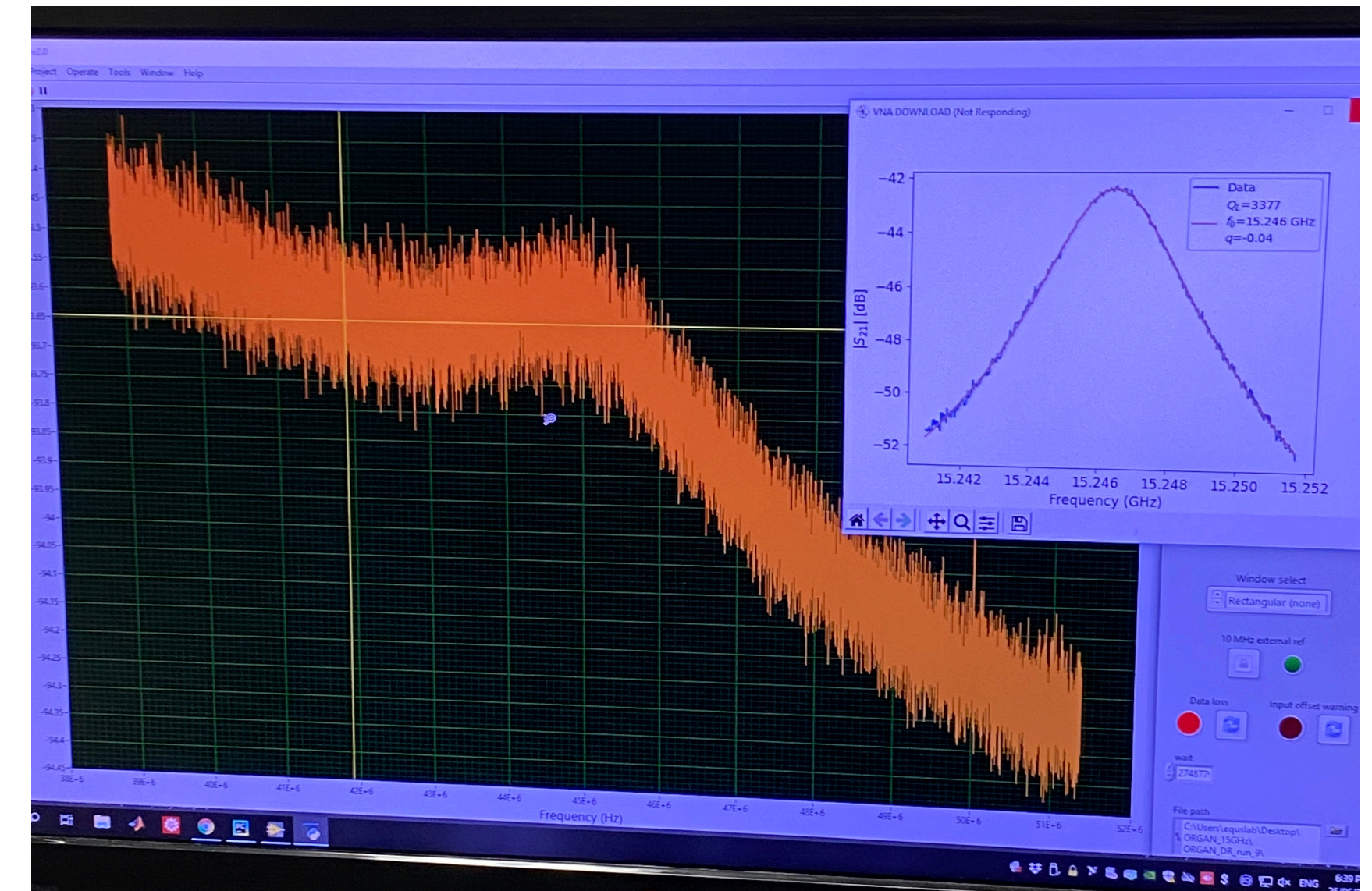
Data Taking

- ~12.5 MHz span, 26,214 point FFT, $\Delta\nu_{bin} \approx 477$ Hz
- IF bandwidth gets cropped to ~6MHz
- IF spectrum is free from contamination
- Visible thermal profile of the cavity mode



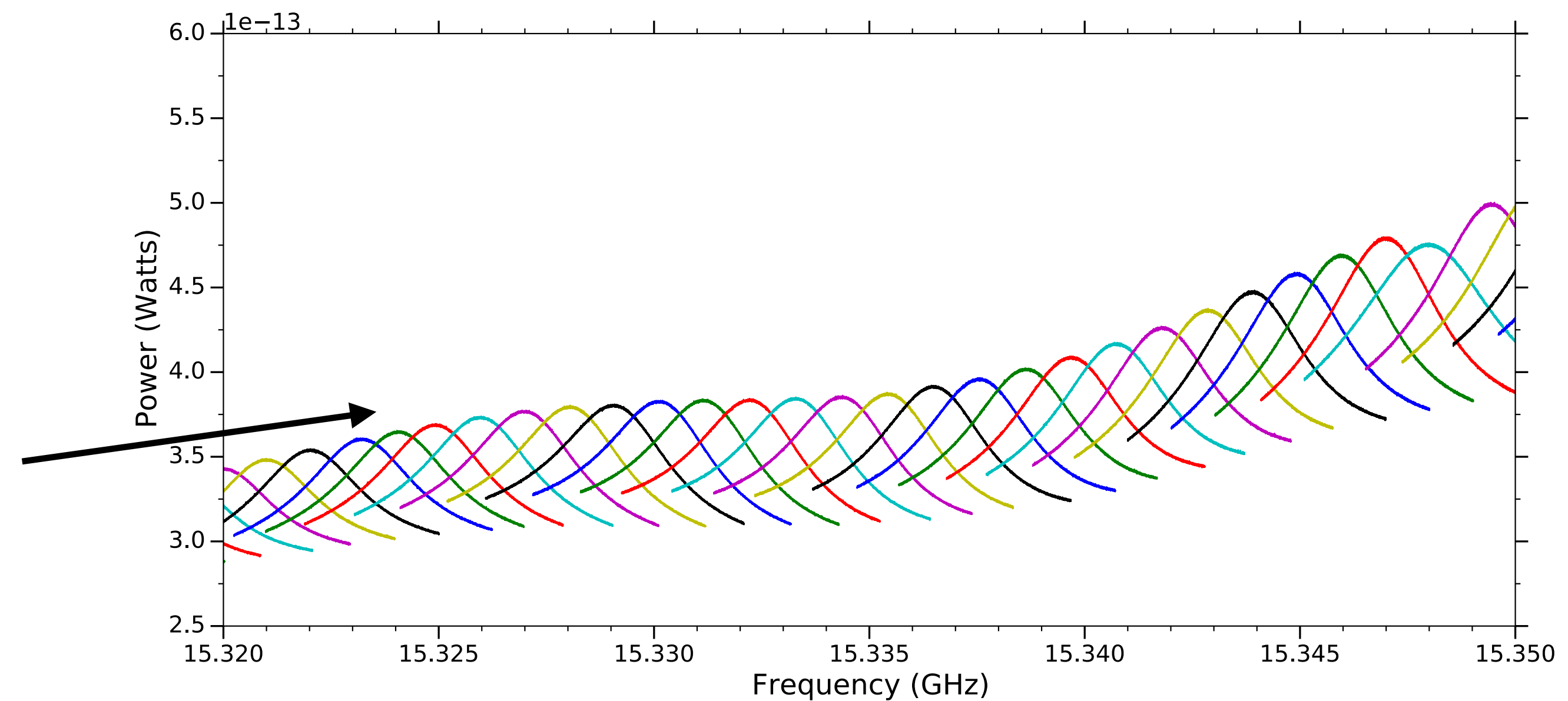
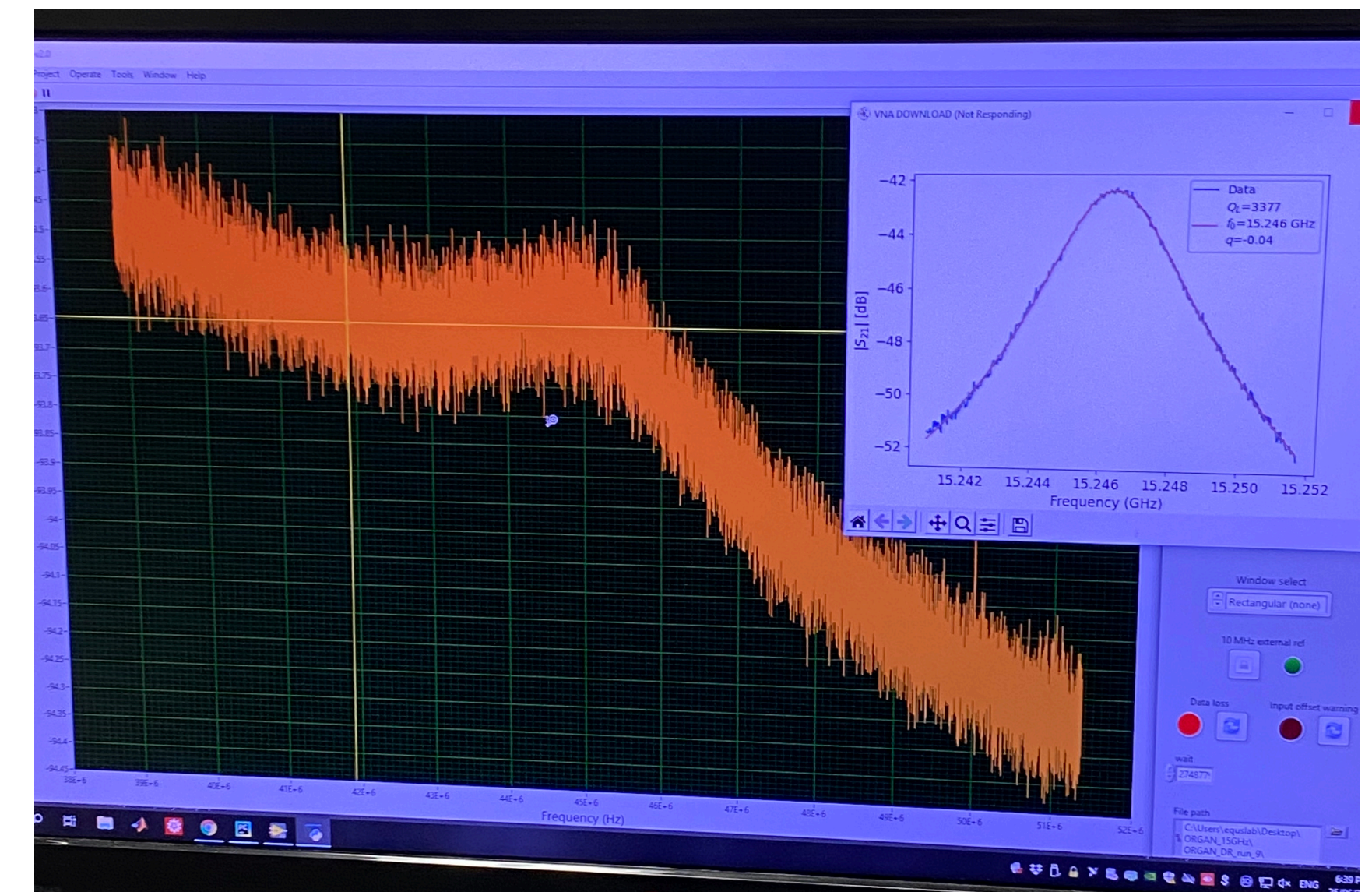
Data Taking

- ~12.5 MHz span, 26,214 point FFT, $\Delta\nu_{bin} \approx 477$ Hz
- IF bandwidth gets cropped to ~6MHz
- IF spectrum is free from contamination
- Visible thermal profile of the cavity mode
- Thermal noise after many averages



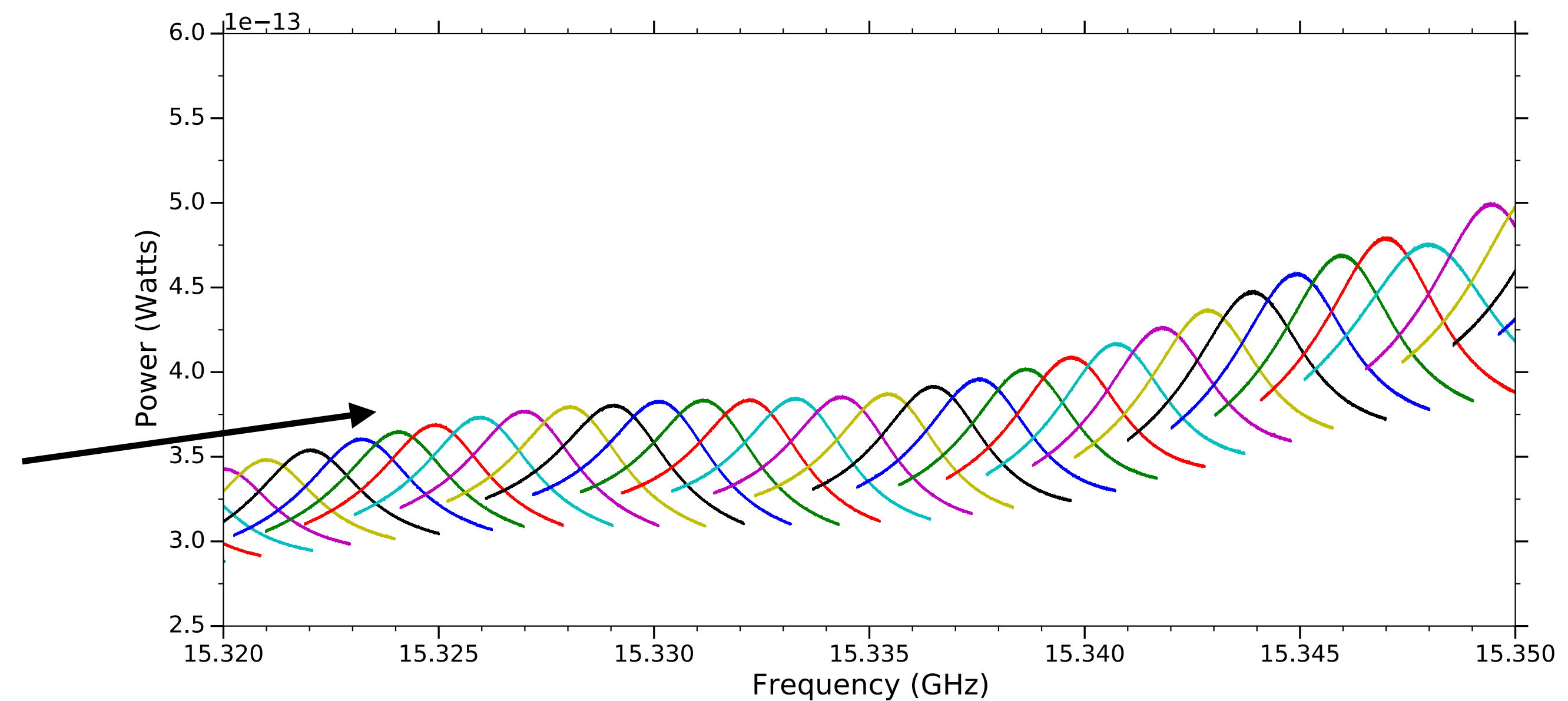
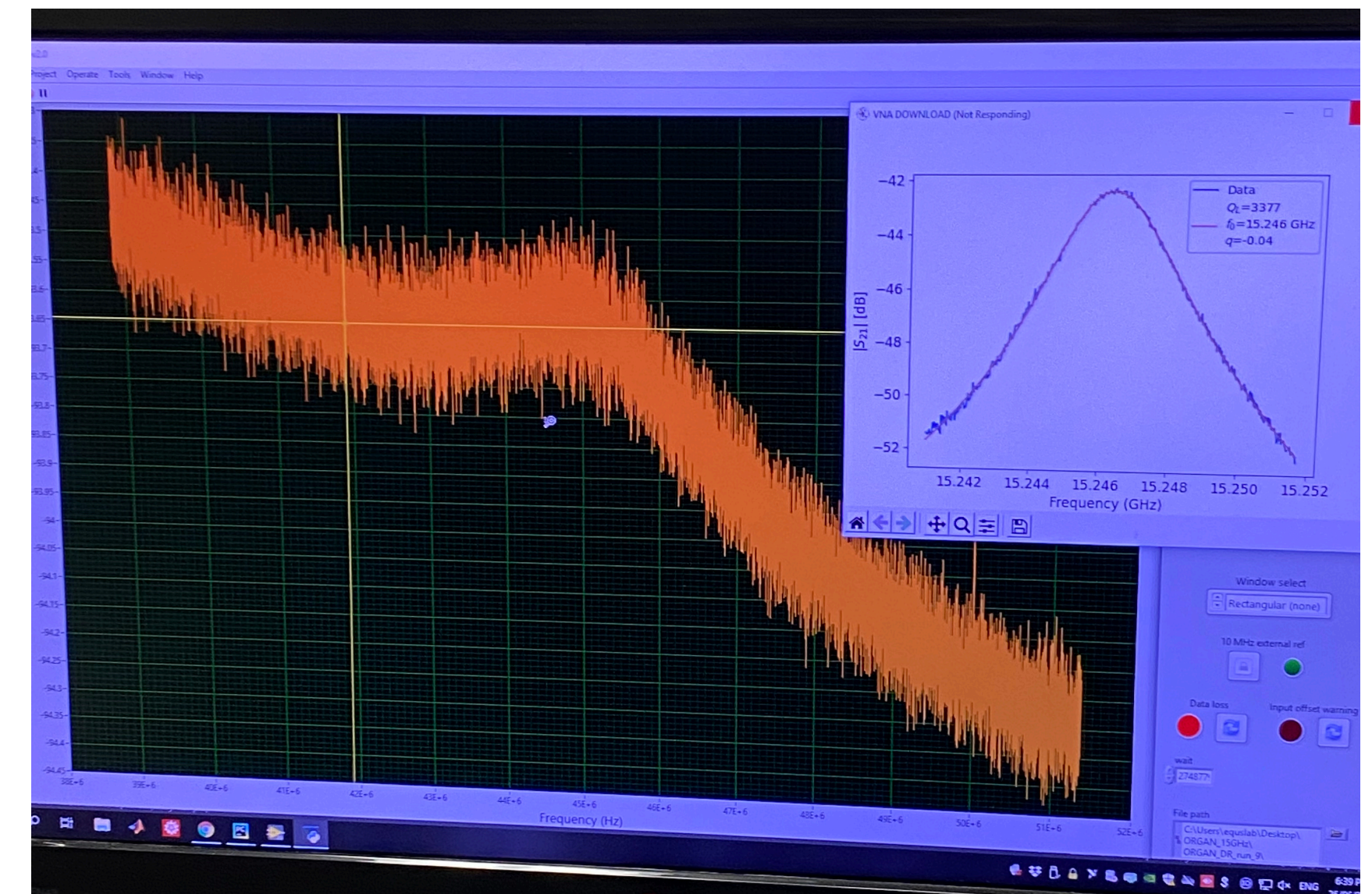
Data Taking

- ~12.5 MHz span, 26,214 point FFT, $\Delta\nu_{bin} \approx 477$ Hz
- IF bandwidth gets cropped to ~6MHz
- IF spectrum is free from contamination
- Visible thermal profile of the cavity mode
- Thermal noise after many averages



Data Taking

- ~12.5 MHz span, 26,214 point FFT, $\Delta\nu_{bin} \approx 477$ Hz
- IF bandwidth gets cropped to ~6MHz
- IF spectrum is free from contamination
- Visible thermal profile of the cavity mode
- Thermal noise after many averages
- ~5 overlapping traces contribute to each RF bin



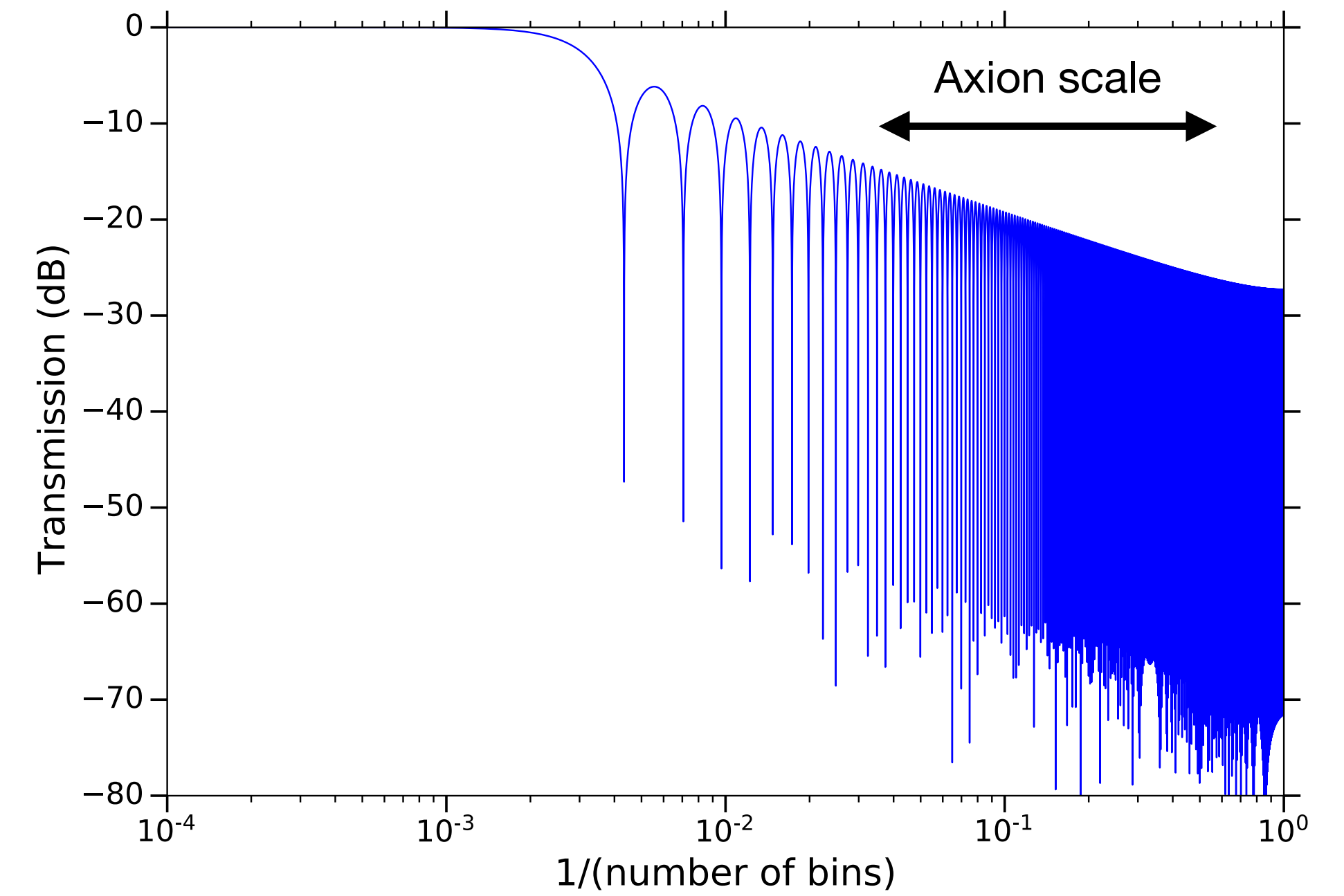
Savitzky-Golay Filter

Savitzky-Golay Filter

- Digital low pass filter parametrised by d (polynomial order) and W ($2W + 1$ point window length)

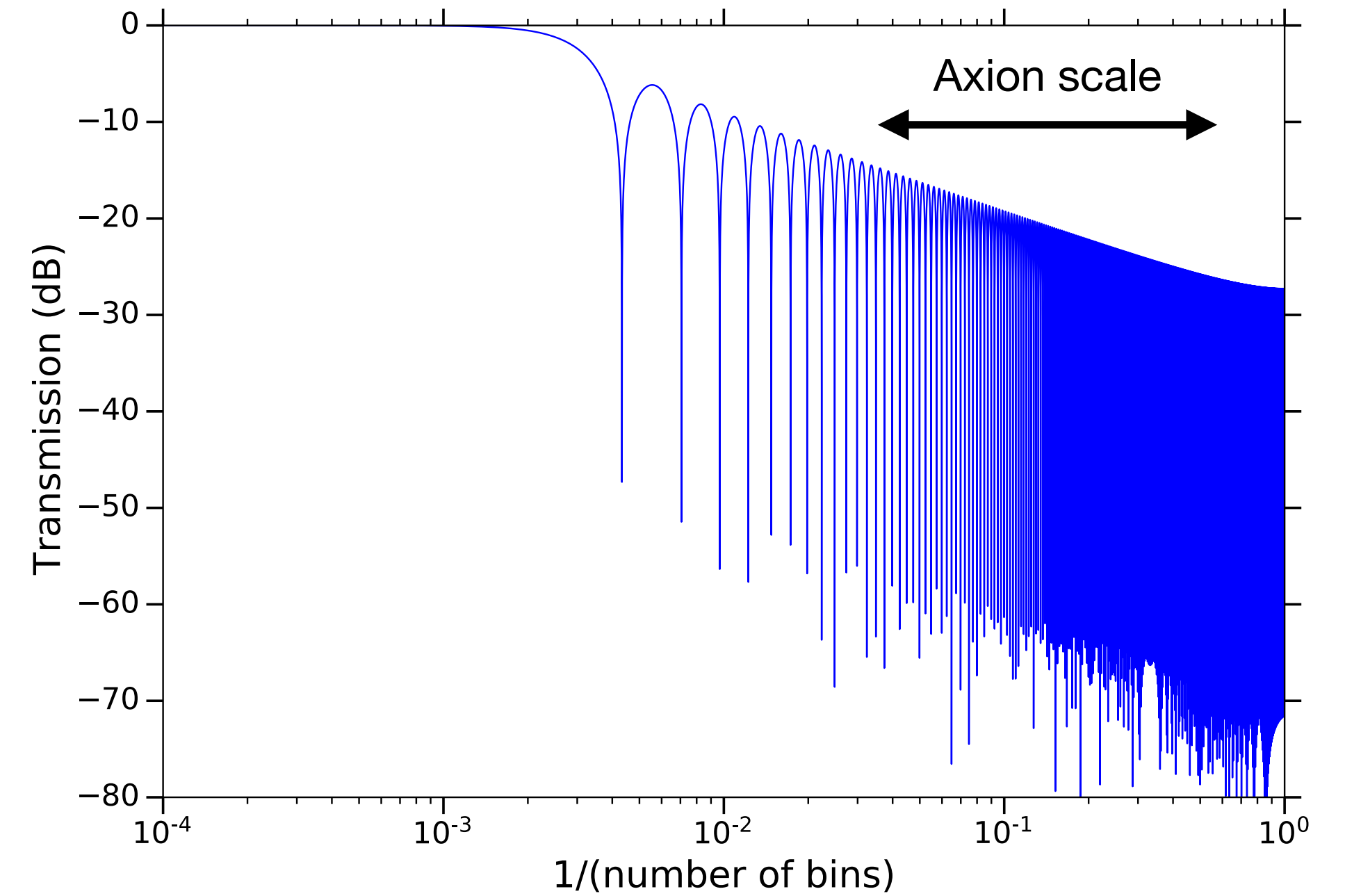
Savitzky-Golay Filter

- Digital low pass filter parametrised by d (polynomial order) and W ($2W + 1$ point window length)



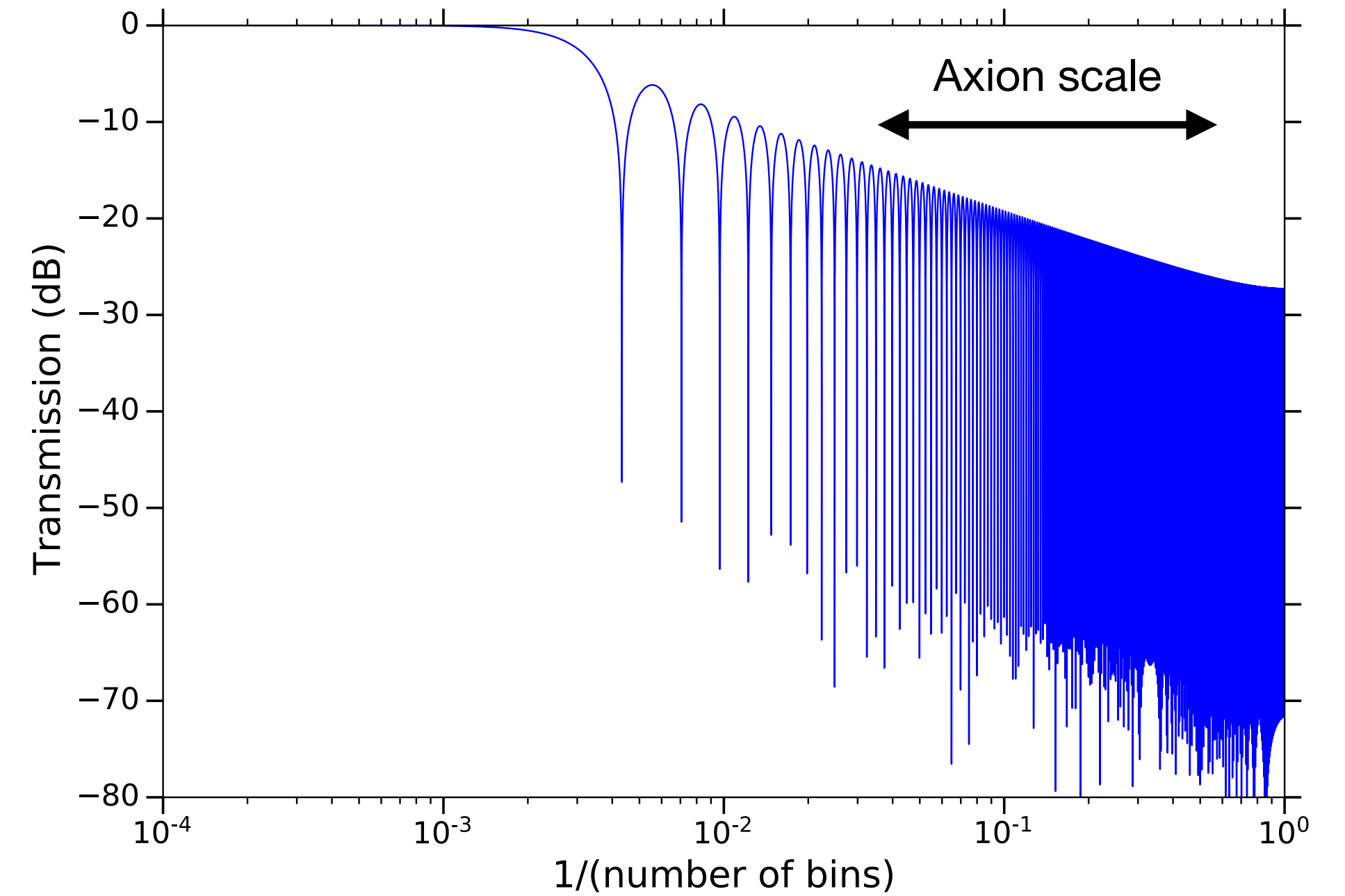
Savitzky-Golay Filter

- Digital low pass filter parametrised by d (polynomial order) and W ($2W + 1$ point window length)
- Removes large scale baseline variations



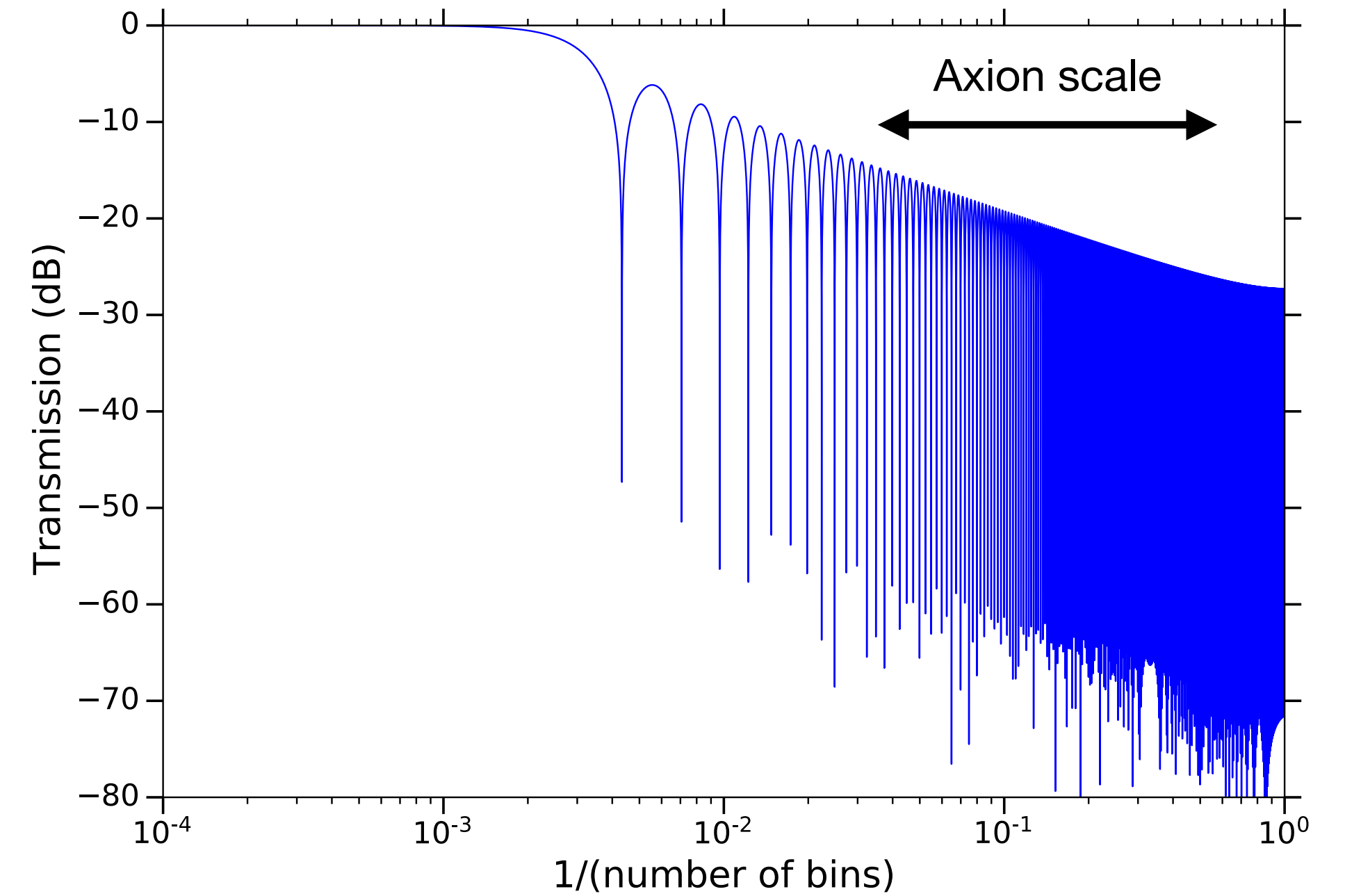
Savitzky-Golay Filter

- Digital low pass filter parametrised by d (polynomial order) and W ($2W + 1$ point window length)
- Removes large scale baseline variations
- Very flat passband and good stop band attenuation



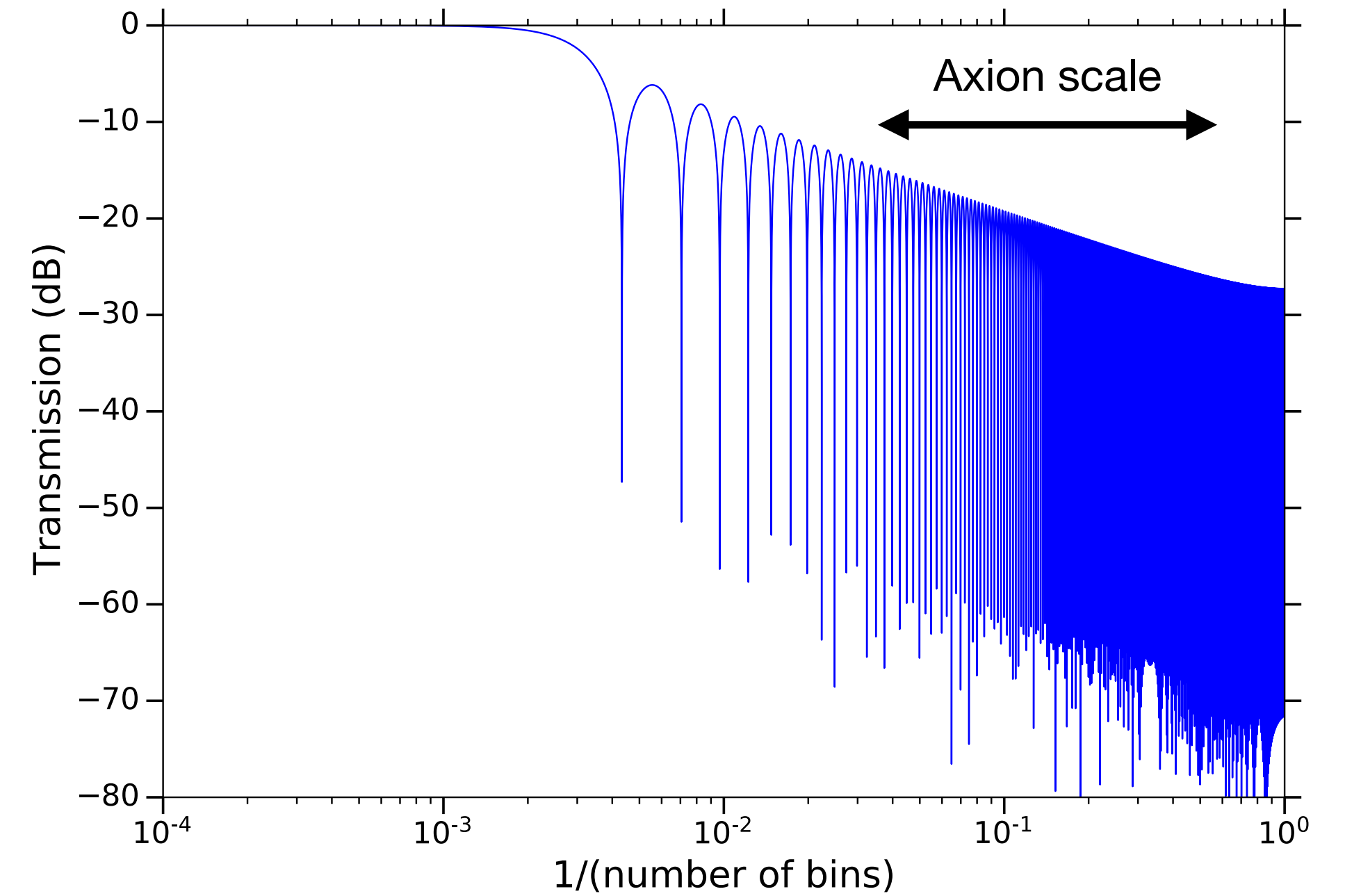
Savitzky-Golay Filter

- Digital low pass filter parametrised by d (polynomial order) and W ($2W + 1$ point window length)
- Removes large scale baseline variations
- Very flat passband and good stop band attenuation
- Imprints small negative correlations between bins



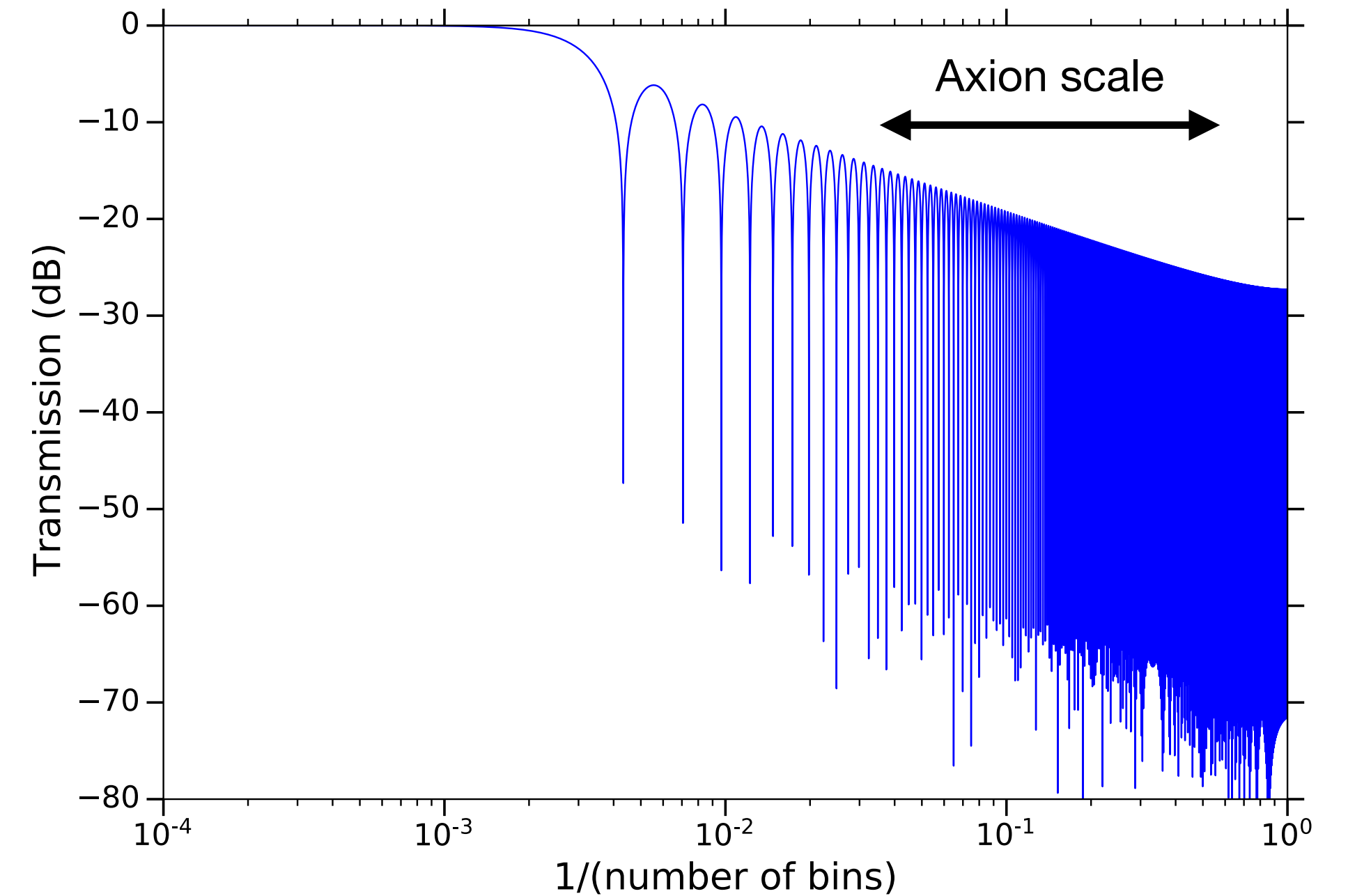
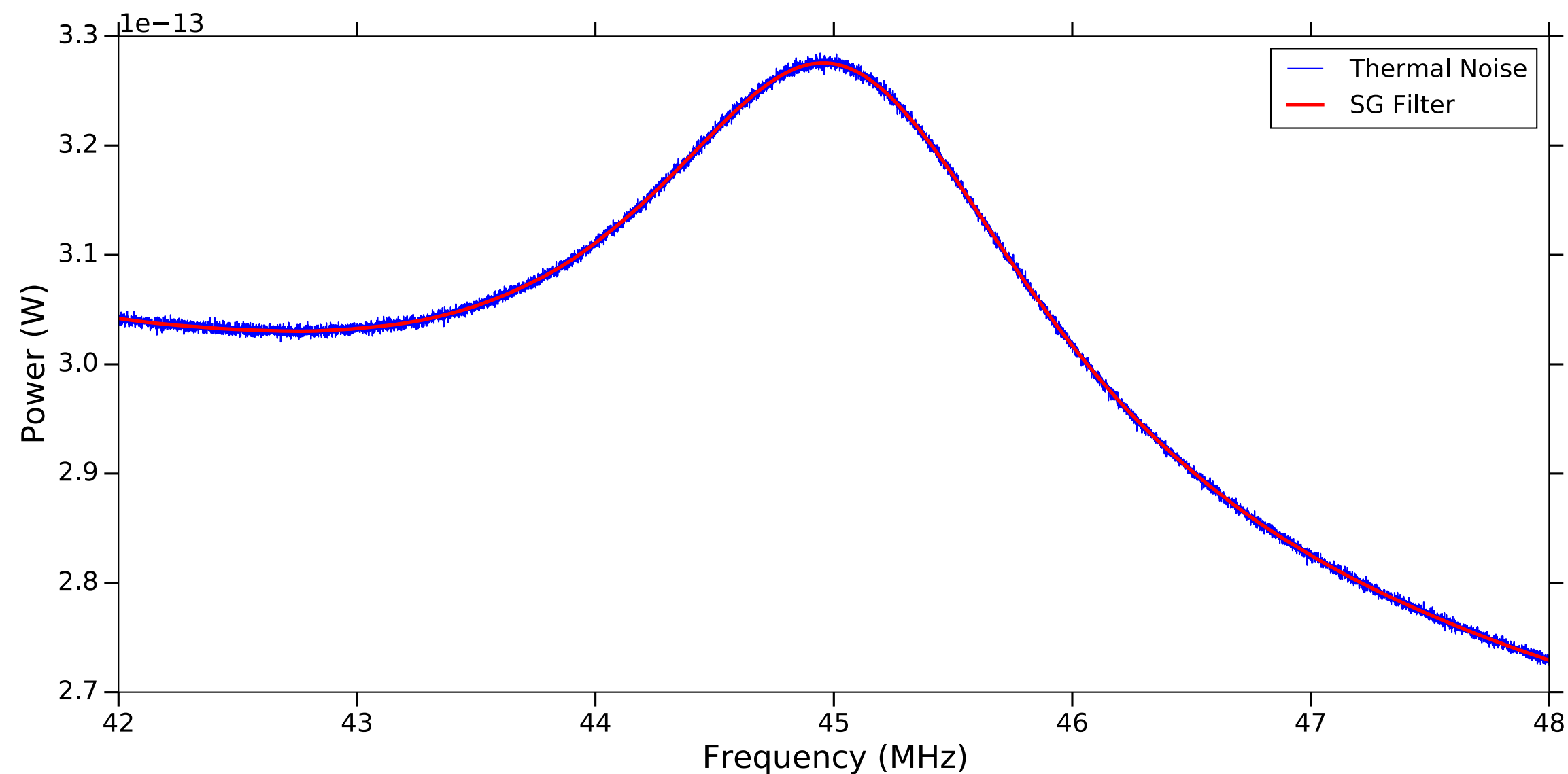
Savitzky-Golay Filter

- Digital low pass filter parametrised by d (polynomial order) and W ($2W + 1$ point window length)
- Removes large scale baseline variations
- Very flat passband and good stop band attenuation
- Imprints small negative correlations between bins
- Choose $d=3$ and $W=400$



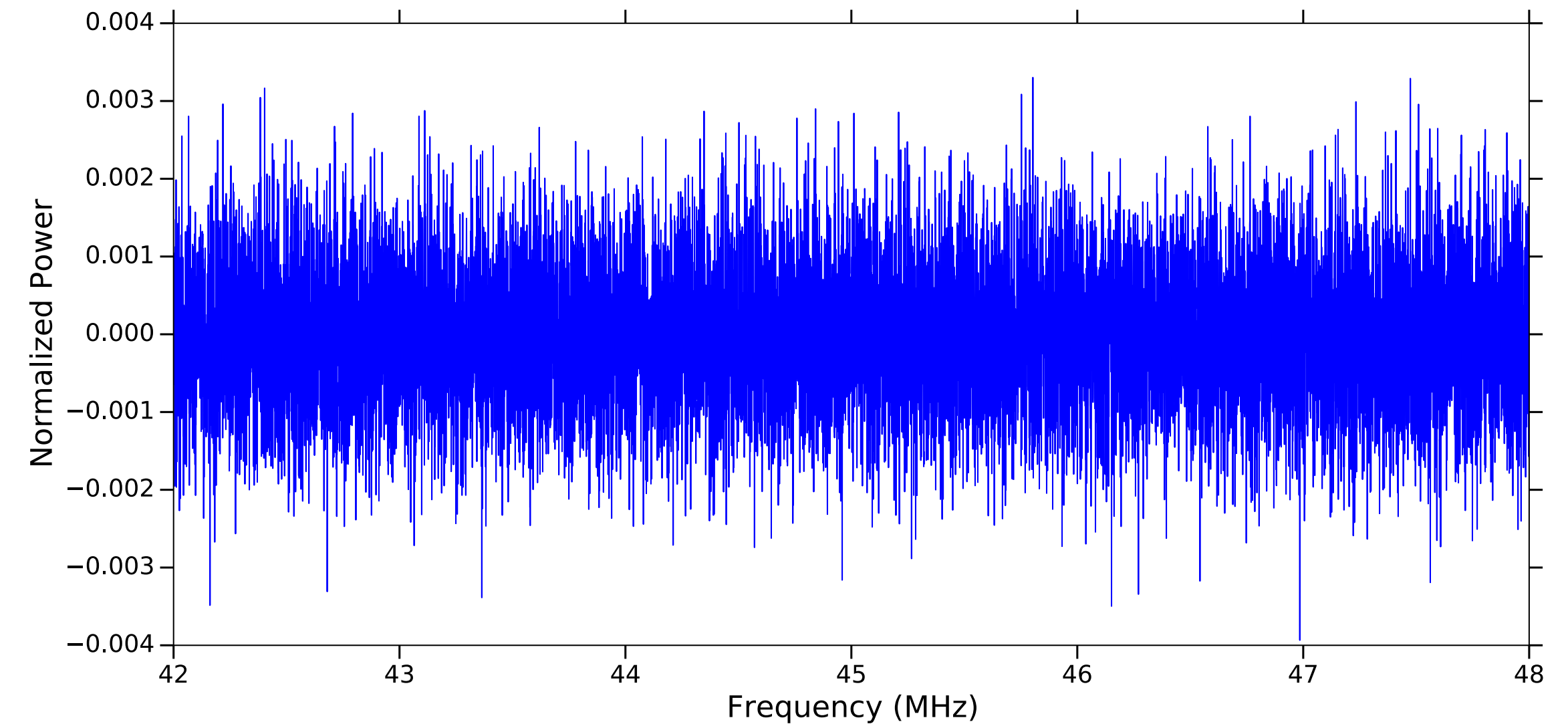
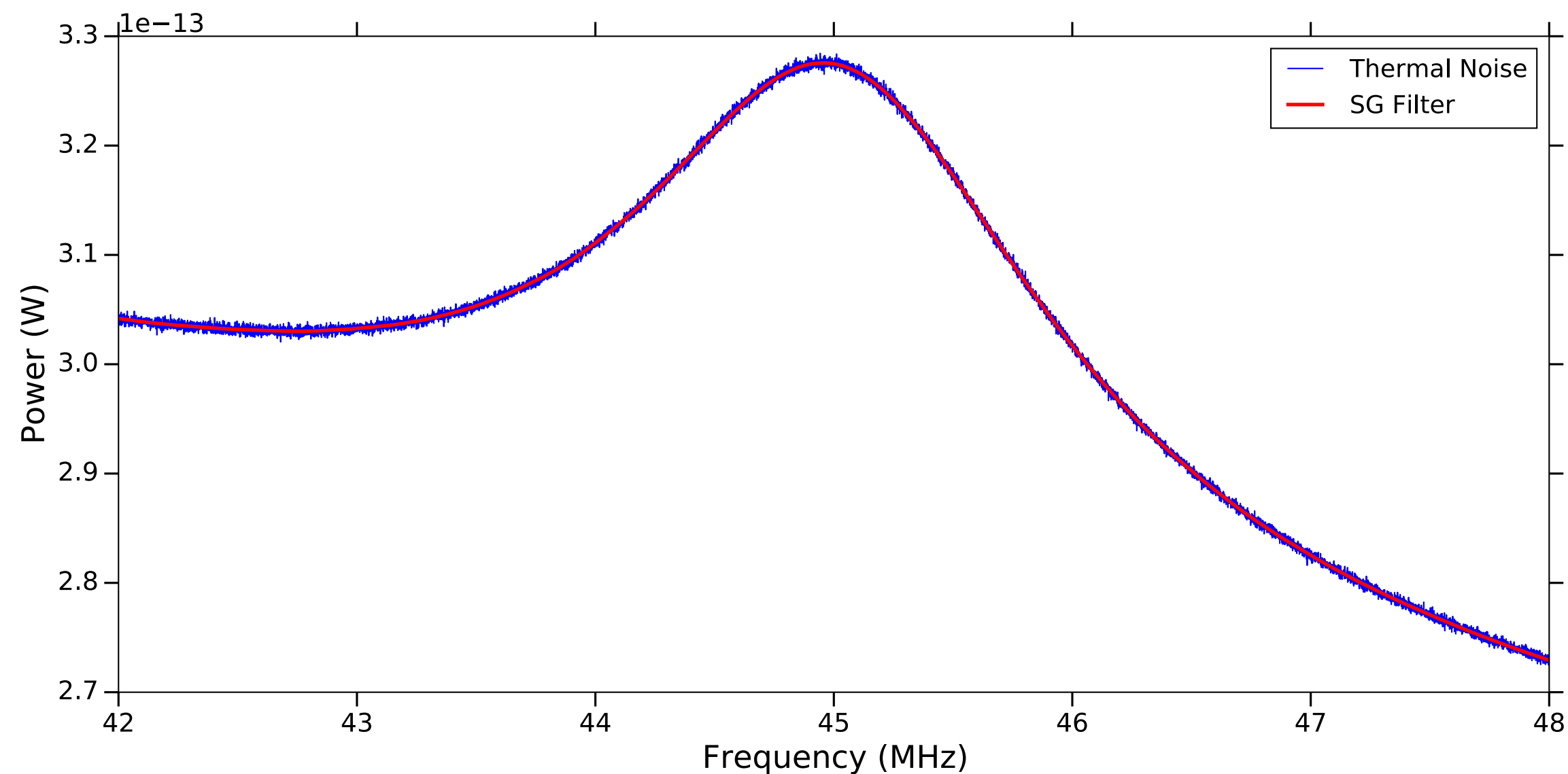
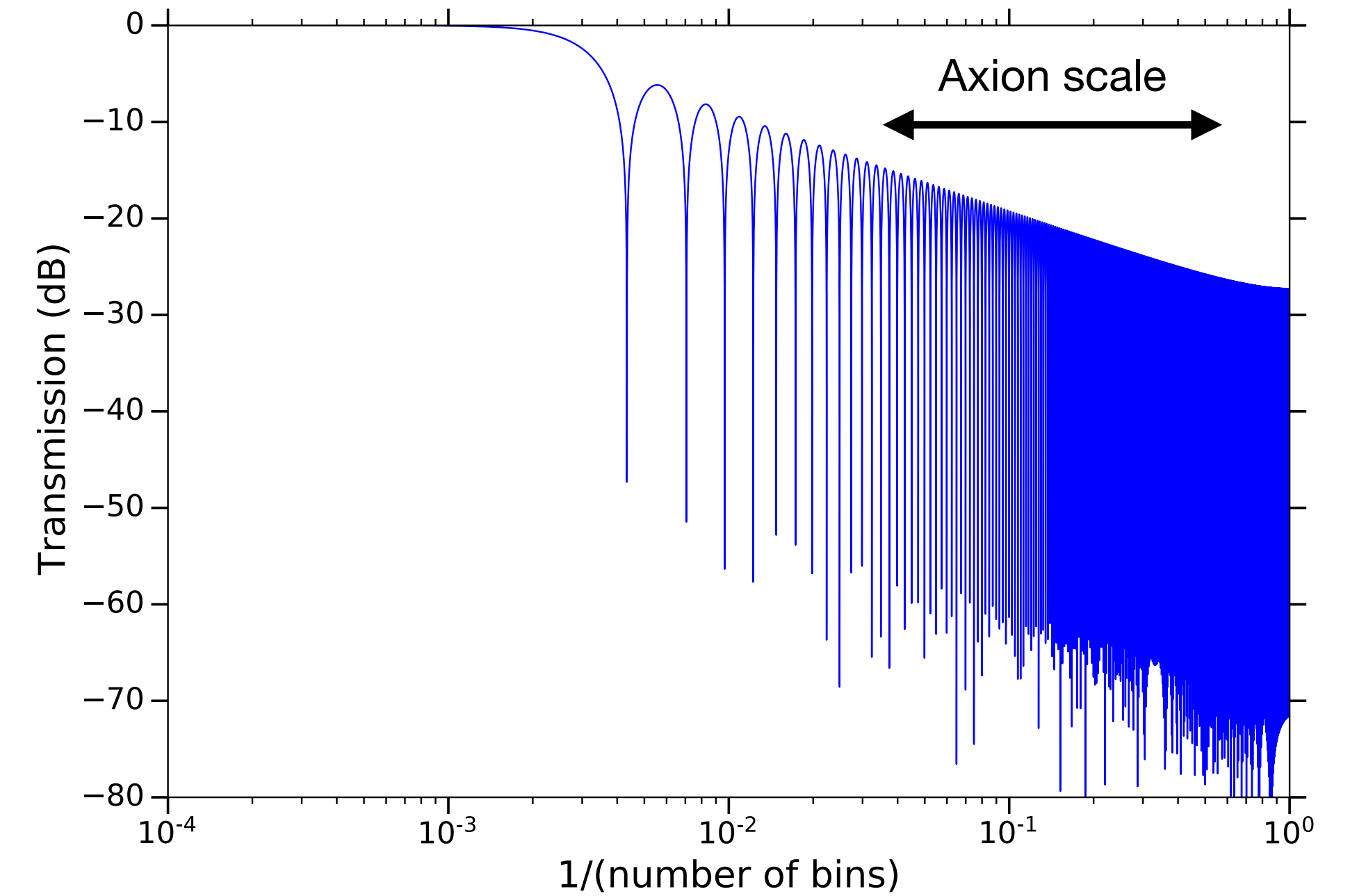
Savitzky-Golay Filter

- Digital low pass filter parametrised by d (polynomial order) and W ($2W + 1$ point window length)
- Removes large scale baseline variations
- Very flat passband and good stop band attenuation
- Imprints small negative correlations between bins
- Choose $d=3$ and $W=400$



Savitzky-Golay Filter

- Digital low pass filter parametrised by d (polynomial order) and W ($2W + 1$ point window length)
- Removes large scale baseline variations
- Very flat passband and good stop band attenuation
- Imprints small negative correlations between bins
- Choose $d=3$ and $W=400$



Combining bins vertically

Combining bins vertically

- Follow the procedure outlined by HAYSTAC

Combining bins vertically

- Follow the procedure outlined by HAYSTAC

PHYSICAL REVIEW D **96**, 123008 (2017)

HAYSTAC axion search analysis procedure

B. M. Brubaker,^{1,*} L. Zhong,¹ S. K. Lamoreaux,¹ K. W. Lehnert,² and K. A. van Bibber³

¹*Department of Physics, Yale University, New Haven, Connecticut 06511, USA*

²*JILA and the Department of Physics, University of Colorado*

and National Institute of Standards and Technology, Boulder, Colorado 80309, USA

³*Department of Nuclear Engineering, University of California Berkeley, Berkeley, California 94720, USA*

(Received 26 June 2017; published 18 December 2017)

We describe in detail the analysis procedure used to derive the first limits from the Haloscope at Yale Sensitive to Axion CDM (HAYSTAC), a microwave cavity search for cold dark matter (CDM) axions with masses above $20 \mu\text{eV}$. We have introduced several significant innovations to the axion search analysis pioneered by the Axion Dark Matter eXperiment (ADMX), including optimal filtering of the individual power spectra that constitute the axion search data set and a consistent maximum likelihood procedure for combining and rebinning these spectra. These innovations enable us to obtain the axion-photon coupling $|g_\gamma|$ excluded at any desired confidence level directly from the statistics of the combined data.

DOI: [10.1103/PhysRevD.96.123008](https://doi.org/10.1103/PhysRevD.96.123008)

Combining bins vertically

- Follow the procedure outlined by HAYSTAC
- Vertically combine overlapping single bins using maximum-likelihood weights

PHYSICAL REVIEW D **96**, 123008 (2017)

HAYSTAC axion search analysis procedure

B. M. Brubaker,^{1,*} L. Zhong,¹ S. K. Lamoreaux,¹ K. W. Lehnert,² and K. A. van Bibber³

¹*Department of Physics, Yale University, New Haven, Connecticut 06511, USA*

²*JILA and the Department of Physics, University of Colorado*

and National Institute of Standards and Technology, Boulder, Colorado 80309, USA

³*Department of Nuclear Engineering, University of California Berkeley, Berkeley, California 94720, USA*

(Received 26 June 2017; published 18 December 2017)

We describe in detail the analysis procedure used to derive the first limits from the Haloscope at Yale Sensitive to Axion CDM (HAYSTAC), a microwave cavity search for cold dark matter (CDM) axions with masses above $20 \mu\text{eV}$. We have introduced several significant innovations to the axion search analysis pioneered by the Axion Dark Matter eXperiment (ADMX), including optimal filtering of the individual power spectra that constitute the axion search data set and a consistent maximum likelihood procedure for combining and rebinning these spectra. These innovations enable us to obtain the axion-photon coupling $|g_\gamma|$ excluded at any desired confidence level directly from the statistics of the combined data.

DOI: [10.1103/PhysRevD.96.123008](https://doi.org/10.1103/PhysRevD.96.123008)

Combining bins vertically

- Follow the procedure outlined by HAYSTAC
- Vertically combine overlapping single bins using maximum-likelihood weights
- SNR of a single bin will change based on the lorentzian factor, T_{sys} , Q_L , β and σ

PHYSICAL REVIEW D **96**, 123008 (2017)

HAYSTAC axion search analysis procedure

B. M. Brubaker,^{1,*} L. Zhong,¹ S. K. Lamoreaux,¹ K. W. Lehnert,² and K. A. van Bibber³

¹*Department of Physics, Yale University, New Haven, Connecticut 06511, USA*

²*JILA and the Department of Physics, University of Colorado*

and National Institute of Standards and Technology, Boulder, Colorado 80309, USA

³*Department of Nuclear Engineering, University of California Berkeley, Berkeley, California 94720, USA*

(Received 26 June 2017; published 18 December 2017)

We describe in detail the analysis procedure used to derive the first limits from the Haloscope at Yale Sensitive to Axion CDM (HAYSTAC), a microwave cavity search for cold dark matter (CDM) axions with masses above $20 \mu\text{eV}$. We have introduced several significant innovations to the axion search analysis pioneered by the Axion Dark Matter eXperiment (ADMX), including optimal filtering of the individual power spectra that constitute the axion search data set and a consistent maximum likelihood procedure for combining and rebinning these spectra. These innovations enable us to obtain the axion-photon coupling $|g_\gamma|$ excluded at any desired confidence level directly from the statistics of the combined data.

DOI: [10.1103/PhysRevD.96.123008](https://doi.org/10.1103/PhysRevD.96.123008)

Combining bins vertically

- Follow the procedure outlined by HAYSTAC
- Vertically combine overlapping single bins using maximum-likelihood weights
- SNR of a single bin will change based on the lorentzian factor, T_{sys} , Q_L , β and σ
- Gaussian noise, as you might expect

PHYSICAL REVIEW D **96**, 123008 (2017)

HAYSTAC axion search analysis procedure

B. M. Brubaker,^{1,*} L. Zhong,¹ S. K. Lamoreaux,¹ K. W. Lehnert,² and K. A. van Bibber³

¹*Department of Physics, Yale University, New Haven, Connecticut 06511, USA*

²*JILA and the Department of Physics, University of Colorado*

and National Institute of Standards and Technology, Boulder, Colorado 80309, USA

³*Department of Nuclear Engineering, University of California Berkeley, Berkeley, California 94720, USA*

(Received 26 June 2017; published 18 December 2017)

We describe in detail the analysis procedure used to derive the first limits from the Haloscope at Yale Sensitive to Axion CDM (HAYSTAC), a microwave cavity search for cold dark matter (CDM) axions with masses above $20 \mu\text{eV}$. We have introduced several significant innovations to the axion search analysis pioneered by the Axion Dark Matter eXperiment (ADMX), including optimal filtering of the individual power spectra that constitute the axion search data set and a consistent maximum likelihood procedure for combining and rebinning these spectra. These innovations enable us to obtain the axion-photon coupling $|g_\gamma|$ excluded at any desired confidence level directly from the statistics of the combined data.

DOI: [10.1103/PhysRevD.96.123008](https://doi.org/10.1103/PhysRevD.96.123008)

Combining bins vertically

- Follow the procedure outlined by HAYSTAC
- Vertically combine overlapping single bins using maximum-likelihood weights
- SNR of a single bin will change based on the lorentzian factor, T_{sys} , Q_L , β and σ
- Gaussian noise, as you might expect

PHYSICAL REVIEW D **96**, 123008 (2017)

HAYSTAC axion search analysis procedure

B. M. Brubaker,^{1,*} L. Zhong,¹ S. K. Lamoreaux,¹ K. W. Lehnert,² and K. A. van Bibber³

¹*Department of Physics, Yale University, New Haven, Connecticut 06511, USA*

²*JILA and the Department of Physics, University of Colorado*

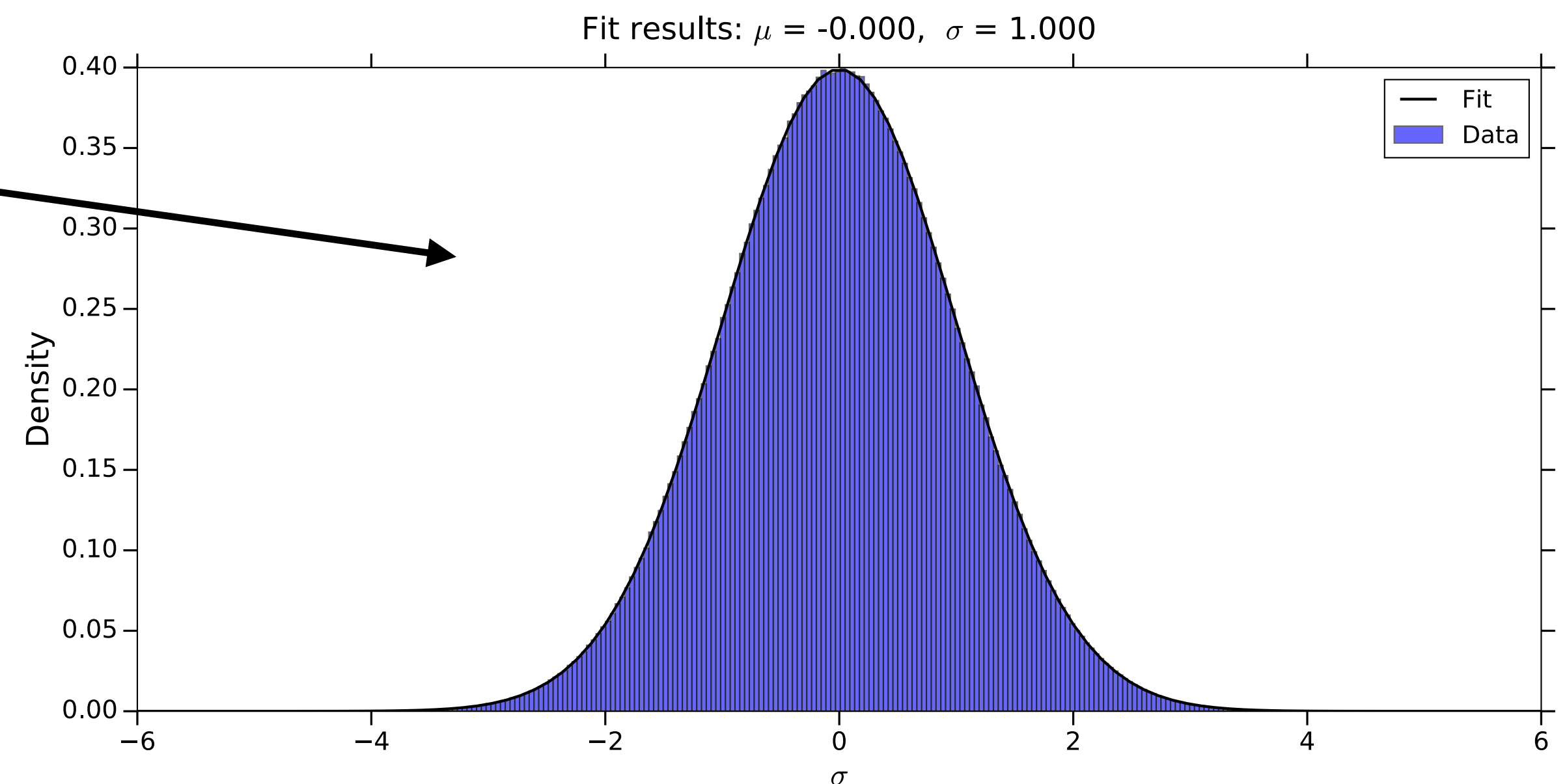
and National Institute of Standards and Technology, Boulder, Colorado 80309, USA

³*Department of Nuclear Engineering, University of California Berkeley, Berkeley, California 94720, USA*

(Received 26 June 2017; published 18 December 2017)

We describe in detail the analysis procedure used to derive the first limits from the Haloscope at Yale Sensitive to Axion CDM (HAYSTAC), a microwave cavity search for cold dark matter (CDM) axions with masses above $20 \mu\text{eV}$. We have introduced several significant innovations to the axion search analysis pioneered by the Axion Dark Matter eXperiment (ADMX), including optimal filtering of the individual power spectra that constitute the axion search data set and a consistent maximum likelihood procedure for combining and rebinning these spectra. These innovations enable us to obtain the axion-photon coupling $|g_\gamma|$ excluded at any desired confidence level directly from the statistics of the combined data.

DOI: [10.1103/PhysRevD.96.123008](https://doi.org/10.1103/PhysRevD.96.123008)



Combining bins vertically

- Follow the procedure outlined by HAYSTAC
- Vertically combine overlapping single bins using maximum-likelihood weights
- SNR of a single bin will change based on the lorentzian factor, T_{sys} , Q_L , β and σ
- Gaussian noise, as you might expect
- No negative correlations between bins, since independent scans

PHYSICAL REVIEW D **96**, 123008 (2017)

HAYSTAC axion search analysis procedure

B. M. Brubaker,^{1,*} L. Zhong,¹ S. K. Lamoreaux,¹ K. W. Lehnert,² and K. A. van Bibber³

¹*Department of Physics, Yale University, New Haven, Connecticut 06511, USA*

²*JILA and the Department of Physics, University of Colorado*

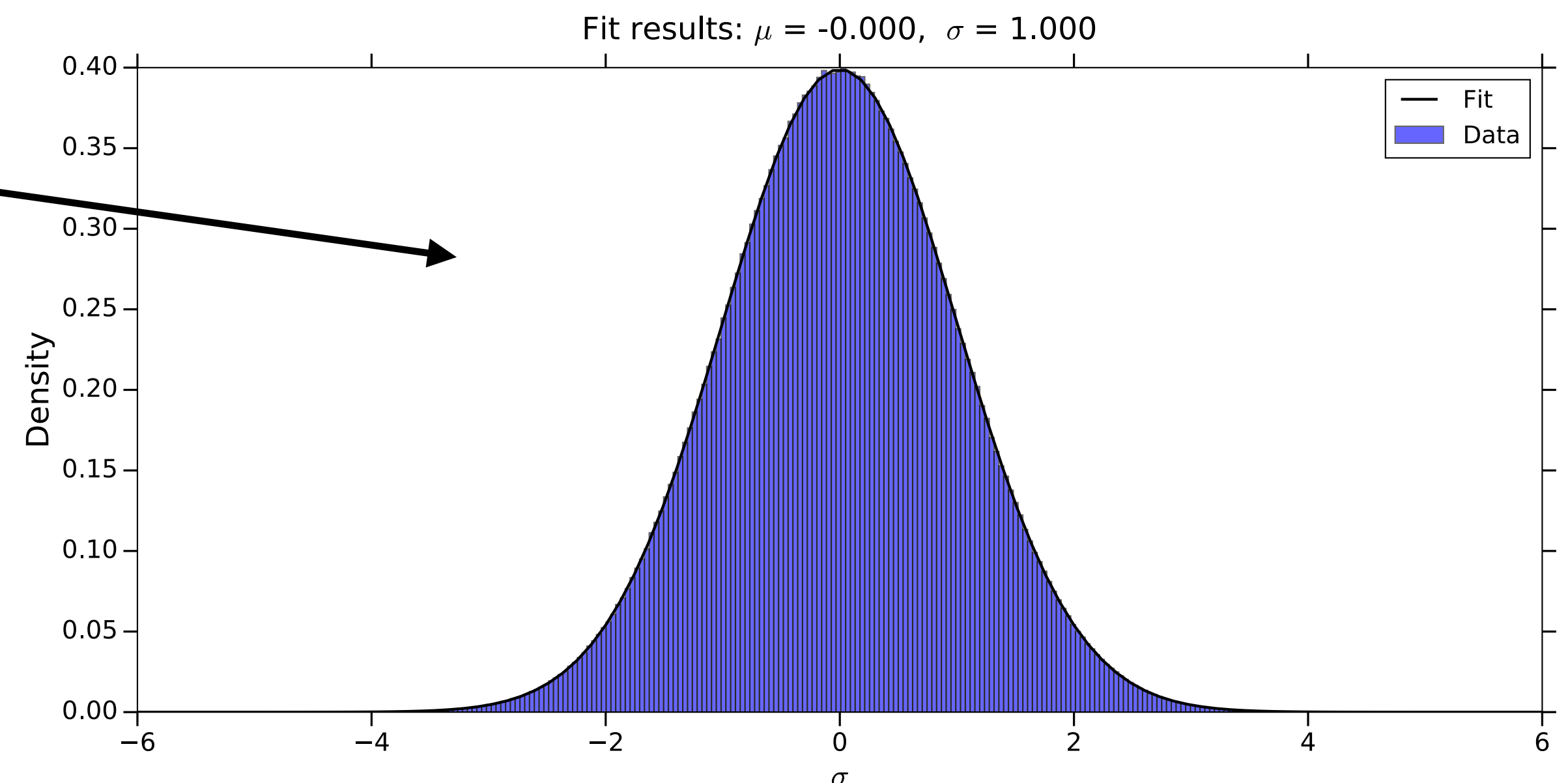
and National Institute of Standards and Technology, Boulder, Colorado 80309, USA

³*Department of Nuclear Engineering, University of California Berkeley, Berkeley, California 94720, USA*

(Received 26 June 2017; published 18 December 2017)

We describe in detail the analysis procedure used to derive the first limits from the Haloscope at Yale Sensitive to Axion CDM (HAYSTAC), a microwave cavity search for cold dark matter (CDM) axions with masses above $20 \mu\text{eV}$. We have introduced several significant innovations to the axion search analysis pioneered by the Axion Dark Matter eXperiment (ADMX), including optimal filtering of the individual power spectra that constitute the axion search data set and a consistent maximum likelihood procedure for combining and rebinning these spectra. These innovations enable us to obtain the axion-photon coupling $|g_\gamma|$ excluded at any desired confidence level directly from the statistics of the combined data.

DOI: [10.1103/PhysRevD.96.123008](https://doi.org/10.1103/PhysRevD.96.123008)



Combining bins horizontally

Combining bins horizontally

- Since $\Delta\nu_a \approx 32\Delta\nu_{bin}$, we must also combine bins horizontally

Combining bins horizontally

- Since $\Delta\nu_a \approx 32\Delta\nu_{bin}$, we must also combine bins horizontally
- First rebin the spectrum to $\Delta\nu_{rebin} = 8 \Delta\nu_{bin}$ by adding non-overlapping bins together (using ML weights)

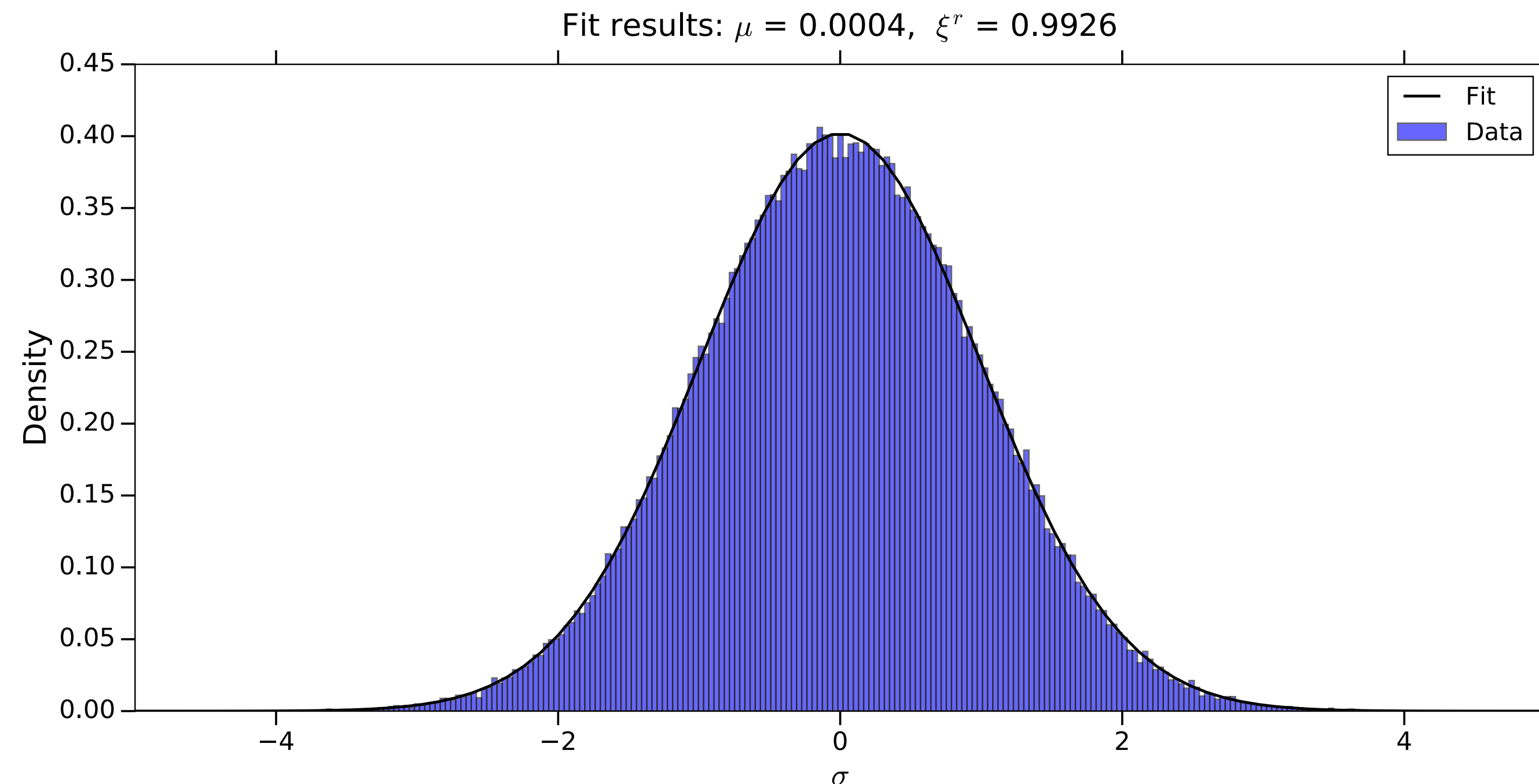
Combining bins horizontally

- Since $\Delta\nu_a \approx 32\Delta\nu_{bin}$, we must also combine bins horizontally
- First rebin the spectrum to $\Delta\nu_{rebin} = 8 \Delta\nu_{bin}$ by adding non-overlapping bins together (using ML weights)
- Because the SG filter induces negative correlations between nearby bins we start to see a non-Gaussian distribution.

Combining bins horizontally

- Since $\Delta\nu_a \approx 32\Delta\nu_{bin}$, we must also combine bins horizontally
- First rebin the spectrum to $\Delta\nu_{rebin} = 8 \Delta\nu_{bin}$ by adding non-overlapping bins together (using ML weights)
- Because the SG filter induces negative correlations between nearby bins we start to see a non-Gaussian distribution.

$$\xi^r = 0.99$$



The Grand Spectrum

The Grand Spectrum

- We must also account for the axion lineshape ie. a Maxwell-Boltzmann distribution

The Grand Spectrum

- We must also account for the axion lineshape ie. a Maxwell-Boltzman distribution
- **Matched filtering:** multiply sets of $\Delta\nu_{grand} = 4 \Delta\nu_{rebin}$ by axion line shape weights

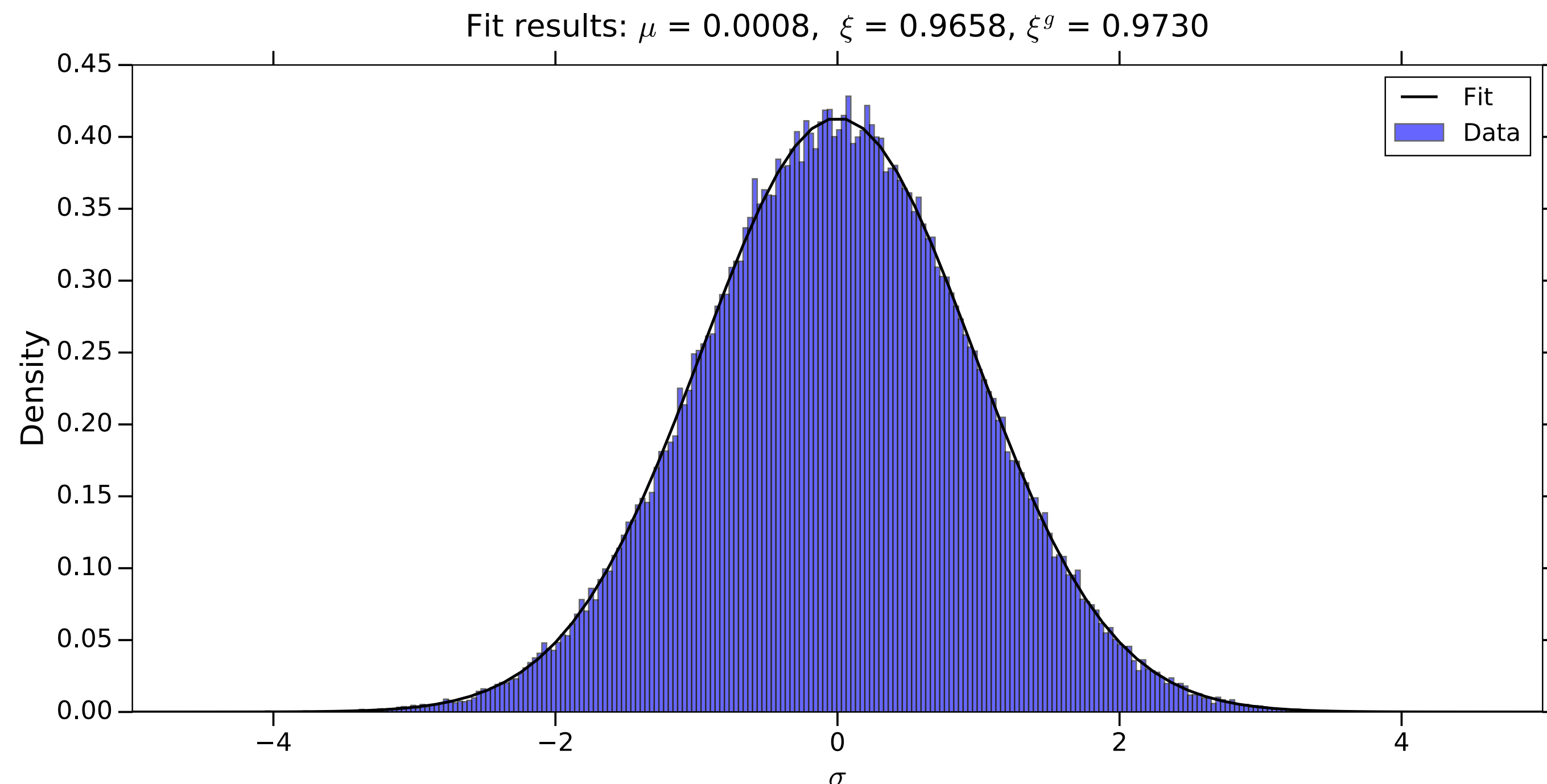
The Grand Spectrum

- We must also account for the axion lineshape ie. a Maxwell-Boltzman distribution
- **Matched filtering:** multiply sets of $\Delta\nu_{grand} = 4 \Delta\nu_{rebin}$ by axion line shape weights
- Further negative correlations between nearby bins reduces the width (ξ) of the histogram

The Grand Spectrum

- We must also account for the axion lineshape ie. a Maxwell-Boltzman distribution
- **Matched filtering:** multiply sets of $\Delta\nu_{grand} = 4 \Delta\nu_{rebin}$ by axion line shape weights
- Further negative correlations between nearby bins reduces the width (ξ) of the histogram

$$\xi^g = \frac{\xi^r}{\xi} = 0.97$$



Accounting for correlations

Accounting for correlations

- Simulate the effect of the SG filter on Gaussian noise

Accounting for correlations

- Simulate the effect of the SG filter on Gaussian noise
- Find the full covariance matrix and compare SG filtered vs non-filtered data for the “rebinned spectrum”

Accounting for correlations

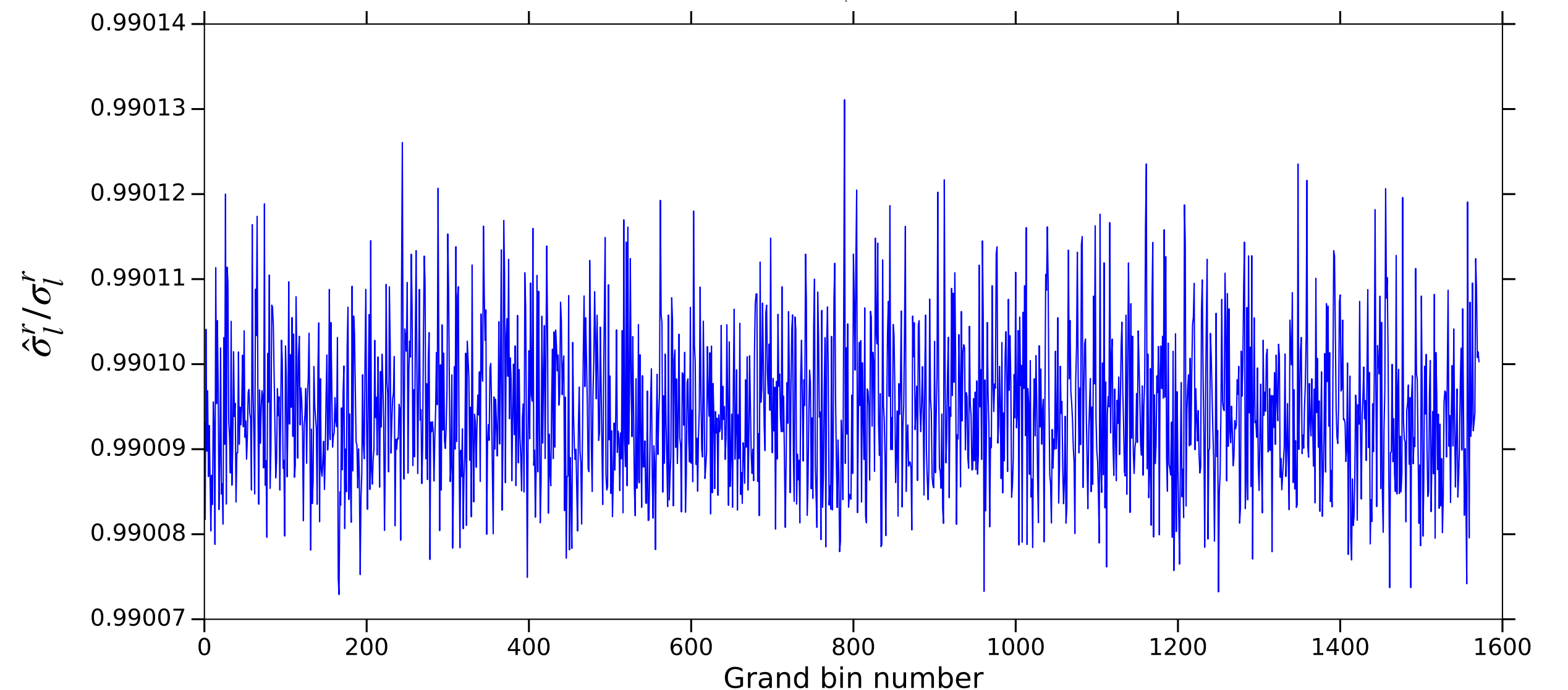
- Simulate the effect of the SG filter on Gaussian noise
- Find the full covariance matrix and compare SG filtered vs non-filtered data for the “rebinned spectrum”
- $\hat{\sigma}_l^r$ is the variance using the full covariance matrix

Accounting for correlations

- Simulate the effect of the SG filter on Gaussian noise
- Find the full covariance matrix and compare SG filtered vs non-filtered data for the “rebinned spectrum”
- $\hat{\sigma}_l^r$ is the variance using the full covariance matrix
- We find $\hat{\sigma}_l^r / \sigma_l^r \sim 0.99$

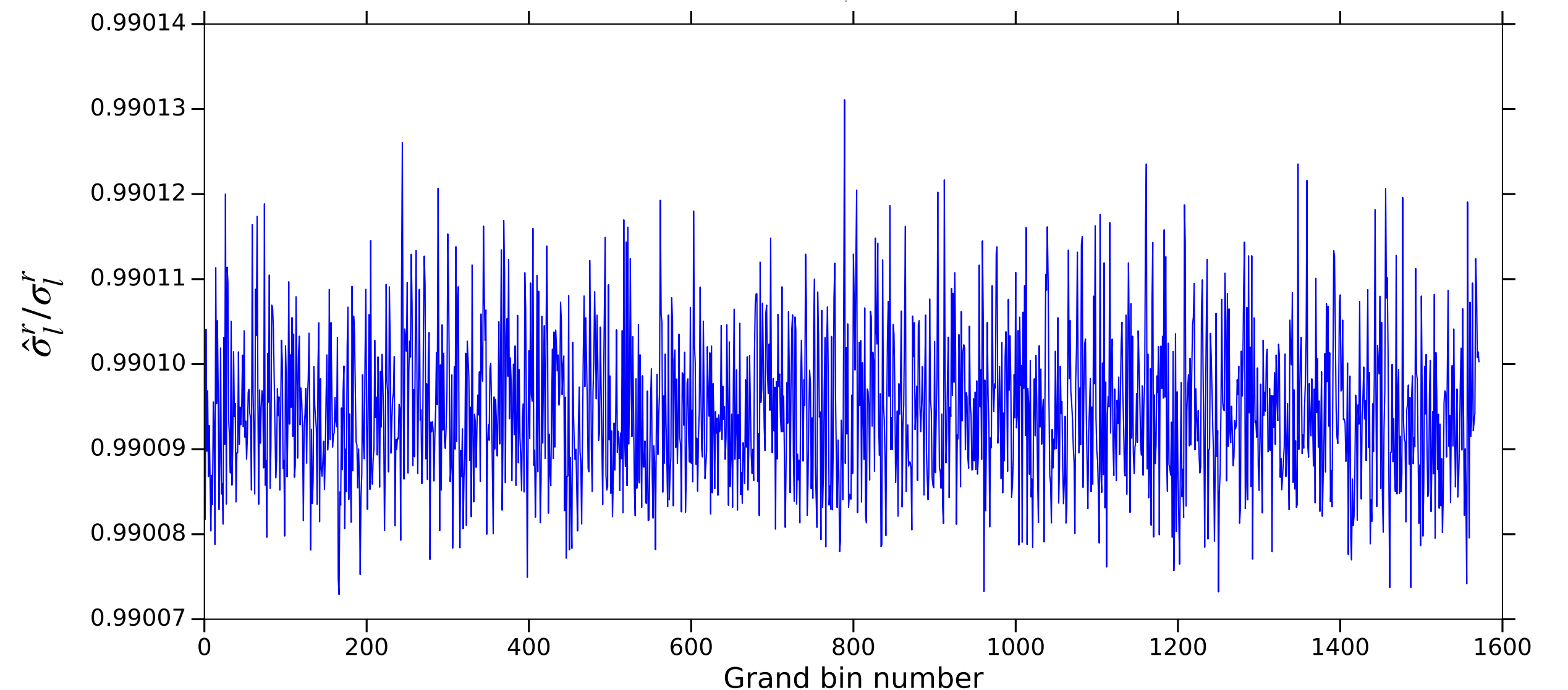
Accounting for correlations

- Simulate the effect of the SG filter on Gaussian noise
- Find the full covariance matrix and compare SG filtered vs non-filtered data for the “rebinned spectrum”
- $\hat{\sigma}_l^r$ is the variance using the full covariance matrix
- We find $\hat{\sigma}_l^r / \sigma_l^r \sim 0.99$



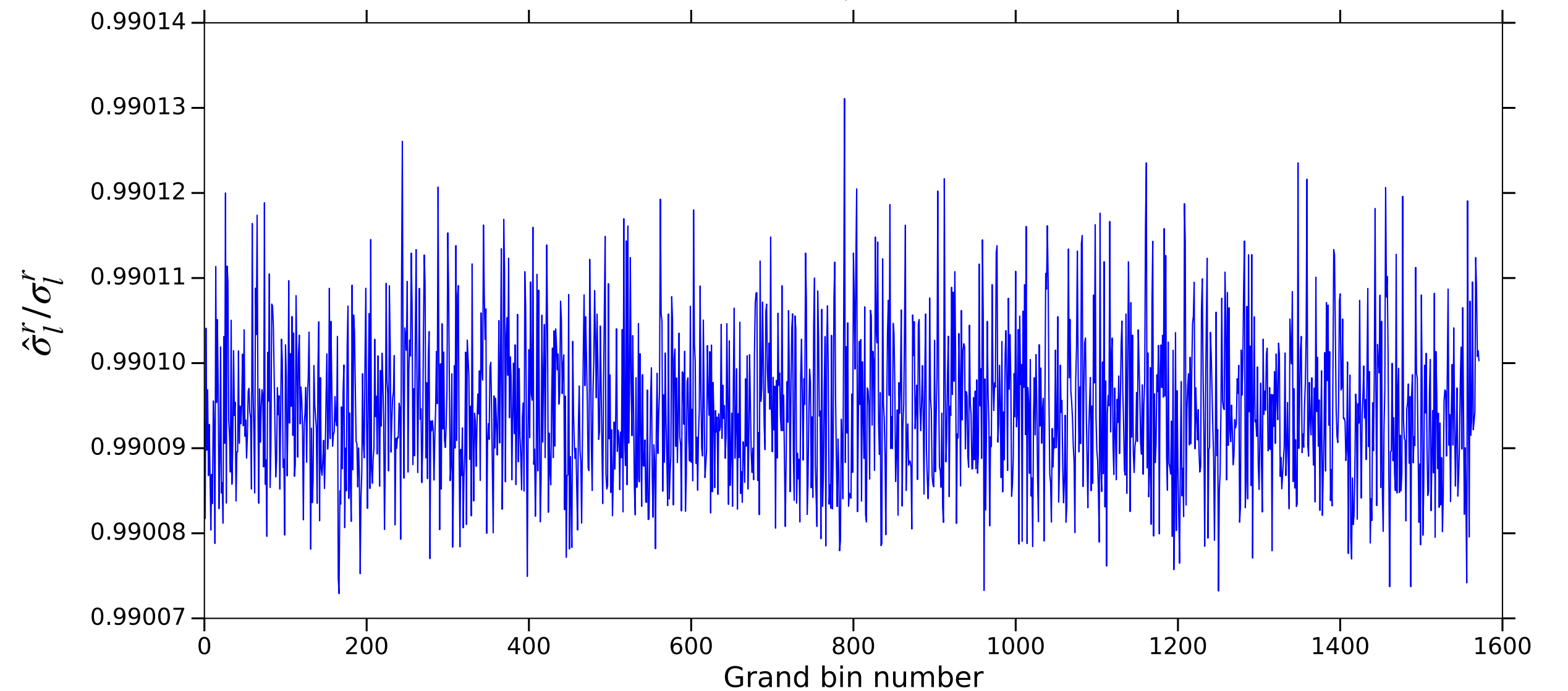
Accounting for correlations

- Simulate the effect of the SG filter on Gaussian noise
- Find the full covariance matrix and compare SG filtered vs non-filtered data for the “rebinned spectrum”
- $\hat{\sigma}_l^r$ is the variance using the full covariance matrix
- We find $\hat{\sigma}_l^r / \sigma_l^r \sim 0.99$
- We expect $\xi^r = \hat{\sigma}_l^r / \sigma_l^r = 0.99$



Accounting for correlations

- Simulate the effect of the SG filter on Gaussian noise
- Find the full covariance matrix and compare SG filtered vs non-filtered data for the “rebinned spectrum”
- $\hat{\sigma}_l^r$ is the variance using the full covariance matrix
- We find $\hat{\sigma}_l^r / \sigma_l^r \sim 0.99$
- We expect $\xi^r = \hat{\sigma}_l^r / \sigma_l^r = 0.99$
- Without the SG filter $\hat{\sigma}_l^r = \sigma_l^r = 1$



Accounting for correlations

Accounting for correlations

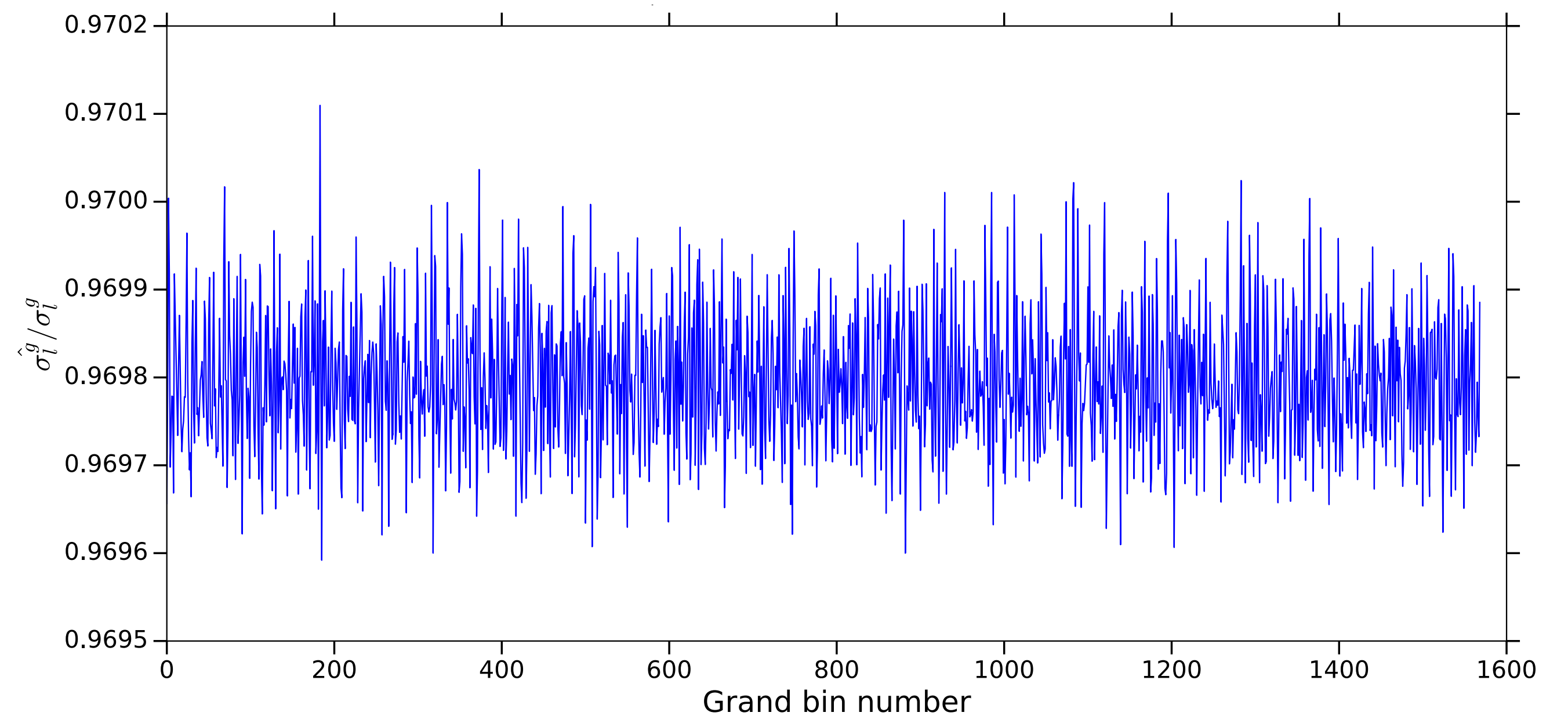
- Follow the same procedure for the “grand spectrum”

Accounting for correlations

- Follow the same procedure for the “grand spectrum”
- We find $\hat{\sigma}_l^g / \sigma_l^g \sim 0.97$

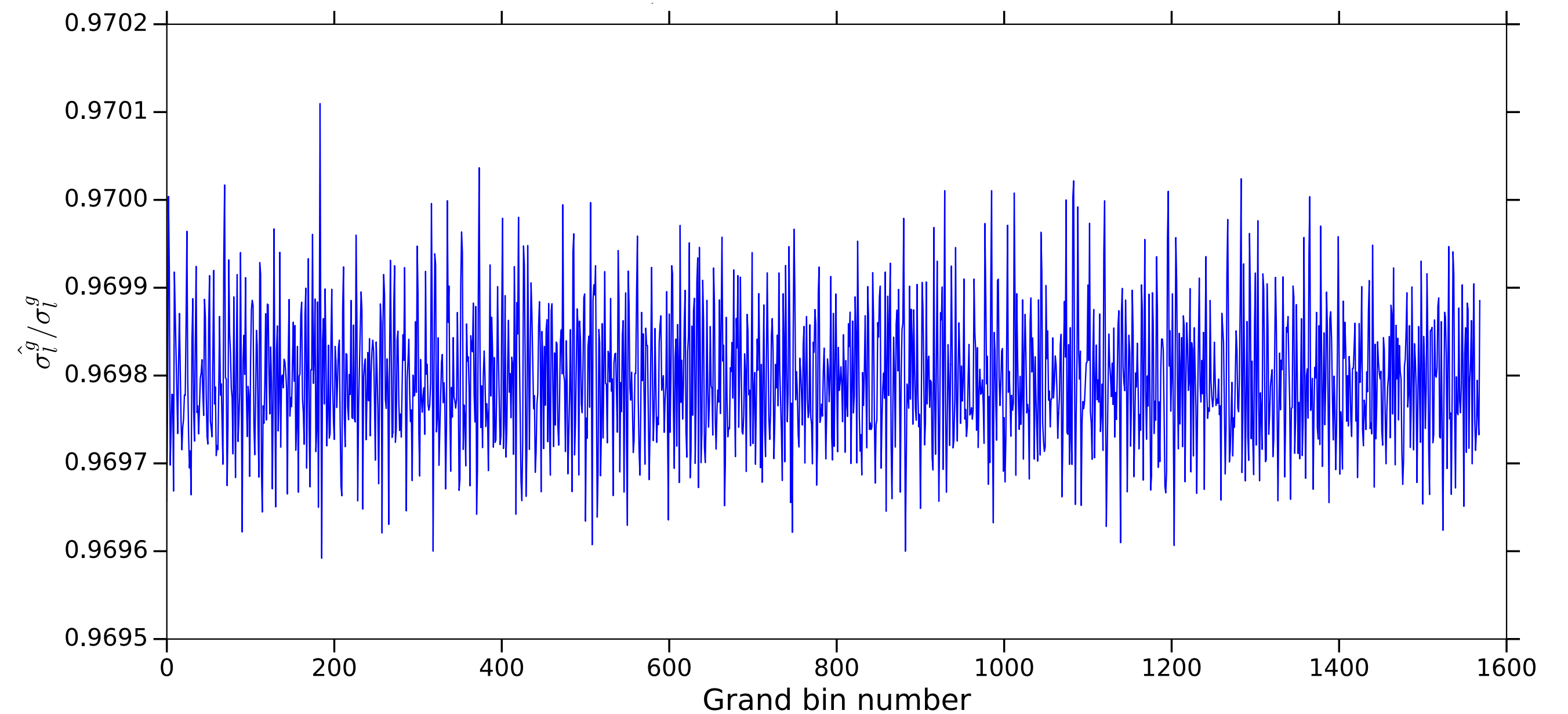
Accounting for correlations

- Follow the same procedure for the “grand spectrum”
- We find $\hat{\sigma}_l^g / \sigma_l^g \sim 0.97$



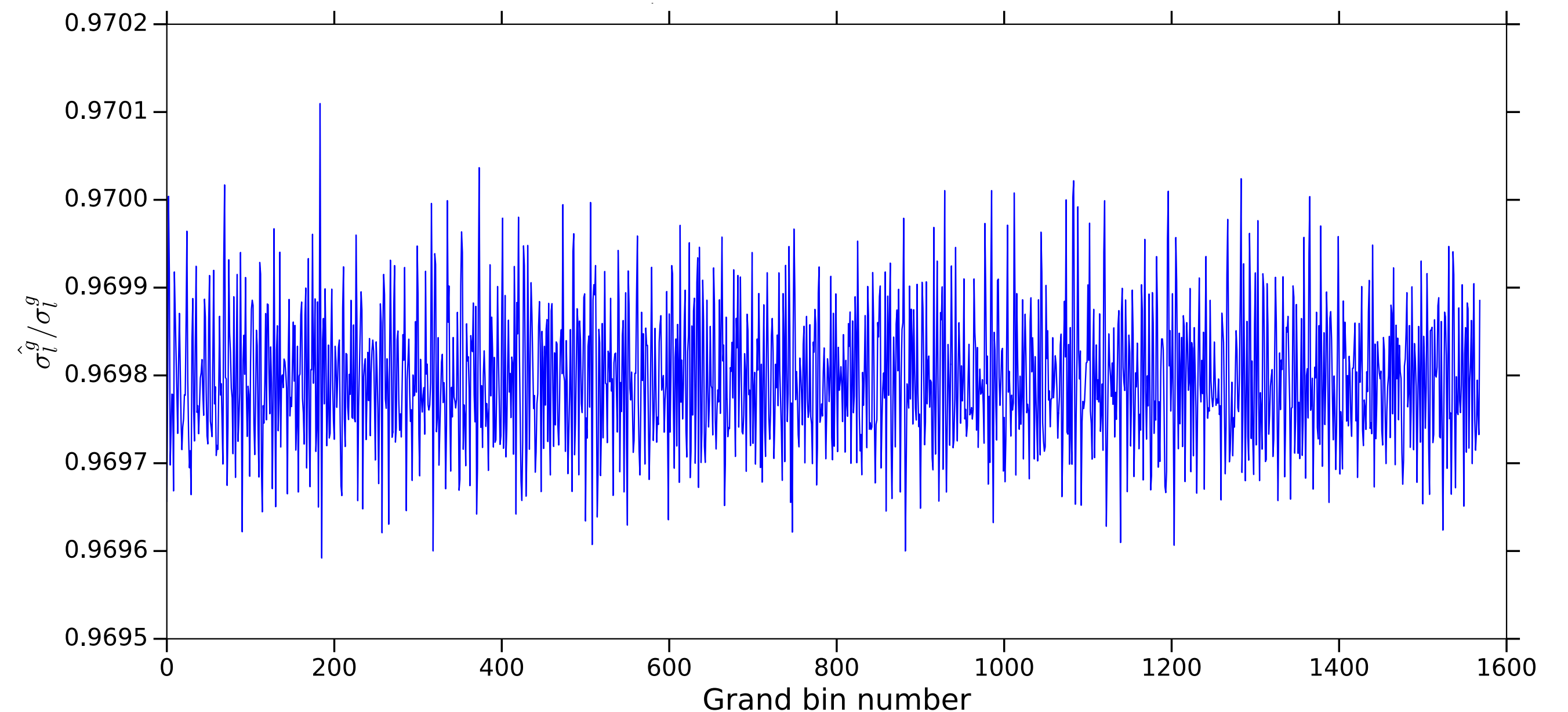
Accounting for correlations

- Follow the same procedure for the “grand spectrum”
- We find $\hat{\sigma}_l^g / \sigma_l^g \sim 0.97$
- We expect $\xi^g = \hat{\sigma}_l^g / \sigma_l^g = 0.97$



Accounting for correlations

- Follow the same procedure for the “grand spectrum”
- We find $\hat{\sigma}_l^g / \sigma_l^g \sim 0.97$
- We expect $\xi^g = \hat{\sigma}_l^g / \sigma_l^g = 0.97$
- Without the SG filter $\hat{\sigma}_l^g = \sigma_l^g = 1$



Simulating an axion

Simulating an axion

- Repeat a similar simulation to account for the attenuation of an axion signal

Simulating an axion

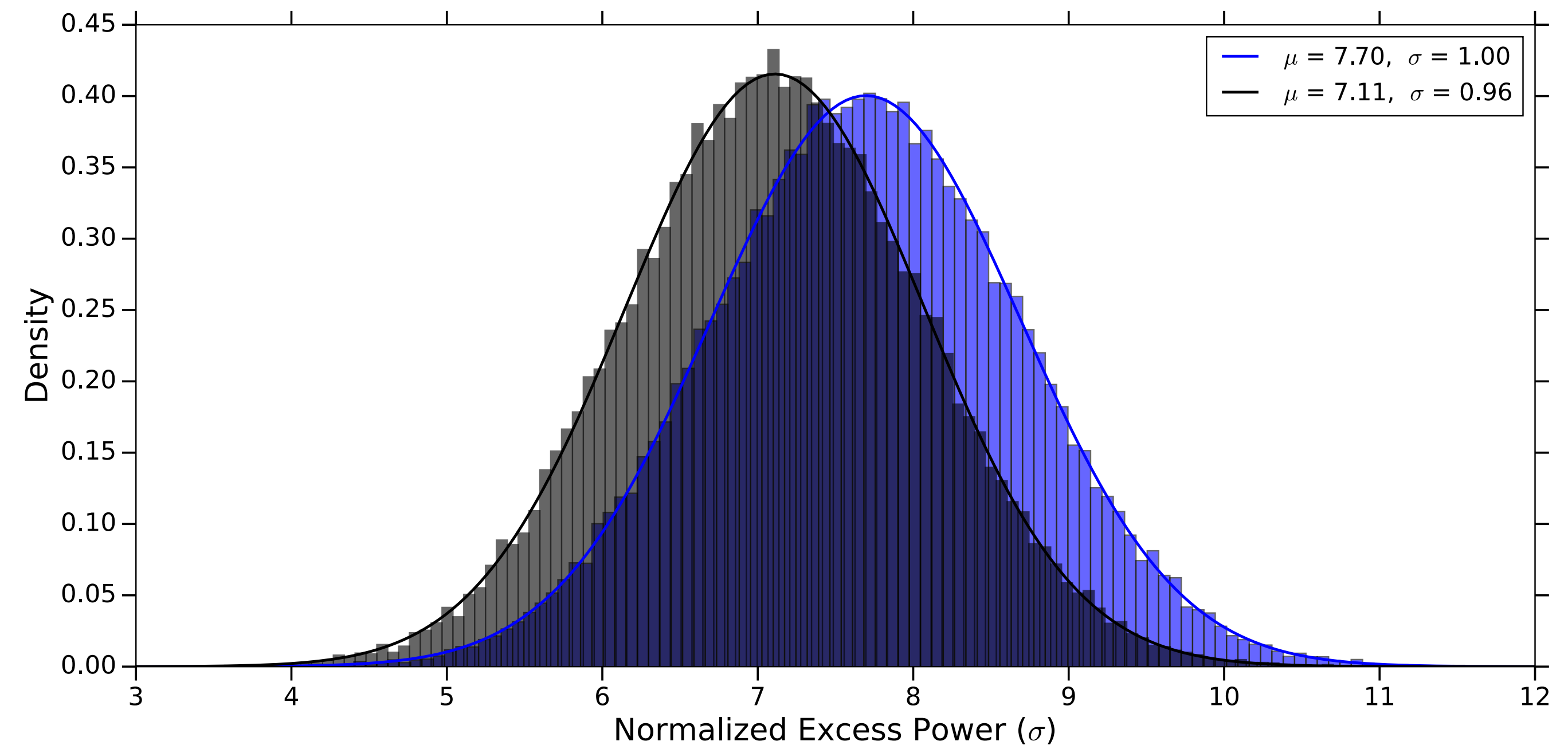
- Repeat a similar simulation to account for the attenuation of an axion signal
- Find the SNR of an axion with a given power buried beneath Gaussian noise

Simulating an axion

- Repeat a similar simulation to account for the attenuation of an axion signal
- Find the SNR of an axion with a given power buried beneath Gaussian noise
- Do this for **non-filtered** and **SG filtered** noise

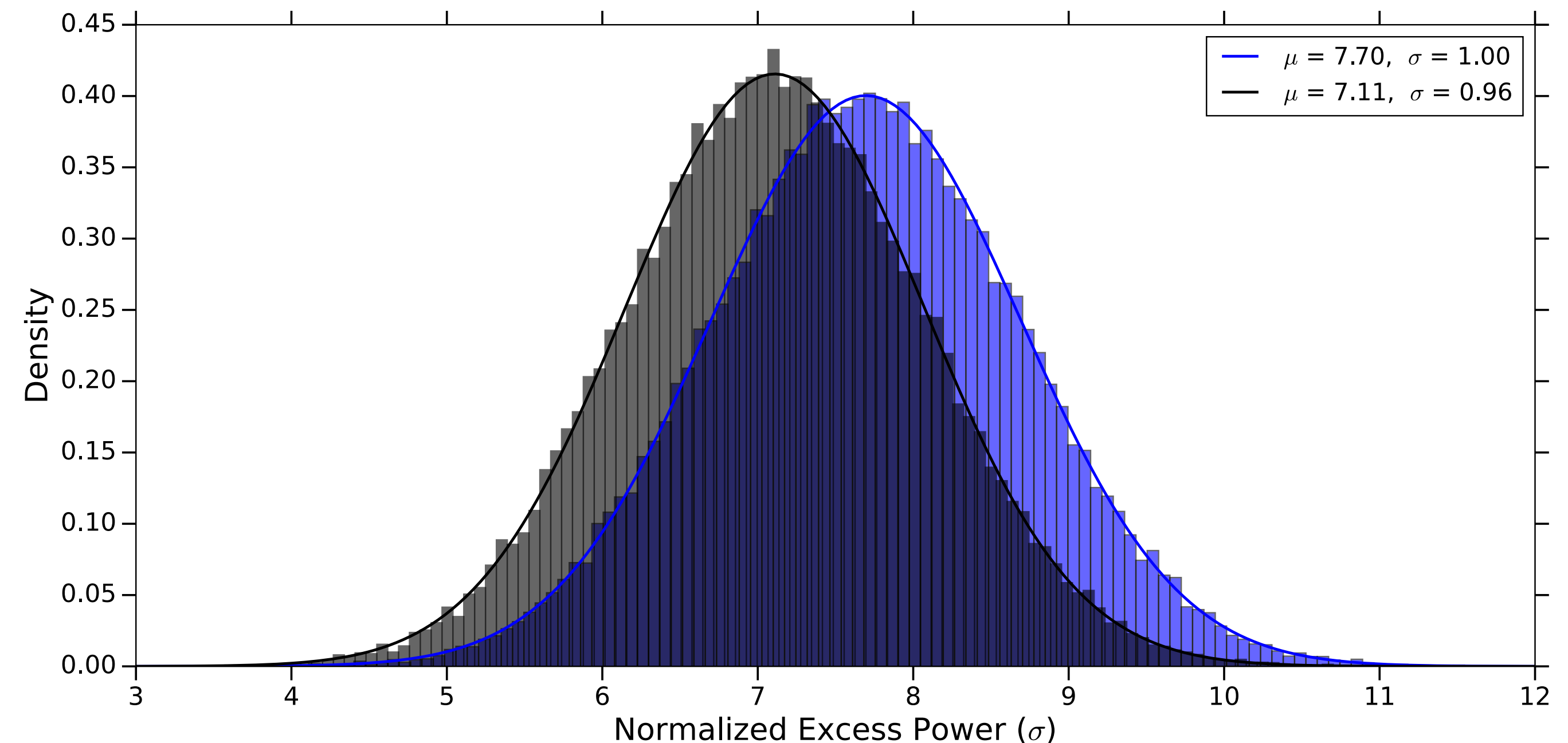
Simulating an axion

- Repeat a similar simulation to account for the attenuation of an axion signal
- Find the SNR of an axion with a given power buried beneath Gaussian noise
- Do this for **non-filtered** and **SG filtered** noise



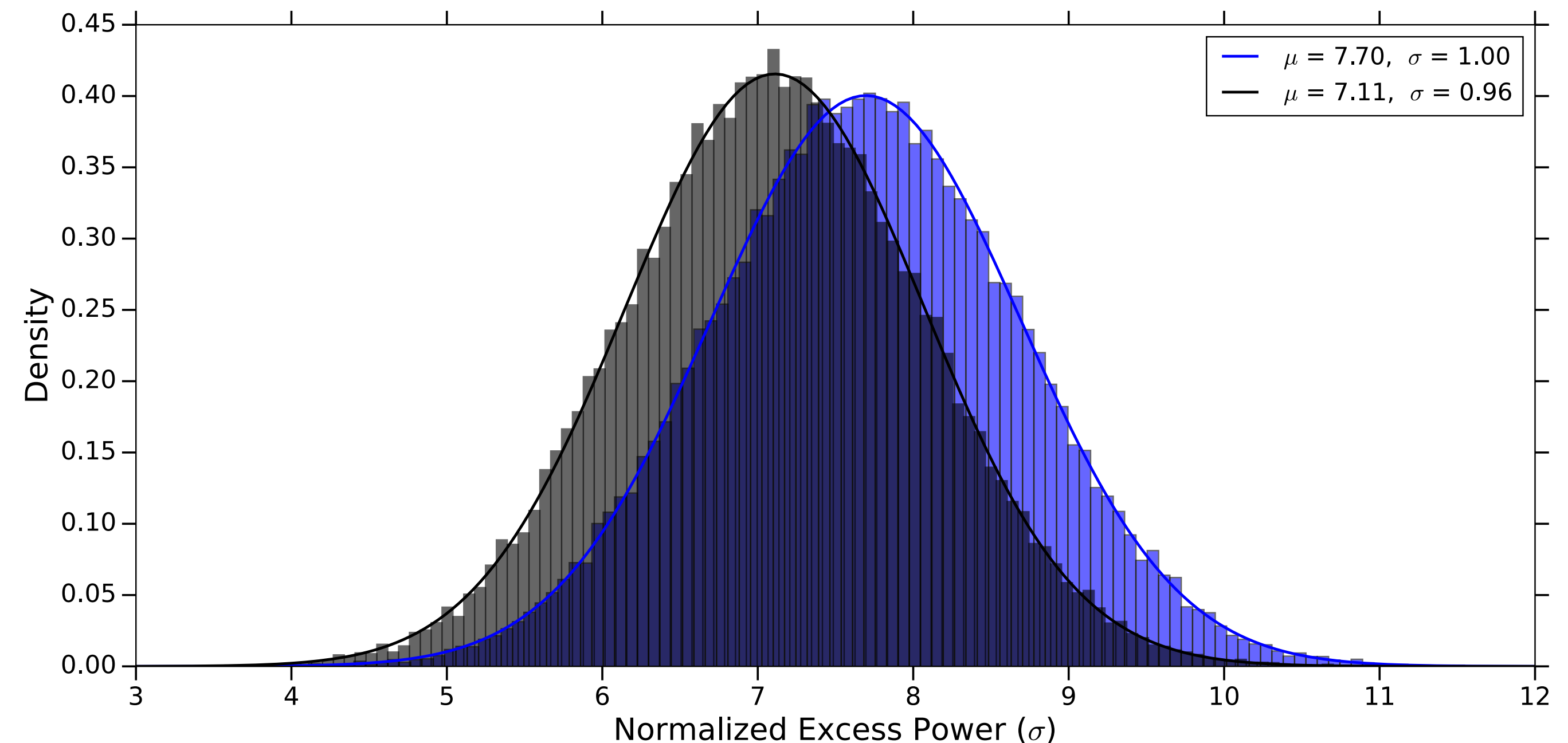
Simulating an axion

- Repeat a similar simulation to account for the attenuation of an axion signal
- Find the SNR of an axion with a given power buried beneath Gaussian noise
- Do this for **non-filtered** and **SG filtered** noise
- We find $\sigma = 1$ for the non-filtered spectrum and $\sigma = 0.96$ for the SG filtered spectrum



Simulating an axion

- Repeat a similar simulation to account for the attenuation of an axion signal
- Find the SNR of an axion with a given power buried beneath Gaussian noise
- Do this for **non-filtered** and **SG filtered** noise
- We find $\sigma = 1$ for the non-filtered spectrum and $\sigma = 0.96$ for the SG filtered spectrum
- The attenuation factor is then ~ 0.92



Preliminary Limits

Preliminary Limits

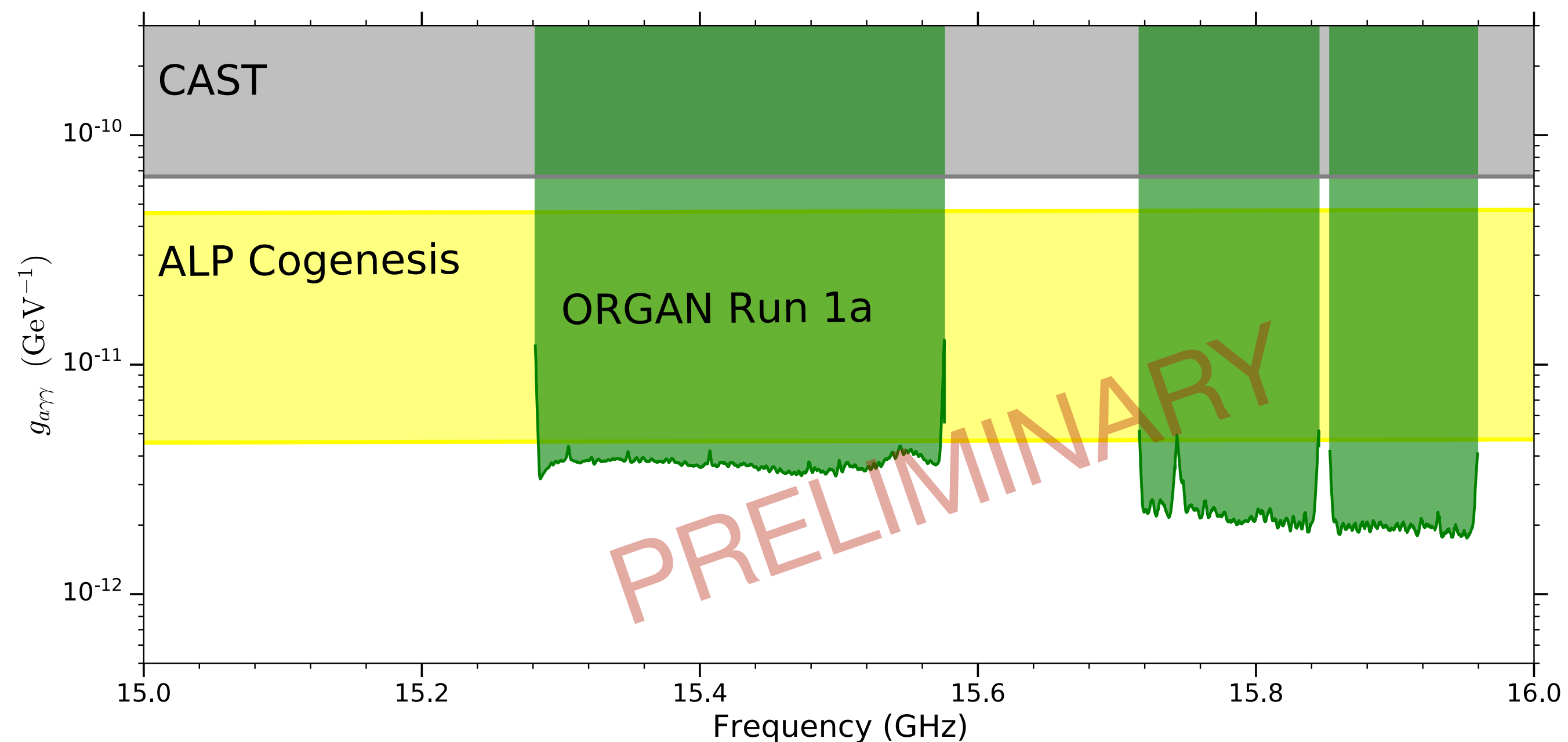
- Using the corrected $\hat{\sigma}_l^g$ and attenuated SNR values we can place limits in statistical manner

Preliminary Limits

- Using the corrected $\hat{\sigma}_l^g$ and attenuated SNR values we can place limits in statistical manner
- We set a 95% confidence limit, beyond the ALP Cogenesis limits

Preliminary Limits

- Using the corrected $\hat{\sigma}_l^g$ and attenuated SNR values we can place limits in statistical manner
- We set a 95% confidence limit, beyond the ALP Cogenesis limits



Preliminary Limits

Preliminary Limits

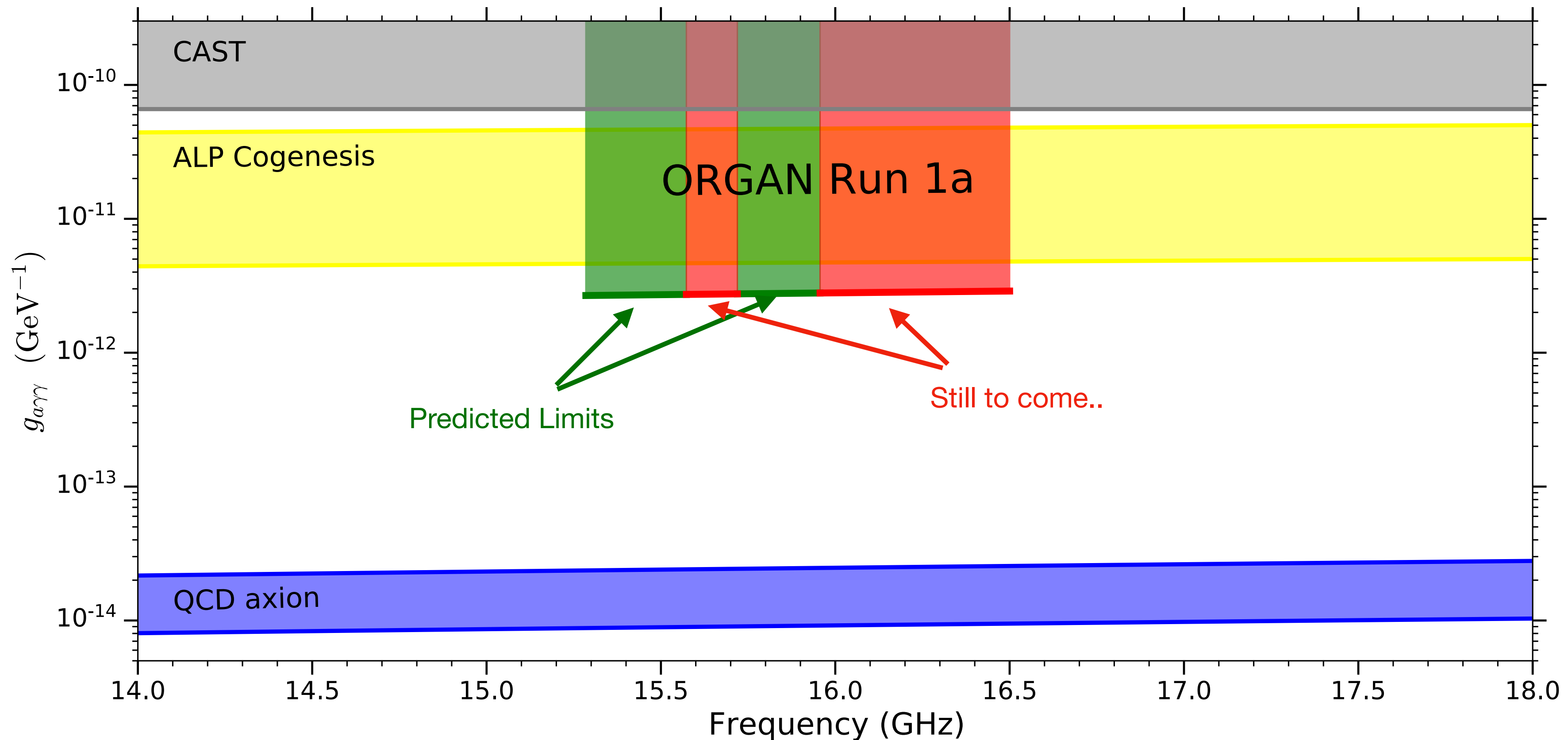
- Predicted limits using $Q_{ave} = 4000$, $T_{sys} = 10K$, $B_0 = 11.5T$

Preliminary Limits

- Predicted limits using $Q_{ave} = 4000$, $T_{sys} = 10K$, $B_0 = 11.5T$
- Set to be place the most sensitive limits in this region

Preliminary Limits

- Predicted limits using $Q_{ave} = 4000$, $T_{sys} = 10K$, $B_0 = 11.5T$
- Set to be place the most sensitive limits in this region



Questions?